Technische Universität München
TUM School of Medicine and Health

Bacterial-Derived Metabolites in the Context of Immune Checkpoint Inhibitor Cancer Therapy

Laura Joachim

Vollständiger Abdruck der von der TUM School of Medicine and Health der Technischen Universität München zur Erlangung einer

Doktorin der Naturwissenschaften (Dr. rer. nat.)

genehmigten Dissertation.

Vorsitz: Prof. Dr. Marc Schmidt-Supprian

Prüfende der Dissertation:

1. Prof. Dr. Hendrik Poeck
2. Prof. Dr. Michael Sattler

Die Dissertation wurde am 04.12.2023 bei der Technischen Universität München eingereicht und durch die TUM School of Medicine and Health am 10.04.2024 angenommen.

PUBLICATION STATEMENT

Journal articles (first author)

Parts of this thesis have been published in the following original research article. In particular, parts of the material and methods section and some figures have been adopted and, in some cases, not been changed.

Joachim L, Göttert S, Sax A, Steiger K, Neuhaus K, Heinrich P, Fan K, Orberg ET, Kleigrewe K, Ruland J, Bassermann F, Herr W, Posch C, Heidegger S, Poeck H. **The microbial metabolite desaminotyrosine enhances T-cell priming and cancer immunotherapy with immune checkpoint inhibitors.** EBioMedicine. 2023 Oct 19;97:104834. doi: 10.1016/j.ebiom.2023.104834.[1]

Journal articles (co-author)

Heidegger S, Stritzke F, Dahl S, Daßler-Plenker J, **Joachim L**, Buschmann D, Fan K, Sauer CM, Ludwig N, Winter C, Enssle S, Li S, Perl M, Görgens A, Haas T, Orberg ET, Göttert S, Wölfel C, Engleitner T, Cortés-Ciriano I, Rad R, Herr W, Giebel B, Ruland J, Bassermann F, Coch C, Hartmann G, Poeck H. **Targeting nucleic acid sensors in tumor cells to reprogram biogenesis and RNA cargo of extracellular vesicles for T cell-mediated cancer immunotherapy.** Cell Rep Med. 2023 Sep 19;4(9):101171. doi: 10.1016/j.xcrm.2023.101171.

Conferences

Partial results of this study have been presented at the following international conference:

Joachim L, Göttert S, Sax A, Steiger K, Neuhaus K, Fan K, Orberg ET, Kleigrewe K, Ruland J, Bassermann F, Herr W, Posch C, Heidegger S, Poeck H. **P237: The microbial metabolite desaminotyrosine enhances T-cell priming and cancer immunotherapy with immune checkpoint inhibitors.** CICON 2023 - 7th International Cancer Immunotherapy Conference, September 2023, Milano, Italy. Poster presentation.

Partial results of this study have been presented in the form of an abstract:

Joachim L, Göttert S, Sax A, Steiger K, Neuhaus K, Kleigrewe K, Thiele-Orberg E, Heidegger S, Poeck H. **V265: The microbial metabolite desaminotyrosine enhances T-cell priming and cancer immunotherapy with anti-CTLA-4.** Oncol Res Treat 2023;46(suppl 5):1–354, October 2023, Hamburg, Germany. Accepted for oral presentation.

TABLE OF CONTENTS

ABSTRACT

Despite considerable progress in immunotherapy for treating tumor diseases such as metastatic melanoma with immune checkpoint inhibitors (ICIs), many patients respond poorly to the treatment. In addition to other known factors, the composition of the gut microbiome has been associated with interindividual differences in treatment response, whereas the underlying molecular mechanisms have not yet been sufficiently explored. Bacterial-derived metabolites have been suggested as the missing link between the gut microbiome and ICI efficacy. In this study the impact of the bacterial-derived metabolites desaminotyrosine (DAT) and indole-3-carboxaldehyde (ICA) on the efficacy of ICI therapy has been investigated using a murine melanoma model. The results indicate that supplementation with DAT and ICA enhances the efficacy of ICI therapy, albeit with variations based on the tumor model and ICI type, dosage, and timing of administration. Furthermore, it was demonstrated that DAT facilitates the activation of immune cells such as T cells and natural killer (NK) cells in combination with anti-cytotoxic T lymphocyte-associated antigen-4 (CTLA-4) therapy, therefore modifying the tumor microenvironment (TME). Host type I interferon (IFN-I) signaling was identified as a critical mediator for the additive effects of DAT and anti-CTLA-4 therapy on tumor control, overall survival (OS), and the activation of immune cells in the TME. Consistently DAT administration promoted the expansion and proliferation of tumor antigen-specific T cells in conjunction with an IFN-I-inducing adjuvant in a vaccination model. Intriguingly, DAT did not directly affect B16.OVA tumor cells, highlighting its selective impact on the immune response. Moreover, DAT administration mitigated the adverse effects on anti-CTLA-4 therapy caused by broad-spectrum antibiotic treatment. Oral supplementation of DAT induced alterations in the gut microbial composition in steady state mice, indicating its potential role in additional gut microbiome modulation. Remarkably, this study highlights that DAT and ICA did not exacerbate anti-CTLA-4-induced immune-related adverse events (irAEs), despite the enhanced T-cell response and the associated inflammatory potential, suggesting their potential as safe and effective adjuncts to existing immunotherapies.

Overall, these findings provide novel insights into the complex interplay between bacterial-derived metabolites, the host immune system, and anti-CTLA-4 therapy, paving the way for the development of more effective and tailored immunotherapeutic approaches for cancer treatment even in the context of broad-spectrum antibiotic therapy.

KURZZUSAMMENFASSUNG

Trotz erheblicher Fortschritte in der Immuntherapie zur Behandlung von Tumorerkrankungen wie dem metastasierenden Melanom mit Immuncheckpoint-Inhibitoren (ICIs) sprechen viele Patienten nur unzureichend oder gar nicht auf die Therapie an. Neben anderen bereits bekannten Faktoren wird das Darmmikrobiom mit den interindividuellen Unterschieden im Therapieansprechen in Verbindung gebracht, wobei die zugrunde liegenden molekularen Mechanismen noch nicht ausreichend erforscht sind. Bakterielle Metabolite wurden als das fehlende Bindeglied zwischen dem Darmmikrobiom und der Wirksamkeit von ICIs erwogen. In dieser Studie wurde der Einfluss der bakteriellen Metabolite Desaminotyrosin (DAT) und Indol-3-carboxaldehyd (ICA) auf die Wirksamkeit der ICI-Therapie mithilfe eines murinen Melanom-Modells untersucht. Die Ergebnisse deuten darauf hin, dass die Supplementierung mit DAT und ICA die Wirksamkeit der ICI-Therapie erhöht, wenn auch mit Schwankungen basierend auf dem Tumormodell und dem ICI-Typ, der Dosierung und dem Zeitpunkt der Verabreichung. Darüber hinaus wurde gezeigt, dass DAT die Aktivierung von Immunzellen wie T-Zellen und natürlichen Killerzellen (NK-Zellen) in Kombination mit der anti-zytotoxisches-T-Lymphozyten-assoziiertes-Antigen-4(CTLA-4)-Therapie erleichtert und somit die Tumormikroumgebung (TME) modifiziert. Die Interferon-Typ-I (IFN-I)-Signalgebung des Wirtes wurde als kritischer Mediator für die additiven Effekte von DAT und der anti-CTLA-4-Therapie auf die Tumorkontrolle, das Gesamtüberleben und die Aktivierung von Immunzellen in der TME identifiziert. Konsequenterweise steigerte die DAT-Verabreichung die Expansion und Proliferation von tumorspezifischen T-Zellen in Verbindung mit einem IFN-I-induzierenden Adjuvans in einem Vakzinierungsmodell. Interessanterweise zeigte DAT keine direkten Auswirkungen auf B16.OVA-Tumorzellen, was somit die selektive Wirkung auf die Immunantwort hervorhebt. Darüber hinaus milderte die DAT-Verabreichung die nach einer Breitbandantibiotikabehandlung verursachten negativen Effekte auf die anti-CTLA-4-Therapie. Die orale Supplementierung von DAT führte zu Veränderungen in der Zusammensetzung des Darmmikrobioms bei Mäusen im Grundzustand, was auf seine potenzielle Rolle bei der zusätzlichen Modulation des Darmmikrobioms hinweist. Bemerkenswerterweise zeigt diese Studie, dass DAT und ICA trotz der verstärkten T-Zell-Antwort und des damit verbundenen entzündlichen Potenzials die durch anti-CTLA-4 induzierten immunvermittelten unerwünschten Effekte (irAEs) nicht verschlimmern, was auf ihr Potenzial als sichere und effektive Ergänzungen zu bestehenden Immuntherapien hinweist.

Insgesamt liefern diese Ergebnisse neue Erkenntnisse über das komplexe Zusammenspiel bakterieller Metabolite, des Wirtsimmunsystems und der anti-CTLA-4-Therapie und ebnen den Weg für die Entwicklung effektiverer und maßgeschneiderter immuntherapeutischer Ansätze zur Behandlung von Krebs, sogar im Zusammenhang mit Breitbandantibiotikatherapie.

LIST OF ABBREVIATIONS

Abbreviation	Term
%	Percentage
°C	Degree Celsius
µM	Micromolar
16S-rRNA	16S ribosomal RNA
AHR	Aryl hydrocarbon receptor
ALR	Absent in melanoma 2-like receptors
AmCyan	Aequorea coerulescens green fluorescent protein
APC (cell)	Antigen-presenting cell
APC	Allophycocyan
ATP	Adenosine triphosphate
BMDC	Bone marrow-derived dendritic cell
BMDM	Bone marrow-derived macrophage
BRAF	B-Raf proto-oncogene, serine/threonine kinase
CAR	Chimeric antigen receptor
CARD	Caspase activation and recruitment domain
CD	Cluster of differentiation
cDC	Conventional DC
cGAS	Cyclic guanosine monophosphate (GMP) - adenosine monophosphate (AMP) synthase
CI	Confidence interval
CLR	C-type lectin receptor
CO_2	Carbon dioxide
CTL	Cytotoxic T lymphocyte
CTLA-4	Cytotoxic T lymphocyte-associated antigen 4
Cy7	Cyanine 7
DAMP	Danger-associated molecular pattern
DAT	3-(4-Hydroxyphenyl)propionic acid (desaminotyrosine)
DC	Dendritic cell
DMSO	Dimethyl sulfoxide
DNA	Deoxyribonucleic acid
ds	Double stranded

EDTA	Ethylenediaminetetraacetic acid
FACS	Fluorescence-activated cell sorting
FBS	Fetal bovine serum
FDA	Food and drug administration
FITC	Fluorescein isothiocyanat
FMT	Fecal microbial transplant
g	Gram
GALT	Gut-associated lymphoid tissue
GF	Germ-free
GM-CSF	Granulocyte-macrophage
h	Hour
H_2O	Water
HEPES	4-(2-hydroxyethyl)-1-piperazineethanesulfonic acid
HLA	Human leukocyte antigen
HRP	Horseradish peroxidase
i.p.	Intraperitoneally
i.v.	Intravenously
I3A	Indole-3-carbaldehyde
ICA	Indole-3-carboxaldehyde
ICI	Immune checkpoint inhibitor
ICOS	Inducible T-cell co-stimulator
IDO	Indoleamine 2,3-dioxygenase
IFN	Interferon
IFNAR(1/2)	Interferon-α/β receptor (alpha/beta chain)
IgG	Immunoglobulin G
IL	Interleukin
IP-10	Interferon-gamma-induced protein 10
irAEs	Immune-related adverse events
ISGs	Interferon-stimulated genes
JAK	Janus kinase
KO	knockout
LAG-3	Lymphocyte-activation gene 3
LPS	Lipopolysaccharide

LRR	Leucine-rich repeat
M	Molar
mAB	Monoclonal antibody
MAMP	Microbe-associated molecular pattern
MAPK	Mitogen-activated protein kinase
MAVS	Mitochondrial antiviral-signaling protein
mg	Milligram
MHC (-I or -II)	Major histocompatibility complex I or II
min	Minute
ml	Milliliter
mm	Millimeter
mM	Millimolar
Mo-DC	Monocyte-derived dendritic cell
MTT	3-(4,5-dimethylthiazol-2-yl)-2,5-diphenyltetrazolium bromide
ng	Nanogram
NK	Natural killer
NLR	NOD-like receptor
NOD	Nucleotide-binding oligomerization domain
OS	Overall survival
OVA	Ovalbumin
pAB	Polyclonal antibody
PAMP	Pathogen-associated molecular pattern
PBS	Phosphate-buffered saline
PD-1	Programmed cell death protein 1
pDC	Plasmacytoid dendritic cell
PD-L1	Programmed death-ligand 1
PE	Phycoerythrin
PEG	Polyethylene glycol
PerCP-Cy5.5	Peridinin chlorophyll protein-Cyanine 5.5
PFS	Progression-free survival
PRR	Pattern recognition receptor
RIG-I	Retinoic Acid-Inducible Gene I
RLR	RIG-I-like receptor

RNA	Ribonucleic acid
RT	Room temperature
s.c.	Subcutaneously
SCFA	Short-chain fatty acid
sec	Second
SOCS	Suppressors of cytokine signaling
SPF	Specific pathogen free
STAT	Signal transducer and activator of transcription
STING	Stimulator of interferon genes
TAA	Tumor-associated antigen
TCM	Central memory T cell
TCR	T cell receptor
tdLN	Tumor draining lymph node
TEM	Effector memory T cell
TGF	Transforming growth factor
Th	T helper
TIR	Toll/interleukin-1 receptor
TLR	Toll-like receptor
TMB	Tumor mutational burden
TME	Tumor microenvironment
T_{reg}	Regulatory T cell
U	Unit
USA	United states of America
VLE	Very low endotoxin
WT	Wild-type
x	multiplied by
α	Alpha
β	Beta
γ	Gamma
µg	Microgram
µl	Microliter
µM	Micromolar

LIST OF TABLES

LIST OF FIGURES

I INTRODUCTION

1. Melanoma

Melanoma is an aggressive disease arising from the uncontrolled proliferation and malignant transformation of melanocytes, which are responsible for the production of melanin, a pigment that determines the color of the skin, hair, and eyes, and offers protection against sun exposure and oxidative stress.[2] The disease mainly involves melanocytes in the epidermis, specifically the innermost layer known as the stratum basale.[2] The malignant transformation of epidermal melanocytes ultimately leads to cutaneous melanoma. Despite being the least common type of skin cancer, malignant melanoma is the most aggressive and life-threatening form.[3] Risk factors include UV exposure, ethnicity, age, and gender.[4] Survival rates vary with localized tumors having up to a 100% 5-year relative survival rate, while distant metastases result in a 32% survival rate.[5] Patients with melanomas at stage I and II have the best prognosis as the tumors are localized and no regional lymph nodes are affected, and surgery holds a high curative potential. However, patients at stages III and IV, with involvement of local or distant lymph nodes or distant organs, as well as some patients at stage II, require adjuvant treatments to halt disease progression.[6,7] While radiotherapy is occasionally used for exceptional cases, its effectiveness is limited due to the radio resistance of melanomas.[8] Similarly, chemotherapy is generally avoided due to its limited activity and lack of survival benefit.[9] Instead, targeted therapies and immunotherapeutic approaches are more widely applied in advanced melanoma. Given the abundance of genetic alterations in genes associated with proliferative signaling pathways, targeted therapy uses small molecule inhibitors to specifically target these pathways.[7] The immunotherapeutic approach started with interleukin-2 (IL-2) and interferon alpha-2b (IFNα-2b) with moderate responses in long-term follow up and high toxicity.[10,11] Since 2011, a significant change has occurred in the role of immunotherapy in melanoma with the approval of the immune checkpoint inhibitor (ICI) ipilimumab. Over the last few years, in addition to ipilimumab other ICIs targeting different immune checkpoints have also been approved and have shown significant results in terms of therapy response and overall survival (OS).[12–15] ICIs allow for the re-establishment of an antitumor immune response by overcoming inhibited T cell functions. Nevertheless, a large percentage of patients do not respond to ICI therapy or develop resistance, and the reasons behind this remain elusive.[16–18] Another aspect is that patients often experience immune-related adverse events (irAEs) due to ICI therapy.[12,19] Another approach for first line treatment for locoregional disease is represented by oncolytic viruses, also in combination with ICIs to generate a systemic antitumor response.[20]

Ultimately, the principal constraint is related to the emergence and subsequent development of treatment resistance for the current state of the art therapies.

2. The immune system

2.1 Basic concepts

The human immune system comprises three key levels: anatomic and physiologic barriers, innate immunity, and adaptive immunity, with deficiencies in any of these levels significantly heightening susceptibility to infection. Anatomic and physiologic barriers, including intact skin, effective mucociliary clearance mechanisms, low stomach pH, and bacteriolytic lysozyme in bodily secretions, serve as the initial defense line against pathogens. Innate immunity supplements the protection provided by anatomic and physiologic barriers by rapidly initiating a protective inflammatory response upon pathogen exposure and facilitating the subsequent activation of the adaptive immune response. The innate immune system identifies invaders through pattern detection, utilizing pattern recognition receptors (PRRs) which recognize distinct and conserved molecular structures in pathogens, the so-called pathogen-associated molecular patterns (PAMPs). These PAMPs are vital for pathogen survival, possessing unique attributes absent in host cells. Consequently, PRRs initiate signaling pathways, triggering immune responses like cytokine release, inflammation, and innate immune cell activation, contributing to pathogen elimination and host-microbe balance.[21–24] PRRs are categorized into important main types based on protein domain homology: these include membrane-bound toll-like receptors (TLRs), C-type lectin receptors (CLRs), and cytosolic receptor families like nucleotide-binding oligomerization domain (NOD)-like receptors (NLRs), RNA-helicases such as RIG-I-like receptors (RLRs), absent in melanoma-2 (AIM2)-like receptors (ALRs), and the Cyclic GMP-AMP synthase (cGAS).[21–25] Furthermore, PRRs can recognize so called danger-associated molecular patterns (DAMPs). Unlike PAMPs, DAMPs are endogenous molecules produced by host cells. The recognition of DAMPs by the innate immune system helps in the clearance of damaged tissues, the repair of injured areas, and the initiation of defense mechanisms against potential threats or infections resulting from tissue damage.[21–24] Additionally, the innate immune system features a humoral component consisting of various well-characterized components, including complement proteins, lipopolysaccharide (LPS) binding protein, C-reactive protein, pentraxins, collectins, and anti-microbial peptides like defensins.[26,27] These circulating innate immune proteins play a crucial role in both pathogen sensing and facilitating the clearance of infections. As adaptive immunity progressed alongside a fully operational innate immune system throughout evolution, the conventional differentiation between innate and adaptive immunity is regarded as overly simplistic, given that numerous adaptive immune responses rely on the fundamental framework established by innate immunity.[26–28] Adaptive immunity is a complex and highly specialized defense mechanism of the immune system that provides long-lasting protection against specific pathogens. This type of immunity is antigen-specific, meaning it recognizes and targets particular antigens. Adaptive immunity also exhibits immunological memory, enabling the immune system to recognize and

mount a stronger and faster response upon subsequent encounters with the same pathogen. Adaptive immunity involves two primary types of immune responses: humoral immunity mediated by B lymphocytes and the antibodies they produce as well as cell-mediated immunity.[27]

2.2. Cell-mediated immune responses

The innate immune system engages a wide array of cells of both hematopoietic and non-hematopoietic origins to provide defense against pathogens. Hematopoietic cells involved in innate immune responses include macrophages, dendritic cells (DCs), mast cells, neutrophils, eosinophils, natural killer (NK) cells, and NK T cells, while non-hematopoietic cells such as those in the skin and the epithelial linings of the respiratory, gastrointestinal, and genitourinary tracts further contribute to innate immune responsiveness. The adaptive immune system on the other hand relies on hematopoietic T and B lymphocytes.[26,27]

2.2.1. T cells

T cells develop in the thymus through chemokine-guided interactions, undergo positive and negative selection, establish central tolerance in the medulla, and exit as mature T cells with unique T cell receptors (TCRs) that recognize diverse antigens. Activation occurs when TCRs interact with antigenic peptides presented by major histocompatibility complex (MHC) molecules, leading to the formation of an immunological synapse and activation of intracellular signaling pathways.[29–31]

The mature T lymphocytes can be identified as either $CD4^+$ T helper (Th) cells or $CD8^+$ cytotoxic T lymphocytes (CTLs). Th cells produce cytokines essential for triggering both humoral and cell-mediated immune responses. The activation of Th cells is regulated, and naive $CD4^+$ cells become active when they encounter antigens presented by MHC complexes (in humans specifically called human leukocyte antigen (HLA)) on professional antigen presenting cells (APCs), like DCs, with the appropriate co-stimulatory molecules. Upon activation, $CD4^+$ T cells differentiate into distinct subsets, including Th1, Th2, Th17, and Tregs, each with specialized functions. Th1 cells promote cell-mediated immunity against intracellular pathogens, Th2 cells facilitate responses against extracellular parasites and allergens, while Th17 cells play a role in inflammation and mucosal defense.[27,32,33] Tregs, on the other hand, help maintain immune tolerance and prevent excessive immune reactions. Tregs are characterized by the expression of the transcription factor FoxP3 and are capable of suppressing the activation and function of other immune cells, such as effector T cells, B cells,

and antigen-presenting cells. By exerting immunosuppressive effects, Tregs help control inflammation and immune reactions, making them essential for immune homeostasis. Dysfunction or deficiencies in Tregs can lead to autoimmune diseases, contribute to chronic inflammatory conditions, and regulate tumor immunity.[34,35]

$CD8^+$ T cells play a critical role in the adaptive immune response by recognizing and eliminating infected or abnormal cells. When they encounter cells displaying antigens on MHC class I (MHC-I) molecules, typically as a result of viral infection or cellular transformation, $CD8^+$ T cells become activated. Upon activation, they undergo clonal expansion and differentiate into effector cells equipped to recognize and destroy the target cells. This process involves the release of cytotoxic molecules, such as perforin and granzymes, which induce apoptosis in the target cells.[36] CTLs can provide a defense against spontaneous tumors by identifying alterations in the antigens of tumor cells. As cells undergo transformation into tumors, their protein composition is modified as well. $CD8^+$ T cells are capable of identifying these antigens presented by MHC-I molecules, which acquire peptides from the internal protein degradation process of a cell and present them on the cell surface. This mechanism enables CTLs to conduct surveillance for any cellular changes, including those occurring in tumor cells.[36,37]

Both $CD4^+$ and $CD8^+$ T cells express T cell activation markers, including early activation marker CD69 and activation marker CD25, upon encountering antigens or other signals. These activation markers are integral to various T cell functions, such as T cell proliferation and cytokine production.[38] In addition to these markers, activated T cells also produce cytokines like interferon-gamma (IFN-γ) as part of their effector function. While IFN-γ is typically not used as a direct marker for identification of activated T cells, its presence in the surrounding environment or its secretion by T cells can serve as an indicator of an ongoing T cell response and activation.[38,39]

After an initial encounter with an antigen, some T cells develop into memory T cells. These cells provide long-lasting immunity and can rapidly respond to re-infection with the same pathogen. These cells come in two primary subtypes: central memory T cells (TCMs) and effector memory T cells (TEMs). TCMs primarily reside in lymphoid tissues, such as lymph nodes and the spleen, and possess a high degree of proliferative potential. They function as a reservoir of memory T cells and contribute to the generation of secondary immune responses. TEMs, on the other hand, circulate in peripheral tissues and have immediate effector functions, swiftly mobilizing to infection sites to combat invading pathogens. Both TCMs and TEMs are derived from previously activated T cells, often naive T cells that have undergone antigen stimulation and differentiation into effector cells during the initial encounter with an antigen.[40]

Memory T cells can play a crucial role in preventing cancer recurrence. This phenomenon is the basis for some immunotherapies and cancer vaccines that aim to stimulate the development of memory T cells specific to tumor antigens.[40,41]

2.2.2 Dendritic cells

DCs are essential antigen-presenting cells found in various tissues, acting as immune system sentinels. They play a crucial role in maintaining the immune balance by promoting immune tolerance under normal conditions. However, when there are disruptions in this balance, often signaled by innate immune activation, DCs become activated and carry antigens to the nearby draining lymph nodes. There, they initiate the activation of naive T cells, a pivotal step in launching immune responses against perceived threats. In essence, DCs serve as a bridge between innate and adaptive immunity, regulating immune responses in both steady state and perturbed conditions. DCs are a heterogenous group of cells that include conventional DCs (cDCs), plasmacytoid DCs (pDCs), and monocyte derived DCs (Mo-DCs). DCs, similar to all other types of leukocytes, originate from hematopoietic stem cells found in the bone marrow. Monocytes, macrophages, granulocytes, megakaryocytes, and erythrocytes go through the process of differentiation from a shared myeloid progenitor.[42–46]

Plasmacytoid DCs, while having lower antigen presentation capabilities than cDCs at baseline, can induce T cell proliferation when stimulated. They express high levels of toll-like receptor (TLR) 7 and TLR9, allowing them to produce type I interferon (IFN-I) in response to nucleic acids, which makes them important in antiviral, antitumor, and autoimmune responses. The pDCs can regulate various immune responses, including those of NK cells, cDCs, macrophages, $CD4^+$ T cells, and $CD8^+$ T cells through IFN-I.[43]

Conventional DCs, expressing CD11c and MHC-II, are categorized into resident and migratory cDCs based on their initial location and migration patterns. Both subsets can be further divided into cDC1s and cDC2s. The cDC1s are characterized by CD103 expression in mice and are critical for cross-presentation to prime $CD8^+$ T cells, particularly in antiviral and antitumor responses. They also present antigens to $CD4^+$ T cells, initiating Th cell differentiation. The cDC2s, on the other hand, are characterized by CD11b expression in mice. They have diverse subsets, and their functions include activating naive $CD4^+$ T cells and directing their differentiation into various Th cell subsets including Th2, Th17, and Tregs, depending on the specific cDC2 subset and inflammatory conditions.[44,45]

Mo-DCs can migrate to lymph nodes and influence $CD4^+$ T cell differentiation through cytokine production, but they are not typically involved in naive T cell priming. Instead, they contribute to shaping $CD4^+$ T cell subsets, particularly during inflammatory states, and can reactivate primed $CD4^+$ T cells in tissues.[46]

2.2.3 Natural killer cells

NK cells are a type of innate immune cell with cytotoxic abilities similar to $CD8^+$ T cells in adaptive immunity. However, they lack CD3 and TCRs and thus do not require prior sensitization or the need for specific antigen recognition. NK cells are primarily found in the blood, constituting around 5-10% of peripheral blood mononuclear cells, and they are present in bone marrow and lymphoid tissues like the spleen as well. These cells originate from common lymphoid progenitor cells in the bone marrow.[47]

In cases of infection and inflammation, NK cells are swiftly recruited and activated, undergoing rapid proliferation, and making significant contributions to both innate and adaptive immune reactions. NK cells can be activated by cytokines like IL-12, IL-15, and IL-18, which stimulate them to produce IFN-γ. Also, interaction with DCs or co-stimulatory signals from other immune cells or target cells can lead to production of IFN-γ by NK cells.[47–49] Like in T cells, IFN-γ can serve as an indicator of an ongoing NK cell immune response or activation. Additionally, they can secrete various cytokines and chemokines, thereby influencing the recruitment and function of other immune cells.[47]

2.3 The significance of type I interferon signaling

IFN-Is, including IFN-α and IFN-β, constitute a vital component of the immune system, functioning as crucial mediators in the immune response. The diverse biological responses initiated by IFN-I are mediated through the ubiquitously expressed heterodimeric interferon alpha/beta receptor (IFNAR), comprised of subunits IFNAR1 and IFNAR2. The IFN-I response is mediated via PRRs. IFNAR1 knockout mice underscore the critical role of this subunit in mediating biological responses and reveal the pleiotropic functions of IFN-I in regulating host responses to viral infections and adaptive immunity. Upon IFNAR receptor occupancy, various signaling cascades, particularly the Janus kinase-signal transducer and activator of transcription (JAK-STAT) pathway, are activated, leading to the transcriptional regulation of numerous IFN-stimulated genes (ISG). Notably, the IFNAR/JAK/STAT1 pathway can induce a negative feedback loop through the transcription of suppressors of cytokine signaling (SOCS) which negatively regulates IFN-I signaling.[50–52]

IFN-I acts directly on immune cells, induces chemokines for immune cell recruitment, and influences cytokine secretion. Notably, IFN-I has diverse effects on various immune cell types, such as enhancing NK cell functions, affecting monocyte and macrophage function and differentiation, and exerting significant regulatory effects on DCs. IFN-I also plays a pivotal role in initiating adaptive immune responses by influencing the differentiation, maturation, and migration of APCs, thereby impacting the overall immune response against infections and

tumors. Furthermore, IFN-I demonstrates adjuvant activities on humoral immune responses, affecting B cells, $CD4^+$ T cells, and $CD8^+$ T cells, promoting antibody production, inducing differentiation of Th1-like T cells, and directly stimulating $CD8^+$ T cells for clonal expansion and memory differentiation.[50,53]

The aberrant expression of IFN-I or signatures of IFN-I-inducible genes are associated with severe autoimmune disorders.[51] Furthermore IFN-Is exert control over autocrine or paracrine circuits in cancer immunosurveillance, with their intact signaling being essential for the efficacy of various cancer treatments.[50,54] For example, mice lacking IFNAR1 show increased tumor growth in response to both syngeneic tumor cell xenografts and carcinogen-induced tumors. A similar outcome is observed when IFNAR1-neutralizing antibodies are administered and in mice with impaired functional IFNAR1.[55–58]

2.4 Regulators of the immune system: immune checkpoints

Immune checkpoints are mechanisms that regulate the immune response, preventing excessive or ill-suited activation of the immune system. By doing so, these regulatory checkpoints play a pivotal role in maintaining self-tolerance and averting the onset of autoimmunity.[59–62] The activation of immune checkpoints is initiated by specific signals from specific molecules, known as checkpoint proteins, which include cytotoxic T-lymphocyte-associated protein 4 (CTLA-4) and programmed cell death protein 1 (PD-1). Upon the binding of these checkpoint proteins to their respective ligands, they transmit signals to initiate the downregulation or inhibition of immune responses.[63]

CTLA-4, discovered in 1987, is a homolog of CD28, a T cell surface molecule that activates T cells during the priming phase by binding to B7-1 (CD80) or B7-2 (CD86) on APCs. Unlike CD28, CTLA-4 has a higher binding affinity for B7-1/2 and generates an inhibitory effect on T cells. Constitutive expression of CTLA-4 on Tregs suppresses immune responses, preventing continuous activation of T cells and maintaining self-tolerance.[63–65] CTLA-4 haploinsufficiency in humans leads to Treg dysregulation and hyperactivation of effector T cells, resulting in lymphocytic infiltrates.[61,66] In animal models, CTLA-4 knockout induces widespread organ inflammation and early mortality.[59,67,68] Conversely, excessive CTLA-4 expression by cancer cells, such as non-small cell lung cancer, nasopharyngeal carcinoma, breast cancer, or melanoma, contributes to immune evasion which promotes cancer progression. [69–73]

PD-1, discovered in 1992, is a costimulatory receptor in the B7/CD28 family, regulating T cell activation through interactions with its ligands PD-L1/B7-H1 and PD-L2/B7-H4. While PD-L1 is constitutively expressed on various immune cells, PD-L2 is inducible and limited to specific cell types. PD-1, expressed broadly in activated T cells, B cells, and monocytes, acts during

the effector phase, inhibiting TCR signaling upon coincident binding with TCR. [74] Complete PD-1 deficiency increases susceptibility to tuberculosis and other autoimmune conditions but does not result in fatal lymphocytic infiltrates. Unlike CTLA-4, PD-1 ligands are expressed in regions where tolerance induction is less critical, causing a milder immune dysregulation when deficient.[60,62,75,76] The role of PD-1 in cancer varies, with cell-intrinsic PD-1 overexpression promoting tumorigenesis in some cancers but having tumor suppressive effects in others.[77–80] PD-L1 expression in tumors is consistently associated with poor prognosis and decreased activated T cell numbers. Unlike CD80 and CD86, PD-1 ligands are not confined to lymphoid cells.[81–86]

3 Immune checkpoint inhibitor therapy

Cancer immunotherapies, including ICIs, have emerged as a revolutionary approach in the treatment of cancer, leveraging the body's own immune system to target and eliminate malignant cells. Unlike traditional treatments like chemotherapy and radiation, which directly attack cancer cells, immunotherapies focus on stimulating the patient's immune response to recognize and target tumors.[87,88] The identification and advancement of monoclonal antibodies targeting inhibitory immune checkpoints, such as CTLA-4 and PD-1, have led to remarkable antitumor responses. One significant contrast between ICI therapy and other systemic cancer treatments lies in its capacity to achieve long-lasting cancer control. These antibodies achieve this by enhancing immune activation at different stages of the immune cycle. Currently, ICI therapies find broad applicability across various types of cancer.[13,89,90]

3.1 Anti-CTLA-4 therapy

In mouse models, anti-CTLA-4 has been shown to significantly increase the antitumor immune response to immunogenic tumors, either alone or in combination with tumor cell vaccines. The anti-CTLA-4 blockade leads to the proliferation and prolonged activation of T cells.[91–94]
Ipilimumab, the first CTLA-4 targeting ICI, was approved in 2011 by the FDA for the treatment of metastatic melanoma after demonstrating a proven benefit in the OS in a randomized phase III clinical trial.[95,96] The long-term clinical response is of special interest because ipilimumab was the first medication to show a durable clinical response in 25% of the patients. However, only a small percentage of patients showed a durable response with 4 doses of 3 mg/kg, while the majority of patients did not benefit from anti-CTLA-4 monotherapy.[96,97] In melanoma

patients, the 3-year OS rate is 34%, and the 5-year OS rate is 26% for patients treated with ipilimumab.[13,89] At present, the decision to use anti-CTLA-4 therapy is primarily based on the clinical condition of the patient and the judgment of the treating oncologist. Biomarker testing may be considered in some cases to provide additional information, but it is not yet a routine practice for all patients. Biomarkers for the response to anti-CTLA-4 can be the inducible costimulatory molecule (ICOS) which is expressed on activated Th1-like CD4 T cells, the tumor mutational burden (TMB) or the abundance of specific immune cell subsets and cytokines.[98,99]

3.2 Anti-PD-1 therapy

In 2014, the first human PD-1 ICI, nivolumab, was approved by the FDA for patients with advanced melanoma.[100] Studies demonstrated that anti-PD-1 monotherapy similarly to anti-CTLA-4 monotherapy significantly extended OS and increased objective response rates.[101] But, compared to anti-CTLA-4 therapy, anti-PD-1 therapy exhibited higher effectiveness in various advanced cancers, with a durable clinical response of 25-47%.[102] For melanoma patients, the 3-year OS rate with nivolumab reached 52%, and the 5-year OS rate was 44%.[13,89] Furthermore, the combination therapy of ipilimumab and nivolumab achieved a 5-year OS rate of 52%.[89] Similar to predictive markers for the anti-CTLA-4 response, biomarkers such as TMB and specific immune cell subsets have been analyzed and identified for anti-PD-1 therapy response.[99,103,104] Additionally, one of the most extensively studied and widely recognized biomarkers is the expression of PD-L1 on tumor cells. Some tumors with higher levels of PD-L1 expression are more likely to respond positively to anti-PD-1 therapy.[103,105]

3.3 Resistance mechanisms

It is differentiated between primary and acquired resistance to ICI therapy. Primary resistance occurs in a large proportion of melanoma patients from the very beginning of the treatment.[101,106] For treatment success the TME and its infiltration by effector T cells plays a pivotal role. Tumor cells have the ability to impair the maturation of DCs and thus their function as APCs by sustaining elevated levels of IL-6, IL-10, or the vascular endothelial growth factor within the tumor microenvironment.[107–111] Additionally, several factors secreted by tumor cells such as IL-10 and transforming growth factor (TGF)-β can guide the maturation process of DCs towards a regulatory phenotype.[112–114] Thus, effector T cells are not recruited to the TME anymore, leading to resistance to ICI. However, not only infiltration into tumors and antigen

recognition are important in anti-cancer immunity, but also activation and functionality of those T cells. T cells from the TME can present with an exhaustion phenotype and thus impaired functionality.[115–117] For example, indoleamine-2,3-dioxygenase (IDO) an enzyme that catalyzes the breakdown of tryptophan is constitutively expressed by a variety of tumors and strongly affects tumor immune resistance by inhibition of T cell proliferation and limitation of their effector functions through tryptophan shortage.[118–120] Within the TME, IDO, among other enzymes, chemokines, and cytokines, achieves immune tolerance by recruiting Tregs, myeloid-derived suppressor cells, and tumor-associated macrophages.[121–124] The JAK-STAT pathway is a central signaling cascade activated by IFN-I. Mutations or dysregulation in key components of this pathway, such as JAK1, JAK2, or STAT1, can compromise the transmission of IFN-I signals within the cell. This leads to a failure in the induction of ISGs that mediate the anti-tumor effects of IFN-I and therefore to a decreased effectiveness of the immune response.[125] Moreover, the canonical function of tyrosine-phosphorylated STAT2 mediates the antiproliferative actions of IFN-I, suggesting a tumor suppressor role, while the progesterone receptor degrades STAT2 to inhibit the IFN response in breast cancer. Unphosphorylated STAT2 exhibits noncanonical functions, promoting tumor progression by enhancing the expression of cytokines and inhibiting STING-mediated IFN-I synthesis, contributing to resistance to DNA damage in tumors.[54] Another primary resistance mechanism is a low TMB. The TMB refers to the number of genetic mutations that have accumulated within a tumor's DNA. Specifically, it counts the nonsynonymous mutations per megabase of the tumor genome, which are changes in the DNA sequence that lead to altered protein products.[126] It can provide insights into the genetic diversity and complexity of a tumor. Tumors with a higher TMB tend to have accumulated more mutations and these mutations can give rise so-called tumor-associated antigens (TAAs), that can be recognized by the immune system as foreign, potentially triggering an immune response against the tumor. Tumors with a low TMB have fewer distinctive mutations and therefore may be less likely to trigger a strong immune response. These tumors can thus evade immunosurveillance.[104,127,128] Intrinsic resistance to ICI therapy can also be mediated by the gut microbiome as well as the tumor microbiome as the microbial composition of the gut and tumor have been observed to differ between patients responding and not responding to ICIs.[129–131]

In contrast to the primary resistance acquired resistance emerges after an initial phase of clinical response to treatment following tumor progression. Subpopulations of tumor cells that develop new genetic and epigenetic traits and undergo selection due to treatment can evade immune surveillance. Examples are the loss of beta-2-microglobulin leading to a subsequent loss of MHC-I expression and the mutation of JAK1/2 that confers resistance to immunotherapy by disrupting the IFN-γ-induced cell growth arrest and the JAK/STAT pathway, including diminished IFN-I signaling, promoting survival and progression of resistant cells.[125,132–135]

Acquired resistance can stem from individual cells adapting their gene expression in response to immune signals, such as upregulating PD-L1 due to immune cytokines like IFN-γ.[136] Additionally, chronic exposure to low doses of IFN-I, observed in cancer cells exposed to repeated or prolonged therapy, contributes to resistance to DNA damage and therefore contributing to acquired resistance.[54] Moreover, several negative regulators exist to modulate the intensity and duration of IFN-I signaling to prevent excessive inflammation. However, the production these negative regulators, such as RIG-I inhibitors or SOCS, can increase over time to attenuate anti-tumor effects of IFN-I.[54,135] These observations highlight the ambiguous role of IFN-I in cancer therapy, where the strength and duration of IFN-I stimulation determine whether it exerts cytotoxic effects in tumors or promotes survival.

3.5 Immune-related adverse events

ICI therapy can lead to a range of side effects, known as immune-related adverse events (irAEs), due to the immune system's increased activity. Common side effects include fatigue, skin rash, diarrhea, colitis, thyroid dysfunction, and liver inflammation.[137] More severe irAEs can affect vital organs and systems, such as the lungs, heart, and endocrine glands.[137] It is important to note that while ICIs have shown great promise in cancer treatment, close monitoring and management of potential side effects are essential to ensure patient safety and optimize treatment outcomes. Around 30% of patients treated with ipilimumab, approximately 15% of those treated with nivolumab, and about 40% of those receiving a combination of present with gastrointestinal irAEs.[106,138–140] Because of their distinct mechanisms, the toxicities linked to anti-CTLA-4 and anti-PD-1 therapies vary slightly, with symptoms from anti-CTLA-4 antibodies often being more severe. Ipilimumab is predominantly associated with a higher incidence of colitis and hypophysitis, while nivolumab and pembrolizumab are more frequently linked to pneumonitis and thyroiditis.[106,139,141,142] The side effects of ICIs are largely manageable and responsive to treatment.[137] Nevertheless, minimizing their occurrence undoubtedly enhances the overall well-being of patients, without posing an increased risk of more severe or life-threatening irEAs. Overcoming these side effects might play an even more significant role for patients who suffer from autoimmune diseases prior to therapy.[143] Further, the composition of the gut microbiome may serve as an indicator to predict whether patients are prone to experiencing colitis or not, and given that the microbiome can be modulated, it might serve as an adjustable element to address and mitigate this concern.[129,131,144]

4. The gut microbiome

All host-associated microorganisms are acquired through vertical transmission following birth and subsequently adapt changes through continuous exposure to the environment throughout their entire lifespan. Gut microbiota, alternatively referred to as the gut microbiome, consist of a diverse array of microorganisms, including bacteria, archaea, fungi, and viruses, that inhabit the digestive tract. The quantity of microbial cells present within the gut lumen is approximately tenfold greater than the count of eukaryotic cells within the human body.[145] The human gut microbiome is increasingly recognized as a significant regulator in human physiology.[145,146] It demonstrates substantial diversity, even among healthy individuals.[147,148] The human gut can undergo modifications influenced by factors such as age and environmental conditions, including dietary habits and nutrition.[145,149] Interestingly, the gut microbiome can serve as an indicator of health status, and an imbalance or disruption in the composition and function of the microbial communities – referred to as dysbiosis – can significantly impact the success of cancer immunotherapy treatment.[149]

4.1 Significance and features of the gut microbiome

In essence, the gut microbiome is an intricately connected ecosystem that influences a wide range of physiological processes, contributing to overall health and disease susceptibility.[150] Microbial enzymes play a pivotal role in breaking down otherwise indigestible substances, such as plant cell walls, into smaller components that can be absorbed by the body. Dietary fibers, found in fruits, vegetables, and whole grains, are composed of complex carbohydrates that human digestive enzymes cannot break down. However, the gut microbiome possesses enzymes that can degrade these fibers through fermentation.[150] As a result, short-chain fatty acids (SCFAs) like acetate, propionate, and butyrate are produced that provide an additional energy source.[151] Furthermore, microbes can convert insoluble forms of minerals like iron, zinc, and magnesium into more soluble and absorbable forms.[152] These processes enhance the bioavailability of nutrients, such as vitamins and minerals, which are released during microbial fermentation and subsequently absorbed by the host.[152] Moreover, the gut microbiome acts as a barrier by competing with potential pathogens for nutrients and attachment sites within the gut lining. This competitive exclusion helps prevent the colonization and overgrowth of harmful microorganisms, ultimately protecting against infections.[153,154] Notable strides in large-scale sequencing and mass spectrometry have enhanced our insights into the impact of the microbiome and its metabolites on the initiation and advancement of intestinal and extraintestinal cancers, as well as their role in shaping the effectiveness of cancer immunotherapy.[155] The impact of the gut microbiome extends to the very early stages of cancer

development, influencing the development of precancerous lesions with specific bacterial genera linked to increased risk.[155,156] Dysbiosis in the intestinal tract can lead to persistent inflammation which is a well-established risk factor for cancer.[157] In general, dietary habits play a pivotal role in shaping the gut microbiome and thus cancer risk as diets can promote the growth of certain beneficial or potentially harmful microbes.[150,158]

4.2 Mechanisms and interactions with the immune system

The interactions between the gut microbiome and the immune system are intricate and multifaceted, playing a pivotal role in upholding immune homeostasis, safeguarding against pathogens, and averting inappropriate immune responses. These interactions manifest through a range of mechanisms that collectively shape and regulate the immune system's functioning. As highlighted earlier, the gut microbiome impacts the innate immune defense by both outcompeting pathogenic bacteria and preserving the integrity of the epithelial barrier.[153,154] A robust gut barrier is crucial in preventing the migration of pathogens from the gut lumen into the bloodstream. The mucus layer enveloping the gut epithelium functions as a physical shield and hosts antimicrobial compounds.[154,159] Certain gut microbes encourage mucus production by epithelial cells, thus contributing to the maintenance of this protective layer.[160–162] Moreover, mucosal immunity finds its footing in structures like the gut-associated lymphoid tissue (GALT), which houses a variety of immune cells. These specialized lymphoid structures, such as the lamina propria, Peyer’s patches, and mesenteric lymph nodes, hold pivotal roles in pathogen recognition and the initiation of an immune responses.[163] The innate (and adaptive) immune response repertoire in the gut is expanded by the interactions of commensal derived microbe-associated molecular pattern (MAMPS) with PRRs such as TLRs and NLRs.[164] This interplay triggers the release of pro-inflammatory cytokines, such as IL-1β and IL-6 which can activate and recruit immune cells.[154,165] Such pro-inflammatory cytokines for example stimulate the differentiation of Th17 cells, which play a crucial role in defense against fungal or bacterial infections by IL-17 secretion.[166,167] Intriguingly, specific gut microbes are indispensable for the development and differentiation of immune cells. This importance becomes evident in the context of germ-free (GF) or antibiotic-treated mice, which display impaired immune cell development.[168–172] Microbial components, such as bacterial LPS and other PAMPs, can stimulate DCs and NK cells via TLRs.[173,174] Thus, immature DCs undergo a maturation process which includes the upregulation of costimulatory molecules and the secretion of cytokines and chemokines.[42,173] Consequently, these actions provide essential signals that support the development and differentiation of lymphocytes. Furthermore, NK cells releasing cytokines are important in contributing to an inflammatory environment and thus

response to infections.[47,174] Moreover, the production of IL-12 and IL-18 induced by gut microbes can implicate the activation of NK cells.[165,175] The transition from innate immunity to adaptive immunity is facilitated by the IFN-I signaling induced by microbiota.[176,177] Moreover, the gut microbiome can significantly contribute to the augmentation of IFN-I signaling. The bacterial-derived metabolite DAT can, through this mechanism, protect the host against viral infection.[178,179] These examples show that the commensal microbiota can influence different immune cell subsets contributing to health and that bacterial-derived metabolites might be linked to this observation.

While the gut microbiome significantly contributes to the host's defense against pathogens, it also plays a foundational role in fostering immune tolerance. The early exposure to diverse microbial communities assists in establishing immune tolerance, thereby mitigating the risk of allergies and autoimmune diseases. Tregs are crucial in maintaining tolerance, and microbial metabolites like SCFAs have been shown to support the generation and function of these cells.[180,181] Additionally, some gut microbes induce a state of tolerogenic antigen presentation by DCs. This phenomenon involves DCs presenting antigens in a manner conducive to Treg development while simultaneously suppressing the activation of pro-inflammatory T cells. The gut microbiome's ability to produce anti-inflammatory cytokines, such as IL-10 and TGF-β, serves to dampen immune cell activation and reduce inflammation, adding another layer to its immunomodulatory impact.[182,183]

4.3 The microbiome and cancer immunotherapy

4.3.1 Correlation between bacterial taxa and treatment outcomes

Over the past years 16S-rRNA sequencing of the gut microbiome revealed that specific bacterial taxa can be associated with the response to ICI therapy. Several studies assessed the microbial composition in melanoma patients that were treated with ICIs. In general, a higher alpha diversity and richness can be associated with longer progression-free survival and response to ICIs in melanoma patients but also in non-melanoma patients.[184–188] Responder to anti-CTLA-4 and anti-PD-1 treatment showed mainly enrichment in bacterial families *Ruminococcaceae*, *Tannerellaceae*, *Bacteriodaceae*, *Lachnospiraceae*, and *Bifidobacteriaceae*. Specific microbes that could be identified in these patients are *Bifidobacterium longum*, *Bifidobacterium adolescentis*, *Collinsella aerofaciens*, *Enterococcus faecium*, *Faecalibacterium prausnitzii*, *Ruminococcus gnavus*, *Bacteroides massiliensis*, *Bacteroides stercoris*, *Bacteroides thetaiotamicron*, and *Parabacteroides distasonis*.[130,184–186,189–193] On family level of non-responding patients to anti-CTLA-4 and anti-PD-1 *Lachnospiraceae*, *Bacteriodaceae*, *Enterobacteriaceae*, and *Lactobacillaceae* were found to

be enriched. Here, specific microbes that could be identified are *Ruminococcus obeum*, *Roseburia intestinalis*, *Escherichia coli*, *Anaerotruncus colihominis*, *Veillonella atypica*, *Lactobacillus gasseri* and *Klebsiella aerogans*.[130,184–186,189–193] When comparing these studies, members of the *Firmicutes* phylum, specifically *Lachnospiraceae* and *Ruminococcaceae*, were found to be more abundant in individuals who responded positively to therapy, while non-responder exhibited a greater presence of the *Bacteroidetes* phylum.[130,184–186,189–193]

Based on these findings, research is increasingly focused on therapies for disrupted microbiomes in diseases such as cancer. One approach that has been introduced is fecal microbiota transplantation (FMT), in which fecal material (stool) from a healthy donor is transplanted into the gastrointestinal tract of a recipient to treat the recipient's potential dysbiosis. FMT is associated with increased response rates in cancer treatment with ICIs in preclinical studies.[189,194–196] Clinical trials in melanoma patients have indicated that FMT from ICI responder patients can improve therapy response in immunotherapy-refractory patients.[184,190]

In recent years, probiotics have gained substantial attention in oncology. Probiotics are live microorganisms that are known for their potential to promote gut health, modulate immune responses, and alleviate treatment-related side effects in cancer therapy. Probiotics are also found in certain foods and fermented products.[197] In preclinical models, patient cohorts, and clinical trials, it has been demonstrated that defined probiotics, including *Bifidobacterium sp.*, *Bacteroides sp.*, *Akkermansia muciniphila*, and *Clostridium butyricum*, enhance response rates to ICI therapy across different types of solid cancers.[198–202] Probiotics and other commensal bacteria in the gut can be affected by prebiotics. Prebiotics are non-digestible fibers and compounds that serve as food for beneficial bacteria in the gut and thus promote the growth and activity of these bacteria.[203,204] Bacteria that benefit from prebiotic intake include *Lactobacilli* and *Bifidobacteria*.[203,204] Higher dietary fiber intake is linked to improved progression-free survival in melanoma patients undergoing ICI treatment, with corresponding results in preclinical models illustrating a compromised response to anti-PD-1 therapy in mice fed low-fiber diets or probiotics, highlighting the clinical significance for cancer patients receiving ICI treatment.[205]

4.3.2 Bacterial-derived metabolites in cancer immunotherapy

Over the last couple of years, the intricate relationship between the human microbiota and cancer has gathered significant attention, unveiling a novel avenue for exploring the therapeutic potential of bacterial metabolites in cancer treatment. The multifaceted nature of bacterial metabolites, produced by various microbial communities residing in the human body,

has sparked interest in their role as influential modulators of the tumor microenvironment and immune response. With mounting evidence suggesting their capacity to impact tumorigenesis, immune regulation, and drug efficacy, investigating the intricate mechanisms underlying the effects of bacterial metabolites on cancer immunotherapy has emerged as promising therapeutic strategy. Increasing numbers of *in vivo* studies suggest several bacterial-derived metabolites as potential cancer therapeutics.[206–210] One study identified the by *Bifidobacterium pseudolongum* produced metabolite inosine to enhance the efficacy of ICIs in murine cancer models. ICI-induced impairment of the gut barrier function results in the systemic translocation of the metabolite inosine, activating T cells dependent upon their expression of the A_{2A} receptor.[206] Another study demonstrated that the probiotic *Lactobacillus reuteri* enhances antitumor immunity and supports ICI treatment by stimulating IFN-γ production in $CD8^+$ T cells within a murine melanoma model. This effect is attributed to the secretion of indole-3-aldehyde (I3A), an aryl hydrocarbon receptor (AhR) agonist and tryptophan metabolite.[210] The anacardic acid 6-pentadecyl salicylic acid was shown to promote antitumor immunity through caspase-8-mediated apoptosis in a breast cancer model. It increases immune cell populations such as NK cells and CTLs by secretion of different cytokines.[207] One study suggests that the SCFAs pentanoate and butyrate enhance the anti-tumor activity of CTLs and CAR T cells by triggering metabolic and epigenetic reprogramming, leading to increased production of effector molecules such as CD25 and IFN-γ.[208] A prospective cohort biomarker study investigated the association between SCFAs and the efficacy of anti-PD-1 therapy in patients with solid tumors. High concentrations of certain SCFAs, particularly acetic acid, propionic acid, butyric acid, valeric acid in fecal samples, and isovaleric acid in plasma, are associated with longer progression-free survival.[209] In general, SCFAs are associated with antitumor effects.[211] But nevertheless there are studies indicating contradictory results. For example, one study found that high blood levels of butyrate and propionate are associated with resistance to anti-CTLA-4 therapy in both mice and patients.[212]

However, bacterial metabolites are still being investigated in preclinical models or cohort biomarker studies in the context of cancer rather than being tested in clinical trials. To date, the metabolite inosine was examined in a single-center, prospective, randomized Phase 2/3 clinical trial in combination with PD-1/PD-L1 for patients with advanced solid tumors (NCT05809336), although the results have not yet been published. This suggests that while some progress has been made, not all mechanisms by which bacterial metabolites operate have been thoroughly investigated, emphasizing the need for further testing and the inclusion of promising candidates in clinical trials.

Understanding the intricate interplay between gut microbiota and cancer therapy holds promise for tailoring treatment approaches, potentially paving the way for personalized interventions and improved outcomes in the realm of cancer care.

5. Aim of the study

The primary objective of this study is to comprehensively investigate the impact of bacterial-derived metabolites, specifically DAT and ICA, on the efficacy and potential side effects of immune checkpoint inhibitor therapy, particularly anti-CTLA-4 treatment. Both metabolites are naturally produced by bacterial species that are abundantly present in both mice and humans.[178,213] Given the crucial role of IFN-I in antitumor immunity, exploring bacterial-derived metabolites that can modulate this response in a favorable manner becomes intriguing. DAT is a recognized IFN modulator, associated with protection from viral infections by enhancing IFN-I signaling.[178,213] Recent research indicates bacterial-derived metabolites as the link between the gut microbiome and the response to ICI therapy.[206–210] Consequently, investigating the impact of metabolites that enhance IFN-I signaling holds particular interest in understanding their potential influence on ICI therapy outcomes and translational potential. ICA, being an indole derivative and a metabolite of tryptophan, emerges as a promising candidate among bacterial metabolites with potential positive effects on therapy. Notably, the indole derivative I3A, has recently been documented for its beneficial impact on ICI therapy.[210] This aims to develop robust therapeutic strategies and to conduct a comparative analysis of indole derivates. Unraveling the effects of both, DAT and ICA, on ICI therapy can provide deeper insights into the complex interplay between microbial metabolites, host immune responses, and cancer. Accordingly, this work aims to clarify if these two metabolites can improve the efficacy of ICI therapy and to investigate the safety of these metabolites regarding irAEs. The objective is to examine the direct effects of DAT on immune cells and on the gut microbiome to determine how DAT mediates potential antitumor effects. Furthermore, another aim is to elucidate if DAT operates in dependence of the pre-existing gut microbiome composition or can act independently. Given its role as IFN-I mediator, the importance of host cell-intrinsic IFN-I signaling in mediating the antitumor response will be investigated.

II MATERIALS AND METHODS

1. Reagents and Materials

1.1 Mouse strains

Table 1: Mouse strains

Line	Alias	Distributor	RRID
C57Bl/6j	WT	Janvier-Labs	IMSR_JAX:000664
B6(Cg)-Ifnar1$^{tm1.2Ees}$/J	*Ifnar1*$^{-/-}$	Bred in house	IMSR_JAX:028288

1.2 Cell lines

Table 2: Cell lines

Line	Description	Background	RRID	Source
B16.OVA	Melanoma	C57Bl/6	CVCL_WM78	Marcel R.M. van den Brink (MSKI, USA)
Panc02	Pancreatic adenocarcinoma	C57Bl/6	CVCL_D627	Marcel R.M. van den Brink (MSKI, USA)

1.3 Reagents

1.3.1 Reagents, chemicals, and buffers

Table 3: Reagents, chemicals, and buffers

Product	Company
2-Mercaptoethanol (50 mM)	Thermo Fisher Scientific, Waltham, USA
2-Propanol	Carl Roth, Karlsruhe, Germany
Aqua	Braun, Melsungen, Germany
Bovine Serum Albumin Powder (≥96%)	Sigma-Aldrich, Taufkirchen, Germany
Collagenase II	Worthington, Lakewood, NJ, USA
DNAse I	Sigma-Aldrich, Taufkirchen, Germany
Ethanol	Merck Millipore, Darmstadt, Germany
Formalin solution, neutral buffered (10%)	Sigma-Aldrich, Taufkirchen, Germany
In vivo-jetPEI	Polyplus, Illkirch-Graffenstaden, France
Isoflurane CP	CP Pharma, Burgdorf, Germany
Ovalbumin (≥98%)	Sigma-Aldrich, Taufkrichen, Germany
Percoll	Sigma-Aldrich, Taufkrichen, Germany
Trypan Blue Stain (0.4%)	Gibco, Fisher Scientific, Waltham, USA
Tween 20	Sigma-Aldrich, Taufkrichen, Germany

1.3.2 Cell culture media and reagents

Table 4: Cell culture media and reagents

Product	Company
0.05% Trypsin-EDTA (1x)	Gibco, Fisher Scientific, Waltham, USA
Advanced DMEM/F-12	Gibco, Fisher Scientific, Waltham, USA
B27 Supplement (50x)	Gibco, Fisher Scientific, Waltham, USA
Cell Stimulation Cocktail (plus protein transport inhibitors)	eBioscience, Fisher Scientific, Waltham, USA
DMEM - high glucose	Sigma-Aldrich, Taufkirchen, Germany
Dulbecco's Phosphate Buffered Saline	Sigma-Aldrich, Taufkirchen, Germany
DMSO	Sigma-Aldrich, Taufkrichen, Germany
EDTA (0.5 M)	Invitrogen, Fisher Scientific, Waltham, USA
FBS Good Forte (VLE)	PAN Biotech, Aidenbach, Germany
HEPES Buffer Solution (1 M)	Gibco, Fisher Scientific, Waltham, USA
L-glutamine (200 mM)	Gibco, Fisher Scientific, Waltham, USA
Lipofectamine 2000	Thermo Fisher Scientific, Waltham, USA
mEGF (50 µg/ml)	Peprotech, Hamburg, Germany
mNoggin (11 µg/ml)	Peprotech, Hamburg, Germany
N2 Supplement (100x)	Gibco, Fisher Scientific, Waltham, USA
N-acetyl cysteine (500mM)	Sigma-Aldrich, Taufkirchen, Germany
NEM-NEAA (100x)	Gibco, Fisher Scientific, Waltham, USA
Opti-MEM (1x)	Gibco, Fisher Scientific, Waltham, USA
PEG 300	Sigma-Aldrich, Taufkirchen, Germany
Penicillin/Streptomycin (10000 U/ml)	Gibco, Fisher Scientific, Waltham, USA
RBC Lysis Buffer (1x)	Invitrogen, Fisher Scientific, Waltham, USA
Recombinant Murine GM-CSF	Peprotech, Hamburg, Germany
RPMI-1640	Sigma-Aldrich, Taufkirchen, Germany
Sodium hydroxide	VWR International, Darmstadt, Germany
Sodium Pyruvate 100 (mM)	Gibco, Fisher Scientific, Waltham, USA
VLE RPMI	Bio&SELL, Feucht, Nürnberg

Table 5: Cell culture media

complete DMEM	**complete RPMI**	**T cell media**	**BMDC media**
in DMEM high glucose	in RMPI-1640	in complete RPMI-1640	in VLE-RPMI
10% FBS	10% FBS	1 mM HEPES	10% FBS
3 mM L-glutamine	3 mM L-glutamine	1x non-essential amino acids	3 mM L-glutamine
100 U/ml penicillin	100 U/ml penicillin	1 mM sodium pyruvate	100 U/ml penicillin
100 µg/ml streptomycin	100 µg/ml streptomycin		100 µg/ml streptomycin
	50 µM β-mercaptoethanol		20 ng/ml GM-CSF

Table 6: Organoid media

complete DMEM/F-12	**Rspondin conditioned media**	**ENR**
in advanced DMEM/F-12	in DMEM high glucose	in advanced complete DMEM/F-12
100 U/ml penicillin	10% FBS	1.25 mM N-acetyl-cystein
100 µg/ml streptomycin	100 U/ml penicillin	1x N2 Supplement
1 mM HEPES	100 µg/ml streptomycin	1x B27 Supplement
1x Glutamax	Conditioned with 293T-HA-Rspol-Fc cells for 7 days	10% Rspondin conditioned media
		50 ng/ml mEGF
		100 ng/ml mNoggin

1.3.3 Drinking water and gavage reagents

Table 7: Drinking water and gavage reagents

Product	**Company**
3-(4-Hydroxyphenyl)propionic acid	Sigma-Aldrich, Taufkirchen, Germany
Amphotericin B, dissolved	Merck Millipore, Darmstadt, Germany
Ampicillin sodium salt	Carl Roth, Karlsruhe, Germany
Aspartame	Fragon, Glinde, Germany
Indole-3-carboxaldehyd	Sigma-Aldrich, Taufkirchen, Germany
Metronidazole	Thermo Fisher Scientific, Waltham, USA
Neomycin	Carl Roth, Karlsruhe, Germany
Vancomycin-Hydrochloride	Thermo Fisher Scientific, Waltham, USA

1.4 Kits

Table 8: Kits

Product	Company
Foxp3/Transcription Factor Staining Buffer Set	eBioscience, Thermo Fisher, Waltham, USA
MEGAshortscript T7 Transcritption Kit	Thermo Fisher, Waltham, USA
Pan T Cell Isolation Kit II	Miltenyi, Bergisch Gladbach, Germany

1.5 Antibodies

1.5.1 *In vivo* antibodies

Table 9: *In vivo* antibodies

Antibody	Clone	Isotype	Company
InVivoMAb anti-mouse NK1.1	PK136	Mouse IgG2a, κ	Bio X Cell, Lebanon, USA
InVivoMAb anti-mouse CD8a	YTS169.4	Rat IgG2b, κ	Bio X Cell, Lebanon, USA
InVivoMAb anti-mouse CD4	GK1.5	Rat IgG2b, κ	Bio X Cell, Lebanon, USA
InVivoMAb anti-mouse CTLA-4	9H10	Syrian hamster IgG	Bio X Cell, Lebanon, USA
InVivoMAb anti-mouse PD-1	RMP1-14	Rat IgG2a, κ	Bio X Cell, Lebanon, USA
InVivoMAb polyclonal Syrian hamster IgG	Polyclonal	Syrian hamster IgG	Bio X Cell, Lebanon, USA
InVivoMAb rat IgG2a isotype control	2A3	Rat IgG2a, κ	Bio X Cell, Lebanon, USA

1.5.2 FACS antibodies

Table 10: FACS antibodies

Fluorophore	Antigen	Isotype	Clone	Company
APC-Cy7	Fixable Near-IR Dead Cell Stain			Thermo Fisher Scientific, Waltham, USA
AmCyan	Fixable Viability Dye eFluor™ 506			eBioscience, Fisher Scientific, Waltham, USA
PerCP-Cy5.5	CD103	Armenian Hamster IgG	2E7	Biolegend, San Diego, USA
APC	CD11b	Rat IgG2b, κ	M1/70	Biolegend, San Diego, USA
Pacific Blue	CD11c	Armenian Hamster IgG	N418	Biolegend, San Diego, USA

Fluorophore	Antigen	Isotype	Clone	Company
FITC	CD11c	Armenian Hamster IgG	N418	Biolegend, San Diego, USA
APC-Cy7	CD25	Rat IgG1, κ	PC61.5	eBioscience, Fisher Scientific, Waltham, USA
FITC	CD3	Rat IgG2b, κ	17A2	Biolegend, San Diego, USA
Pacific Blue	CD4	Rat IgG2b, κ	GK1.5	Biolegend, San Diego, USA
PerCP-Cy5	CD4	Rat IgG2b, κ	GK1.5	Biolegend, San Diego, USA
PE-Cy7	CD4	Rat IgG2b, κ	GK1.5	Biolegend, San Diego, USA
Pacific Blue	CD44	Rat IgG2b, κ	30-F11	eBioscience, Fisher Scientific, Waltham, USA
APC-Cy7	CD45.2	Mouse IgG2a, κ	104	Biolegend, San Diego, USA
PE	CD62L	Rat IgG2a, κ	MEL-14	eBioscience, Fisher Scientific, Waltham, USA
PerCP	CD69	Armenian Hamster IgG	H1.2F3	Biolegend, San Diego, USA
PerCP-Cy5.5	CD8	Rat IgG2a, κ	53-6.7	Biolegend, San Diego, USA
APC	CD8	Rat IgG2a, κ	53-6.7	Biolegend, San Diego, USA
Pacific Blue	CD80	Armenian Hamster IgG	16-10A1	Biolegend, San Diego, USA
PE	CD86	Rat IgG2a, κ	GL1	eBioscience, Fisher Scientific, Waltham, USA
APC (AF647)	FoxP3	Rat IgG2a, κ	FJK-16s	eBioscience, Fisher Scientific, Waltham, USA
PE-Cy7	IFN-γ	Rat IgG1, κ	XMG1.2	Biolegend, San Diego, USA
FITC	MHC-II (I-A/I-E)	Rat IgG2b, κ	M5/114.15.2	Biolegend, San Diego, USA
APC	MHC-II (I-A/I-E)	Rat IgG2b, κ	M5/114.15.2	Biolegend, San Diego, USA
APC	NK1.1	Mouse IgG2a, κ	PK136	Biolegend, San Diego, USA
PE	T-bet	recombinant human IgG1	REA102	Miltenyi, Bergisch Gladbach, Germany

1.6 Materials

Table 11: Consumables

Product	**Company**
100 Sterican Gr. 17 needle	Braun, Melsungen, Germany
50 ml, 15 ml tubes cellstar	Greiner bio-one, Kremsmünster, Austria
BD GazPak EZ Anaerobe gas generating pouch system with indicator	Becton, Dickinson and Company, Dublin, Ireland
BD Plastipak syringes Sub-Q 26 G or 27 G	BD Biosciences, New Jersey, USA
Cellstar pipettes (5 ml, 10 ml, 25 ml, 50 ml	Greiner bio-one, Kremsmünster, Austria
Counting Chamber BLAURAND	Brand, Wertheim, Germany
CryoPure tube 1.6ml	Sarstedt, Nümbrecht, Germany
ELISA plate 96-well	Fisher Scientific, Waltham, USA
Falcon Cell Strainers	Fisher Scientific, Waltham, USA
Feather disposable scalpel	pfm medical, Köln, Germany
Glass bottles	Schott, Duran, Deutschland
Glass bulbs	Schott, Duran, Deutschland
magnetic stirring cylinders	Labsolute, Th. Geyer, Renningen, Germany
Micro Sample Tube K3 EDTA	Sarstedt, Nümbrecht, Germany
Micro test plates u-bottom, 96-well	Hartenstein, Würzburg, Germany
Millex Filter unit 100 µm	Merck Millipore, Darmstadt Germany
Millex-GV 0.22 µm syringe filter	Merck Millipore, Darmstadt Germany
Omnifix-F 1ml syringe	Braun, Melsungen, Germany
pH indicator strips, pH 0–14	Merck Millipore, Darmstadt Germany
Pipette tips	Sarstedt, Nümbrecht, Germany
Plate Safe Sealers	Biozol, Eching, Germany
Reusable animal feeding needle 7912	Fisher Scientific, Waltham, USA
SafeSeal Reaction Tubes (0.5-2.0 ml)	Sarstedt, Nümbrecht, Germany
Schaedler Blood Agar Plates PB5034A	Fisher Scientific, Waltham, USA
Supra blood lancets	Megro, Wesel, Deutschland
Syringe Injekt	Braun, Melsungen, Germany
Tissue culture flasks 25-150 cm^2	TPP, Trasadingen, Switzerland
Tissue Culture Test Plates (different sizes)	TPP, Trasadingen, Switzerland
Tubes for flow cytometry, 5 ml	Sarstedt, Nümbrecht, Germany

1.7 Software

Table 12: Software

Software	**Company**
FACSDiva	BD Biosciences, Heidelberg, Germany
FlowJo V10.9.0	Tree Star Inc., Ashland, USA
GloMax Discover 3.0.0	Promega, Walldorf, Germany
GraphPad Prism	GraphPad Software, Boston, USA
Inkscape V1.3	GitLab, open source
Mendeley	Elsevier Inc., New York, USA
Microsoft office 365	Microsoft, Redmond, USA
R and R Studio	Gnu project

1.8 Devices

Table 13: Technical equipment and devices

Device	**Company**
120 mm forceps	Lab logistics group, Meckenheim, Deutschland
160 mm, 130 mm surgical scissors	Lab logistics group, Meckenheim, Deutschland
3-1810 mini centrifuge	neoLab Migge, Heidelberg, Germany
Accu jet pro	Brand, Wertheim, Germany
Axiovert 40C Microscope	Zeiss, Aalen, Germany
BD FACSAria III	BD Biosciences, New Jersey, USA
BD FACSCanto II	BD Biosciences, New Jersey, USA
Cat RM5 roller mixer	CAT, Ballrechten-Dottingen, Germany
Centrifuge 5810R with rotor A-4-81	Eppendorf, Hamburg, Germany
CO_2 incubator model CB	Binder, Tuttlingen, Germany
Envair eco safe comfort hood	Envair Technology, Heywood, UK
Freezer (-20 °C)	Liebherr, Biberach an der Riß, Germany
Freezer (-80 °C)	Binder, Tuttlingen, Germany
GloMax Discover	Promega, Walldorf, Germany
LLG thermometer compact	Lab logistics group, Meckenheim, Deutschland
LLG-uniVACUUSYS	Lab logistics group, Meckenheim, Deutschland
M523i-M precision scale	VWR International, Darmstadt, Germany
Magnetic stirring plates RT5	IKA-Werke, Staufen, Germany
Pipets: Discovery, Comfort, variable volumes	HTL Lab Solutions, Warsaw, Poland
Refrigerators (4 °C)	Siemens, Munich, Germany
Tabletop centrifuge 5417R	Eppendorf, Hamburg, Germany
Thermomixer compact	Eppendorf, Hamburg, Germany
Vacusafe Comfort with Vacuboy	Integra, Biebertal, Germany
Vortex-Genie2 vortexer	Scientific Industries, New York, USA
Water bath WTB	Memmert, Schwabach, Germany

2. Methods

2.1 *In vitro* experiments

2.1.1 Cell lines and culture conditions

The full-length chicken ovalbumin expressing B16 murine melanoma cell line (here referred to as B16.OVA) was cultured in complete DMEM medium. Panc02 cells were cultured in complete RPMI medium. Cells were cultured at 37°C and 5% CO_2. All *in vitro* assays and reagents were performed using sterile techniques and under a laminar flow hood. Tumor cells were regularly passaged to new culture flasks by aspirating the culture medium, rinsing the adherent cells with PBS, and subsequently detaching them with 1% trypsin-EDTA solution at RT for 1 to 5 min. Inactivation of trypsin was achieved by adding the respective serum-containing complete medium, followed by reseeding the cells in a 1:20 ratio after a single washing step with complete medium. For viability and cell number determination *in vitro* and *in vivo* assays, cells were subjected to trypan blue exclusion using a Neubauer hemocytometer. The characteristic of dying cells is a decreased membrane integrity, which allows the absorption of the dye. In contrast, living cells are impermeable to trypan blue, thereby facilitating the exclusion of dead cells from observation under the light microscope due to the distinctive blue intracellular staining. The density per ml of a single-cell suspension was calculated with the following formula: $\text{cells (per ml)} = \text{mean cell count} \times \text{dilution factor} \times 10^5$. Cell density, signs of cell death, and microbial contaminations were periodically monitored using light microscopy. The cells were expanded from a mycoplasma-free and tested master stock. Vials with early passage numbers were stored in liquid nitrogen. To freeze the cells, the trypsinized cells, which were suspended in complete medium to halt the enzyme activity, were centrifuged at 400xg for 5 minutes at 4 °C. Subsequently, they were resuspended in FBS with 10% DMSO at a density of $4x10^6$ cells/ml. The cells were transferred into cryo vials and placed in a freezing container ensuring a cooling rate of 1 °C/min in a -80 °C freezer. After 24 hours, the vials were transferred to a liquid nitrogen tank. The cells were thawed quickly by transferring them to a 37°C water bath, followed by the addition of 9 ml of pre-warmed complete medium for each 1 ml of cell suspension in freezing medium. The cell suspension was then centrifuged at 400xg for 5 min at 4 °C. Subsequently, the cells were resuspended in pre-warmed complete medium and transferred into a cell culture flask. The cells used for the experiments were at early passages 5-10. Prior to *in vivo* experiments, the cells were thawed one week in advance and passaged three times to ensure optimal viability and consistency. The cells were routinely tested for mycoplasma and have been validated using STR analysis with 18 STR markers.

2.1.2 Stimulation of BMDCs

For stimulation of BMDCs with DAT $5x10^5$ BMDCs/ml (see 2.3.2) were seeded in BMDC medium in 48-well cell culture treated flat-bottom plates. All cells were treated with 100 ng/ml LPS or the vehicle (PBS). In addition, DAT was added at concentrations of 100 µM or 1 mM or cells were left untreated. After 24 h of incubation at 37 °C and 5% CO_2 cells were harvested and stained for subsequent flow cytometry analysis.

2.1.3 Stimulation of T cells

For stimulation of T cells with DAT $5x10^5$ panT cells/ml (see 2.3.3) were seeded in a 48-well cell culture treated flat-bottom well in T cell media and supplemented with 30 IU IL-2 and 5 µl of Dynabeads™ Mouse T-Activator CD3/CD28 beads per well or 30 IU IL-2. DAT (neutralized solution) was added at concentrations of 100 µM or 1 mM or cells were not treated. After 24 h of incubation at 37 °C and 5% CO_2 cells were harvested and stained for subsequent flow cytometry analysis.

2.2 *In vivo* experiments

2.2.1 Animals

C57Bl/6j mice were acquired from Janvier-Labs and are herein referred to as WT mice. Mice lacking the interferon-α receptor 1 (B6(Cg)-Ifnar1tm1.2Ees/J; referred to as *Ifnar1*$^{-/-}$) have been previously characterized and were selectively bred in the animal facility at the University Hospital Regensburg.[214] For ease of husbandry, female mice were predominantly procured for most experiments. Nevertheless, male mice from the KO strain, bred in-house, were also utilized. No significant disparities in tumor growth were observed between male and female mice. At the onset of experiments, mice ranged between 6 and 10 weeks of age and were housed under specific pathogen-free (SPF) conditions in a controlled environment. The housing conditions included a 12-hour light-dark cycle (12 h light/12 h darkness), a constant temperature of 24 °C, and a humidity level maintained between 55% and 65%. *Ad libitum* access to autoclaved standard laboratory chow and water, including any special treatments, was ensured throughout. To enhance their welfare, environmental enrichment such as nesting material, houses, and chew toys was provided. Animals were acclimated in the facility where the experiments occurred for a minimum of one week before initiating any experiments. All animal studies were approved by the local regulatory agency (Regierung von Oberbayern, Munich, Germany, TV 55.2-2532.Vet_02-19-159).

2.2.2 Tumor growth dynamics and survival

To assess the treatment effect, measure the tumor volume over time, and determine the continuous survival a syngeneic tumor model with B16.OVA cells was established. 2.4 x 10^5 tumor cells in 60 µl PBS were injected subcutaneously (s.c.) into the right flank of the animals. For some experiments the Panc02 pancreatic adenocarcinoma cell line was used and 1.5 x 10^6 cells were injected s.c. into the right flank of the animal. For easier measurement of the tumor volume the mice were shaved at the injection side one day prior to the tumor inoculation. The immune checkpoint therapy when tumors of palpable size had formed with an average volume of 50 mm^2 to 75 mm^2. Tumor dimensions (length and width) were measured daily with a Vernier caliper, and their volumes were calculated using an ellipsoid volume formula: $\text{volume}\ (\text{mm}^3) = \frac{\pi}{6} \times \left(\frac{(\text{length} \times \text{width})}{2}\right)^3$. Immune checkpoint inhibitors of CTLA-4 or PD-1 were injected intraperitoneally (i.p.) in 200 µl PBS on days 7 (200 µl), 10 (100 µl), and 13 (100 µl) in the B16.OVA model. As Panc02 cells led to palpable tumors of sufficient size earlier than B16.OVA tumor cell inoculation the treatment with checkpoint inhibitors was conducted on days 4, 7, and 10. The standard DAT treatment was started on the day of tumor cell injection with 100 mM DAT in the drinking water and continued until the end of the experiment. For the 'late' DAT treatment group, drinking water containing 100 mM DAT was provided starting from day 5 after tumor cell injection and continued until the end of the experiment. In the gavage treatment groups, mice received 100 µM DAT in 200 µl of 5% EtOH and water or 100 µM ICA in 20% DMSO and 40% PEG in water once per day via gavage, starting from the day of tumor cell injection and continuing until the end of the experiment. To analyze tumor antigen-specific T cells in the B16.OVA model blood was collected from the vena facialis on day 15 and directly transferred to a EDTA Microvette tube.

2.2.2.1 Supplementation with broad-spectrum antibiotics

For some experiments, WT animals with B16.OVA tumors received broad-spectrum antibiotics (Abx) to deplete most of the gut microbiota. The administration of Abx was conducted via the drinking water, containing 1 mg/ml ampicillin, 1 mg/ml neomycin, 0.5 mg/ml vancomycin, 1 mg/ml metronidazole, 0.01 mg/ml amphotericin B, and 2.5 mg/ml aspartame, starting 5 days prior to the tumor cell inoculation, and continuing until day 20. In some groups, Abx and DAT were combined in one drinking water bottle from the day of tumor cell inoculation. The amount of water intake by the mice was tested and observed to assure that the mice do not suffer from dehydration and take up enough of the treatment mixture.

2.2.2.2 Depletion of immune cell subsets

To investigate the growth dynamics of B16.OVA tumors in dependence on DAT and different immune cell subsets, WT mice were injected with depletion antibodies. 250 µg depletion antibodies for either CD4, CD8, or NK cells were injected i.p. 5 and 2 days prior to the tumor cell injection. One day prior to the tumor challenge, blood was collected from the vena facialis to confirm the depletion of the respective immune cell subset. After that the injections of the antibodies were scheduled every 7 days with a dose of 125 µg and the depletion was confirmed again two weeks later. Mice were treated with DAT in the drinking water from the day of tumor cell inoculation with B16.OVA cells.

2.2.3 Vaccination and lung pseudo-metastases

A vaccine was prepared by mixing 10 µg 3pRNA with 3.5 µl in vivo-jetPEI and 50 µg ovalbumin protein in 5% Glucose at a total volume of 20 µl. 3pRNA was generated as described earlier.[215] The mixture was pre-incubated for 15 min before injection. WT Mice were injected s.c. into the upper thigh with the vaccine or the vehicle control that contained in vivo-jetPEI in 5% glucose. On day 7 after the vaccination, blood was collected from the vena facialis to analyze the expansion of OVA antigen-specific T cells. One week prior to the vaccination DAT administration via the drinking water was started and continued throughout the experiment. For some experiments mice were challenged with 10^6 B16.OVA cells injected s.c. into the right flank or 3 x 10^6 B16.OVA cells injected i.v. into the tail vein on day 7 after vaccination. As described before, the s.c. tumor were measured daily. On day 14, the mice were euthanized, and their lungs were subjected to intracardial injection with 20 ml of PBS before. Subsequently, superficial pulmonary pseudo-metastases of each lung were counted by eye.

2.2.4 Induction of a subclinical colitis

To provoke an anti-CTLA-4-induced colitis WT mice that were administered with DAT in the drinking water or ICA gavage and the respective controls from day 0 on were injected i.p. with anti-CTLA-4 on days 7 (200 µg), 10 (100 µg), and 13 (100 µg). Mice were sacrificed for subsequent analysis of the small intestine and colon using an organoid assay, a neutrophil-granulocyte influx assay, and immunohistochemical staining on day 15.

2.2.5 Collection of stool samples for 16S-rRNA analysis

For the DAT effects on the microbiome in the steady state, WT mice were administered with DAT in the drinking water for 7 days. After 7 days fecal samples were collected and snap-frozen in 1.5 ml Eppendorf reaction tubes in liquid nitrogen before long-term storage at -80 °C. For some experiments fecal samples were collected after tumor bearing mice were treated with immune checkpoint inhibitors.

2.3 *Ex vivo* analysis and processing of murine cells

2.3.1 Isolation of tumor infiltrating leukocytes and cells from tumor-draining lymph nodes

Tumors and tumor-draining inguinal lymph nodes (tdLNs) were extracted immediately after sacrificing each mouse using surgical scissors and forceps. The second inguinal lymph node and spleen were harvested for single-stain samples for subsequent analysis. The organs were placed in ice-cold PBS in a 24-well plate until all mice were processed and all samples were handled on ice. Before submerging the tumors in PBS, the tumor weight was determined using a precision scale. Single cell suspensions were gained by mashing tumors or tdLNs with 20 ml of cold PBS through 100 µm and 70 µm nylon cell strainers into a 50 ml Falcon tube. The cells were pelleted by centrifugation at 400xg for 5 min at 4 °C and the supernatant was discarded. After resuspension in 600 µl of PBS, the cell suspension was equally divided into three parts, each transferred into a separate 96-well round-bottom plate and kept on ice. Alternatively, the cells were incubated in 200 µl of T cell media with 1x Cell Stimulation Cocktail (plus protein transport inhibitors) per well if IFN-γ was to be stained for 3 hours with a subsequent PBS washing step before subsequent analysis.

2.3.2 Isolation of BMDCs

To generate BMDCs, bone marrow from C57BL/6 mice was isolated from the tibia and femur of both hind legs. The bones were disinfected with 80% EtOH and equilibrated in BMDC media under sterile conditions. After cutting the epiphysis off each end with surgical scissors, the bones were flushed with BMDC medium using a syringe with a needle and filtered through a 100 µm nylon cell strainer. Cells were then pelleted at 400xg for 5 min at 4 °C, and the supernatant was discarded. The cell pellet was resuspended in 2 ml of red blood cell lysis buffer to remove erythrocytes and incubated for 5 min at RT. The enzymatic reaction was stopped by adding 20 ml of BMDC medium. After another centrifugation step at 400xg for 5 min

at 4 °C, the cells were seeded in non-cell culture-treated 10 cm bacterial dishes in 10 ml BMDC medium at a density of $5x10^5$ cells/ml. The cells were cultured at 37 °C and 5% CO_2 for 7 to 10 days. On day 3 of culture 10 ml of fresh medium was added and on day 6 10 ml of the medium from each dish was collected and centrifuged at 400xg for 5 min at RT and the cells were resuspended in 10 ml fresh medium and put back into the cell culture dish. Cells were harvested between day 7 and 10 of culture by flushing the plate with a serological pipette to also collect loosely adherent cells.

2.3.3 Isolation of splenic T cell populations

cells were extracted from C57Bl6/J mouse spleens. The spleen was minced through a 100 µm nylon cell strainer using ice-cold PBS and then subjected to centrifugation (all centrifugation steps for 5 min, 4 °C, 400xg). All subsequent steps were carried out with pre-cooled reagents and on ice. Following the removal of the supernatant, cells underwent a 2 min incubation in 2 ml of red blood cell (RBC) lysis buffer per spleen, with the subsequent addition of 15 ml of PBS. The mixture was filtered through a 70 µm strainer and then centrifuged again. The resulting cell pellet was resuspended in 10 ml of PBS, filtered through a 40 µm nylon cell strainer, and centrifuged. The supernatant was discarded, and the T cells were isolated using the Pan T Cell Isolation Kit II for mice, following the manufacturer's protocol. In brief, cells were resuspended in 40 µl of MACS buffer per 10^7 total cells and 10 µl of a Biotin-Antibody Cocktail per 10^7 total cells were added. After a 5 min incubation time in the refrigerator 30 µl of buffer per 10^7 total cells were added as well as 20 µl of anti-Biotin MicroBeads per 10^7 total cells following a 10 min incubation time in the 4 °C dark refrigerator. The LS column was prepared by rinsing with 3 ml of MACS buffer. The cell suspension was applied onto the column and the flow through containing the desired cell population was collected as was the flow through after washing the column with additional 3 ml of buffer. Cells were centrifuged and subsequently washed with PBS before seeding.

2.3.4 Neutrophil granulocyte influx

The neutrophil granulocyte influx was used as a surrogate marker for the degree of intestinal inflammation.[216] The distal third of the small intestine was removed using surgical scissors and forceps. The intestine was flushed with cold PBS and opened using an artery scissor with a ball tip. The opened intestine was cut into 1 cm pieces using a scalpel and the pieces were washed with cold PBS until the supernatant was clear. The intestinal pieces were then incubated in PBS containing 10% FBS and 0.1 mM EDTA in Erlenmeyer pistons on a shaker (225 rpm) for 20 min at 37°C. Afterwards the tissue pieces were washed and filtered through

a 100 µm nylon cell strainer. Next, the intestinal pieces were incubated in 20 ml complete RPMI supplemented with 200 U/ml collagenase II and 0.05 mg/ml DNAse for 60 min in Erlenmeyer pistons on a shaker (225 rpm) at 37°C until the pieces dissolved. Then, the solution was filtered through a 100 µm nylon cell strainer and 20 ml of PBS were used to flush the strainer. The cell suspension was centrifuged at 400xg for 5 min at RT. The pellet was resuspended in 4 ml of 80% Percoll and transferred into a 15 ml falcon. Next, 4 ml of 40% Percoll and on top of that 3 ml of 20% Percoll were added carefully. The Percoll gradient was centrifuged at 3000 rpm for 30 min at RT without brakes. Cells from the interphase between 80% and 40% were collected and transferred to a clean 15 ml Falcon tube. 14 ml of PBS were added, and the suspension was centrifuged at 400xg for 5 min at 4°C. Afterwards cells were transferred into 96-well round-bottom plates for subsequent analysis.

2.3.5 Organoid preparation

The whole small intestine (duodenum - ileum) was extracted using surgical scissors and forceps and flushed with cold PBS. Then the intestine was opened using an artery scissor with a ball tip and cleaned carefully with a microscopy slide before transferring it into cold PBS and vortexing for 5 sec. The intestine was cut into 1 cm pieces using a scalpel and the pieces were washed with cold PBS until the supernatant was clear. The samples were washed once with PBS containing 10 mM EDTA and were then incubated with PBS containing 10 mM EDTA for 30 min at 100 rpm at 4°C. After a washing step with PBS, 20 ml of PBS were added, and the tubes were shaken firmly to detach the crypts. Everything was filtered through a 100 µm nylon cell strainer and flushed additionally with 10 ml of PBS. The filtering process was repeated once again. After centrifuging the samples at 250xg for 5 min at 4°C the supernatant was discarded, and the pellet was resuspended in 10 ml of cold PBS. Two 10 µl drops per sample were pipetted onto a microscopy slide, and the crypts were counted to calculate the mean crypts per ml. Material for 200 crypts per sample was transferred into a 1.5 ml Eppendorf reaction tube and centrifuged at 250xg for 5 min at 4°C to remove the PBS. A mixture of 20 µl of ice-cold Matrigel and 10 µl of ice-cold PBS was used to resuspend the 200 crypts per sample. The Matrigel drops containing the crypts were pipetted onto a 24-well flat-bottom plate and 600 µl of ENR medium were added after the Matrigel drop solidified at 37 °C. After 3 days the organoids per drop were counted under a microscope.

2.3.6 Processing of blood samples

Blood samples were processed further for subsequent flow cytometric analysis. Each sample (approximately 50 µl) was transferred into a 96-well round-bottom plate and diluted with 100

µl of PBS. The plate was then centrifuged at 400xg for 5 min at RT, and the supernatant containing serum was discarded. The cell pellet, comprising red and white blood cells, was resuspended in 100 µl of red blood cell lysis buffer and incubated for 5 min at RT. After the incubation, 100 µl of PBS was added to each sample, and the samples were centrifuged at 400xg for 5 min at RT. The process of red blood cell lysis was repeated after discarding the supernatant. Following the red blood cell lysis, the samples were washed once with cold PBS.

2.4 Analytical assays and techniques

2.4.1 Flow cytometry

All flow cytometry analysis were performed using a FACSCanto II. The FACSCanto II was set up with three different lasers. A blue argon-ion laser with a wavelength of 488 nm facilitates the detection of fluorochromes fluorescein isocyanate (FITC), phycoerythrin (PE), the Cy7-coupled tandem-dye PE-Cy7, and peridinin chlorophyll protein (PerCP). The second red diode laser with a wavelength of 633 nm excites the fluorochromes allophycocyanin (APC) and the tandem-dye APC-Cy7. Additionally, the third laser, a violet diode laser with an excitation wavelength of 405 nm, excites fluorochromes Pacific Blue (PB) and Anemonia majano Cyan Fluorescent Protein (AmCyan). Emission spectra that were shared between some of the fluorophores and caused spectral overlap were compensated before acquiring the samples to minimize spillover. All samples were stained in 96-well round-bottom well plates and centrifuged at 400xg for 5 min at 4 °C. To minimize light exposure the staining and incubation were carried out in the dark.

2.4.1.1 Live/dead staining and Fc receptor blocking

To distinguish live cells from dead cells all samples were stained with a live/dead dye. The plates with cells were centrifuged to remove the supernatant. To each well 50 µl of PBS with the respective live/dead marker (1:1000) and anti-CD16/CD32 FcRχ block (1:200) were added and the cells resuspended in that solution. After the incubation for 20 min at 4°C, 150 µl of PBS were added to each well, the plate was centrifuged, and the supernatant discarded. Cells were washed with 200 µl of PBS per well and subsequent extracellular staining was performed.

2.4.1.2 Extracellular staining

Following the live/dead staining each sample was resuspended in 100 µl of PBS containing the respective fluorophore-coupled antibodies for surface markers (see 2.4.1.4 Staining panels and cell populations). The cells were incubated with the surface staining (1:400 for each antibody and 1:160 for the OVA tetramer) for 50 min at RT before 100 µl of PBS per well were added and the plate was centrifuged. The cells were washed twice with 200 µl of PBS per well to remove excessive dye. If the samples were analyzed for surface markers only, the cells were resuspended in 180 µl PBS per well and transferred into flow cytometry tubes. Otherwise, cells were processed further for intracellular staining.

2.4.1.3 Intracellular staining

The intracellular staining was performed with the FoxP3/Transcription factor staining buffer set. To prepare the staining for intracellular antigens cells were resuspended in 50 µl of fixation buffer after the extracellular staining and centrifuged. Then the supernatant was discarded, and the cells were resuspended in 100 µl fixation buffer per well. Following an incubation of 45 min at RT the plates were centrifuged, and the supernatant was discarded. The cells were washed once in permeabilization buffer. The fluorophore-coupled antibodies for the respective intracellular markers (see 2.4.1.4 Staining panels and cell populations) were diluted in permeabilization buffer (1:200) and 100 µl of the staining solution was added to each sample. After an incubation of 50 min at RT 100 µl of permeabilization buffer was added to each well. The plate was centrifuged, and the supernatant was discarded. Cells were washed once with 200 µl of permeabilization buffer per well and twice with 200 µl of PBS per well. In the end samples were resuspended in 180 µl of PBS and transferred into flow cytometry tubes.

2.4.1.4 Staining panels and cell populations

Cells from tumors and tdLNs were analyzed as follows:
Immune cell activation panel (Table 14; Fig. 1A): activated $CD4^+$ and $CD8^+$ T cells were defined as live $CD45^+$ $CD3^+$ $CD4^+$ IFN-γ^+ cells or as live $CD45^+$ $CD3^+$ $CD4^-$ IFN-γ^+ cells respectively. OVA antigen specific T cells were defined as $CD45^+$ $CD3^+$ $CD4^-$ H-$2k^b$-$OVA_{257-264}$-$Tetramer^+$ cells. Natural killer cells were characterized as live $CD45^+$ $CD3^-$ $NK1.1^+$ cells and described as activated when cells expressed IFN-γ.
T cell panel (Table 14; Fig. 1B): cytotoxic T cells ("$CD8^+$ cells") were defined as live $CD45^+$ $CD3^+$ $CD8^+$ cells and Th cells ("$CD4^+$ cells") as live $CD45^+$ $CD3^+$ $CD4^+$ cells. It was differentiated between all $CD4^+$ cells, $CD4^+$ cells without regulatory T cells (live $CD45^+$ $CD3^+$ $CD4^+$ $FoxP3^-$), and regulatory T cells (live $CD45^+$ $CD3^+$ $CD4^+$ $FoxP3^+$). $CD4^+$ and $CD8^+$ T cells were further

defined as naïve T cells (CD62L$^+$ CD44$^-$), central memory T cells (CD62L$^+$ CD44$^+$), and effector memory T cells (CD62L$^-$ CD44$^+$) with the respective other markers.

DC panel (Table 14; Fig. 1C): dendritic cells were defined as CD45$^+$ CD11c$^+$ MHC-II$^+$ cells. Activation of these cells was measured as mean fluorescence intensity (MFI) of CD86.

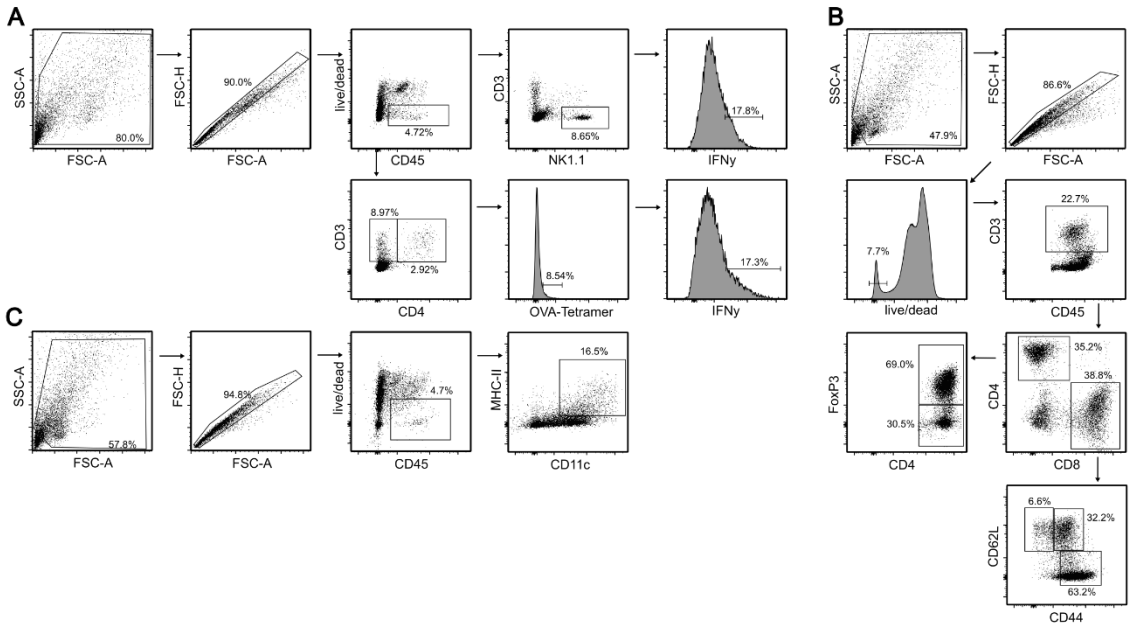

Figure 1: Gating strategy for TME and tdLN analysis
Representative dot plots of **(A)** the immune cell activation panel, **(B)** the T cell panel, and **(C)** the DC panel.

Table 14: Staining panels for tumors and tdLNs

T cell panel		**Immune cell activation panel**		**DC panel**	
Antigen	**Fluorochrome**	**Antigen**	**Fluorochrome**	**Antigen**	**Fluorochrome**
Live/dead	AmCyan	Live/dead	AmCyan	Live/dead	AmCyan
CD3	FITC	CD3	FITC	CD45.2	APC-Cy7
CD4	PE-Cy7	CD4	PerCP-Cy5.5	CD103	PerCP-Cy5.5
CD44	Pacific Blue	CD45.2	APC-Cy7	CD11b	APC
CD45.2	APC-Cy7	H-2k^b-OVA$_{257-264}$-Tetramer	PE	CD11c	Pacific Blue
CD62L	PE	IFN-γ	PE-Cy7	CD86	PE
CD8	PerCP-Cy5.5	NK1.1	APC	MHC-II (I-A/I-E)	FITC
FoxP3	APC (AF647)				

Tumor antigen specific T cells from the blood were characterized as live CD3$^+$ CD4$^-$ H-2k^b-OVA$_{257-264}$-Tetramer$^+$ cells (Table 15; Fig. 2A).

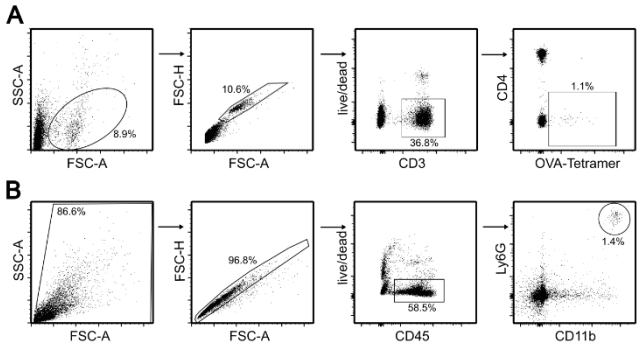

Figure 2: Gating strategy for tumor antigen-specific T cells and neutrophils
Representative dot plots of **(A)** the OVA tetramer panel and **(B)** the neutrophil-granulocyte influx.

Table 15: Staining panel for tumor antigen specific T cells

OVA tetramer panel	
Antigen	**Fluorochrome**
Live/dead	APC-Cy7
CD3	FITC
CD4	APC
H-2k^{b}-OVA$_{257-264}$-Tetramer	PE

Neutrophils in the neutrophil granulocyte influx assay were defined as live CD45^{+} CD11b^{high} Ly6G^{high} cells (table 16; Fig. 2B).

Table 16: Staining panel for neutrophils

Neutrophil granulocyte influx	
Antigen	**Fluorochrome**
Live/dead	AmCyan
CD45.2	Pacific Blue
CD11b	PE
Ly6G	PE-Cy7

For *in vitro* studies (table 17), isolated and treated T cells were characterized as live CD4^{+} and CD8^{+} cells and analyzed for either CD25^{+}, CD69^{+}, IFN-γ^{+}, or T-bet^{+} cells (Fig. 3A). From bone marrow isolated and treated DCs were defined as CD11c^{+} MHC-II^{+} cells and analyzed for MFI of CD80 and CD86 (Fig.3B).

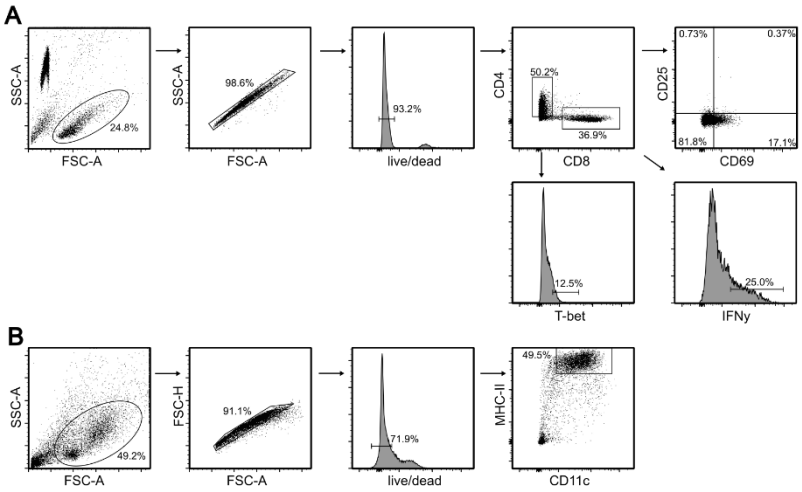

Figure 3: Gating strategy for *in vitro* assays
Representative dot plots of **(A)** the T cell panel and **(B)** the DC panel.

Table 17: *In vitro* staining panels

T cell panel		**DC panel**	
Antigen	**Fluorochrome**	**Antigen**	**Fluorochrome**
Live/dead	AmCyan	Live/dead	APC-Cy7
IFN-γ	PE-Cy7	CD11c	FITC
CD69	PerCP	MHC-II (I-A/I-E)	APC
CD25	APC-Cy7	CD80	Pacific Blue
CD4	Pacific Blue	CD86	PE
CD8	APC		
T-bet	PE		

2.4.2 Targeted metabolomics

Targeted metabolomics was performed by the Bavarian Biomolecular Mass Spectrometry Center (BayBioMS) who utilized their own machines and reagents, and provided the following protocol.

About 20 mg of mouse feces was measured and placed in a 2 mL bead beater tube (FastPrep-Tubes, Matrix D, MP Biomedicals Germany GmbH), which was then mixed with 1 ml of methanol for resuspension. The samples were subjected to extraction using a bead beater FastPep-24TM 5G (MP Biomedicals Germany GmbH) equipped with a CoolPrepTM (MP Biomedicals Germany, cooled with dry ice). This involved a total of 3 cycles, each consisting of 20 seconds of beating at a speed of 6 m/s, with a 30-second pause in between.

Quantification ICA or DAT was carried out using the 3-NPH method.[217] In summary, 40 µl of the fecal extract and 15 µl of isotopically labeled standards (approximately 50 µM) were mixed with 20 µl of 120 mM EDC HCl-6% pyridine-solution and 20 µl of 200 mM 3-NPH HCl solution. This mixture was then subjected to a 30-minute incubation at 40°C with shaking at 1000 rpm using an Eppendorf Thermomix. Subsequently, 900 µl of acetonitrile/water (50/50, v/v) was added after which the clear supernatant was used for analysis. For the measurement, a QTRAP 5500 triple quadrupole mass spectrometer (Sciex) coupled to an ExionLC AD (Sciex) ultrahigh-performance liquid chromatography system was employed. The electrospray voltage was set to -4500 V, curtain gas to 35 psi, ion source gas 1 to 55 psi, ion source gas 2 to 65 psi, and the temperature to 500°C. The MRM-parameters were optimized using commercially available standards. Chromatographic separation was achieved on a 100×2.1 mm, 10 nm, 1.7 µm, Kinetex C18 column (Phenomenex) utilizing 0.1% formic acid (eluent A) and 0.1% formic acid in acetonitrile (eluent B) as elution solvents. An injection volume of 1 µl and a flow rate of 0.4 ml/min were used. The gradient elution was initiated at 23% B and was maintained for 3 minutes. Subsequently, the concentration was raised to 30% B at 4 minutes, further increased to 40% B at 6.5 minutes, with a switch to 100% B at 7 minutes, maintained for 1 minute, and then equilibrated to the initial conditions at 8.5 minutes. The column oven was set to 40°C, while the autosampler was set to 15°C. Data acquisition and instrumental control were managed using Analyst 1.7 software (Sciex), and data analysis was carried out using MultiQuant 3.0.3 (Sciex).

2.4.3 Immunohistochemistry

Immunohistochemistry was conducted by the Institute of Pathology of the TUM School of Medicine and Health and Technical University of Munich who utilized their own machines and products, and provided the following protocol. The samples were analyzed by Katja Steiger.
The colon tissues from the mice were fixed in a 10% neutral-buffered formalin solution for a period of 48 hours. Subsequently, the tissues were dehydrated following standard protocols (Leica ASP300S) and then embedded in paraffin. Serial 2 µm-thin sections were prepared using a rotary microtome (HM355S, ThermoFisher Scientific) and were subjected to both histological and immunohistochemical examinations. Immunohistochemistry was conducted with a Bond RXm system (Leica, using all reagents from Leica) employing a primary antibody against cleaved caspase-3 (Clone 5A1E, at a dilution of 1:150, Cell Signaling). In brief, slides were deparaffinized using a deparaffinization solution and then treated with Epitope retrieval solution 1 (equivalent to citrate buffer pH6) for a duration of 20 minutes. The primary antibody was allowed to incubate for 15 minutes at room temperature. Antibody binding was detected utilizing a polymer refine detection kit without the post-primary reagent, and visualization was

achieved with DAB resulting in a dark brown precipitate. Hematoxylin was used for counterstaining. Subsequently, the slides were cover-slipped and digitally scanned using an AT2 scanner system (Leica Biosystems). The staining reaction was evaluated using Imagescope (12.4.0.2018, Leica Biosystems).

2.4.4 16S-rRNA sequencing

16S-rRNA sequencing was done by the ZIEL - Institute for Food & Health Central of the Technical University of Munich who utilized their own machines and products, and provided the following protocol.

Murine fecal samples were gathered at various intervals during the experiments and promptly frozen in liquid nitrogen. The processing of these samples followed previously outlined procedures, albeit with some modifications.[218] In essence, after DNA isolation, targeted 16S-rRNA gene amplicons were generated using a two-step PCR method, which involved the incorporation of barcodes and adapters. The specific primers employed were 341F (5'-CCT ACG GGN GGC WGC AG-3') and 785R (5'-GAC TAC HVG GGT ATC TAA TCC-3'), as previously documented.[219] DNA isolation was performed using the MaxWell RSC Fecal Microbiome DNA Kit from Promega, utilizing bead beating with the FastPrep-24 (MP Biomedicals) instrument, accompanied by a CoolPrep cooled with dry ice. This process involved three 20-second rounds of beating at a speed of 6 m/s, with each session followed by a 30-second pause for cooling. Modifications were made to the cycle times for the initial and secondary PCR stages, adjusting denaturation to 10 seconds, annealing to 20 seconds, and extension to 45 seconds. Subsequent to library preparation and equimolar pooling of the amplicons, the samples underwent sequencing using a MiSeq (Illumina) platform. For the DAT DW data, a total of 60 samples with a read length of 301 bp were examined, while the responder/non-responder data encompassed 17 samples with a similar read length. Raw sequencing data underwent analysis via a UPARSE-based pipeline that clustered sequences into denoised operational taxonomic units (zOTUs) using www.imngs2.org, incorporating the TIC algorithm.[220,221] Downstream analysis of zOTU tables was carried out using Rhea and default settings. This involved the normalization of reads and the removal of spurious taxa.[222,223]

2.4.5 MTT (3-(4,5-dimethylthiazol-2-yl)-2,5-diphenyltetrazolium bromide) assay

$4x10^4$ B16.OVA cells were seeded in a 96-well flat-bottom cell culture treated plate in 100 µl complete DMEM per well. DAT or ICA were added at concentrations of 1 µM, 10 µM, 50 µM, 100 µM, 200 µM, 400 µM, and 800 µM or cells were treated with PBS as negative control or 3

µg/ml 3pRNA as positive control. The 3pRNA was pre-incubated with 0.2 µl Lipofectamine 2000 per well in OptiMEM for 15 min before adding it to the wells. After 24 h of incubation at 37 °C and 5% CO_2 the cell culture supernatant was discarded and 100 µl complete DMEM containing 0.5 mg/ml MTT was added per well. The cells were incubated for 3 h at 37 °C and 5% CO_2 with the MTT media. Next, the MTT solution was discarded and 150 µl of DMSO per well were added and the plate was incubated for 3 h at 37 °C. The absorption was measured with a plate reader at 560 nm.

2.5 Statistical analysis

The corresponding sample sizes were determined based on preliminary internal studies, previous research, and other ongoing projects. In the case of the B16 tumor model, it was shown that a minimum of 5 mice per group was practical for detecting variations in tumor growth post-therapy.[224] Correspondingly, the impact of DAT and ICA were observed in a separate internal project with comparable group sizes. Adherence to ethical guidelines was also considered, ensuring the use of the minimum animals necessary while maintaining statistical validity. Adjustments to the sample size for subsequent analyses were made to accommodate limitations in resources. Mean values with a 95% confidence interval (CI) were used for graphs where parametric tests were applicable, while non-parametric tests were represented with median and corresponding CI at a 95% confidence level. Evaluation of normality was conducted through visual assessment using a QQ plot, and homoscedasticity was assessed via the Brown-Forsythe test and visual inspection of plotted values. Unpaired parametric t-tests were utilized for data with normal distribution, with Welch's correction applied in cases where standard deviations differed. ANOVA with Tukey's multiple comparison test was used for analyses involving three or more groups, while specific pre-selected pairs were analyzed using Bonferroni's multiple comparison test. Instances where the data did not meet ANOVA criteria employed the Kruskal-Wallis test with Dunn's post-hoc test. Tumor growth curves were assessed using two-way ANOVA with Tukey's post-hoc test, with the hypothesis being that tumor volume in the DAT treated group differed from the control groups over time. The reported p-values in the graphs indicated the latest time point for conducting the test, depending on the included groups. Overall survival was analyzed using the Log-rank (Mantel-Cox) test, with the survival experiments initiated at day 0 and monitored until day 80, with the event of interest typically starting around day 10. All statistical analyses were performed using GraphPad Prism.

III RESULTS

1. Impact of the bacterial-derived metabolites on ICI therapy

1.1 Supplementation with the metabolites DAT and ICA enhances anti-CTLA-4 therapy

To address the role of the bacterial-derived metabolites DAT and ICA on tumor immunosurveillance and therapy, C57Bl/6j mice were provided with 3.4 mg DAT or 3.0 mg ICA per mouse per day via controlled oral gavage. Supplementation with DAT or ICA was initiated on the day of tumor cell inoculation with B16.OVA cells. On days 7, 10, and 13 the mice were injected with anti-CTLA-4 or the isotype control antibodies. The controlled application of DAT did not result in significant differences in tumor growth compared to that in the control mice on day 7 before the anti-CTLA-4 treatment (Fig. 4A). When comparing the overall tumor growth, there was a non-significant trend hinting at improved tumor control in mice administered with DAT and a combination of anti-CTLA-4 treatment (Fig. 4B). Nonetheless, a significant increase in long-term survival was observed in mice receiving the combination of DAT and anti-CTLA-4 compared to those treated with anti-CTLA-4 alone (Fig. 4C). Interestingly, sole gavage of DAT did not have an effect on tumor growth and survival (Fig. 4B and C). Similar results were obtained by the administration of ICA. While the tumor growth did not differ between mice that received ICA and control mice (Fig. 4D and E), the combination of ICA and anti-CTLA-4 significantly enhanced the anti-CTLA-4 effect (Fig. 4E). The OS improved with the combinatorial treatment compared to control mice treated with anti-CTLA-4, whereas sole ICA administration did not influence the survival rate (Fig. 4F).

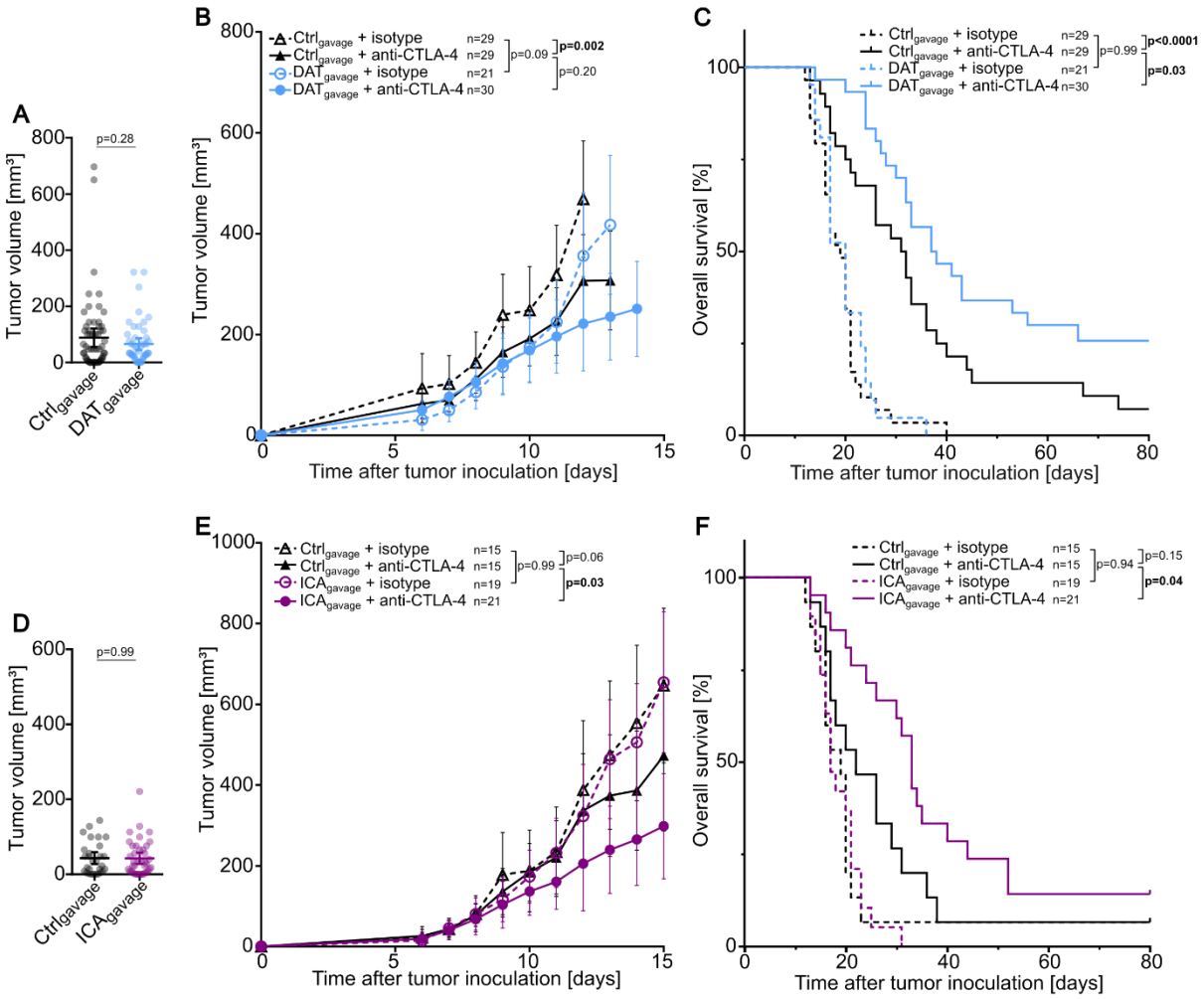

Figure 4: Treatment with DAT or ICA enhances the efficacy of anti-CTLA-4 therapy in melanoma
C57Bl/6j mice were injected s.c. with B16.OVA tumor cells on day 0 and treated with anti-CTLA-4 or isotype control antibodies on days 7, 10, and 13. From the day of tumor cell inoculation on mice were administered with DAT, ICA, or the respective solvent via oral gavage once per day until the end of the experiment. **(A)** Tumor volume on day 7 comparing control mice with mice that received DAT via gavage [unpaired t-test]. **(B)** Tumor growth curves and **(C)** overall survival of the DAT gavage experiments. **(D)** Tumor volume on day 7 comparing control mice with mice that received ICA via gavage [two-way ANOVA with Tukey's multiple comparison test on day 12 for growth curves and Log-rank (Mantel-Cox) test for Kaplan-Meier survival]. **(E)** Tumor growth curves and **(F)** overall survival of the ICA gavage experiments [two-way ANOVA with Tukey's multiple comparison test on day 15 for growth curves and Log-rank (Mantel-Cox) test for Kaplan-Meier survival]. The data were obtained from 3 independent experiments. All graphs show mean with 95% CI.

In order to investigate the priming and expansion of tumor antigen-specific T cells, blood samples were collected two days after the final anti-CTLA-4 treatment. The circulating tumor antigen-specific T cells were analyzed via flow cytometry. Compared to mice receiving the isotype control antibody, mice that were treated with anti-CTLA-4 showed increased frequencies of tumor antigen-specific T cells (Fig. 5A and B). Equivalent to sole metabolite administration, the combination of anti-CTLA-4 and DAT or ICA did not have any additive effect regarding the expansion of tumor antigen-specific T cells (Fig. 5A and B).

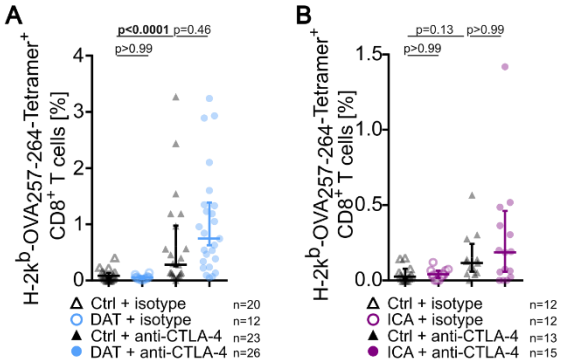

Figure 5: DAT and ICA do not increase the frequencies of tumor antigen-specific T cells
On day 15 blood was collected from the vena facialis from the experimental mice described in figure 5 and circulating tumor antigen-specific T cells were analyzed via flow cytometry. H-2k^b-OVA$_{257-264}$-Tetramer$^+$ CD8$^+$ T cells after anti-CTLA-4 and **(A)** DAT or **(B)** ICA administration [Kruskal-Wallis test with Dunn's multiple comparison test]. The data were obtained from 3 independent experiments. All graphs show median with the CI at the requested confidence level of 95%.

1.2 DAT but not ICA improves anti-PD-1 therapy in a murine model of pancreatic ductal adenocarcinoma

To account for the high immunogenicity of the B16.OVA melanoma model and ensure that the effects of DAT and ICA were not restricted to this issue, the metabolites were administered through oral gavage in a subcutaneous model of murine pancreatic adenocarcinoma. Additionally, this approach was combined with anti-PD-1 therapy as the Panc02 model was more sensitive to sole anti-PD-1 treatment than the B16.OVA model. DAT in combination with anti-PD-1 led to slightly enhanced tumor control, leading to a significantly extended survival rate (Fig. 6A and B). In contrast, ICA did not contribute to enhancing the anti-PD-1 effect, neither in tumor growth dynamics nor in survival (Fig. 6C and D). Combining these data, it becomes evident that oral DAT supplementation enhances the efficacy of both anti-CTLA-4 and anti-PD-1 ICI immunotherapies across various tumor models whereas the effect of ICA seems to be restricted to the B16.OVA tumor model and anti-CTLA-4 treatment.

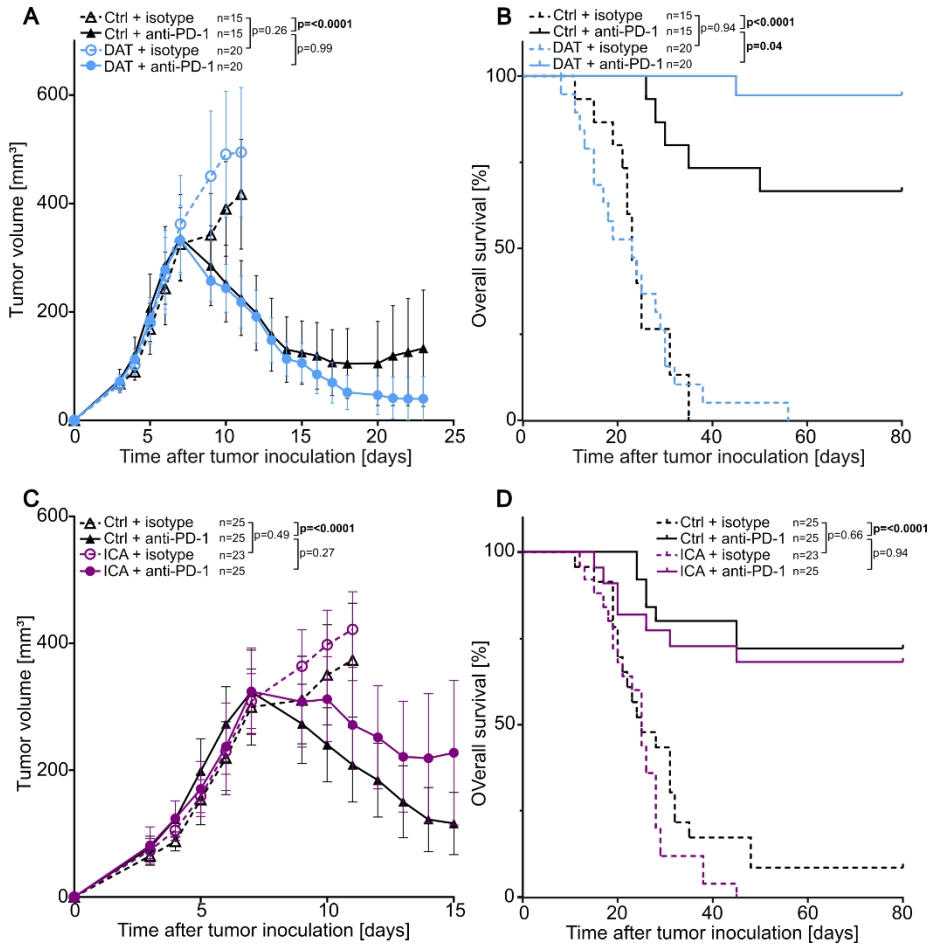

Figure 6: DAT but not ICA improves anti-PD-1 therapy in a murine model of pancreatic carcinoma
C57Bl/6j mice were injected s.c. with Panc02 tumor cells on day 0 and treated with anti-PD-1 or isotype control antibodies on days 4, 7, and 10. From the day of tumor cell inoculation on mice were administered with DAT, ICA, or the respective solvent via oral gavage once per day until the end of the experiment. **(A)** Tumor growth curves and **(B)** overall survival of mice that received DAT [two-way ANOVA with Tukey's multiple comparison test on day 11 for growth curves and Log-rank (Mantel-Cox) test for Kaplan-Meier survival]. **(C)** Tumor growth curves and **(D)** overall survival of mice that received ICA [two-way ANOVA with Tukey's multiple comparison test on day 11 for growth curves and Log-rank (Mantel-Cox) test for Kaplan-Meier survival]. The data were obtained from 3 independent experiments. All graphs show mean with 95% CI.

1.3 The additive effect of DAT and anti-CTLA-4 immunotherapy varies based on dosage and method of administration

Because of its chemical properties, DAT could be dissolved in higher doses than ICA and administered via drinking water without causing acute toxicity by single gavage of a high dose. Furthermore, the oral uptake via the drinking water better reflects the oral drug intake in humans. This characteristic prompted investigations into its potential under these conditions excluding ICA. The approach of DAT in the drinking water has been described previously and was adjusted to meet experimental criteria.[178] As before, DAT was administered from the day

of B16.OVA tumor cell inoculation on and on days 7, 10, and 13 the mice were injected with anti-CTLA-4 or the isotype control antibodies. Administration of DAT via drinking water (100 mM) showed no difference in the total tumor volume on day 7 before anti-CTLA-4 treatment (Fig. 7A). However, in contrast to the low dose via oral gavage, it resulted in 50% of tumor-free mice on day 7 with the tumors becoming visible two to three days later in the DAT treated group (Fig. 7B). The overall tumor control with DAT administration via the drinking water significantly enhanced the anti-CTLA-4 efficacy (Fig. 7C). Similar to low dose gavage the sole DAT administration here did not lead to improved tumor control (Fig. 7C and D). Furthermore, the additive effect of DAT and anti-CTLA-4 was evident in the OS rate (Fig. 7D). Even the high dosage of DAT did not impact the expansion of tumor antigen-specific T cells (Fig. 7E). In summary, the administration of a higher dose of DAT resulted in an even more prominent antitumor effect and a potent model for further mechanistic studies.

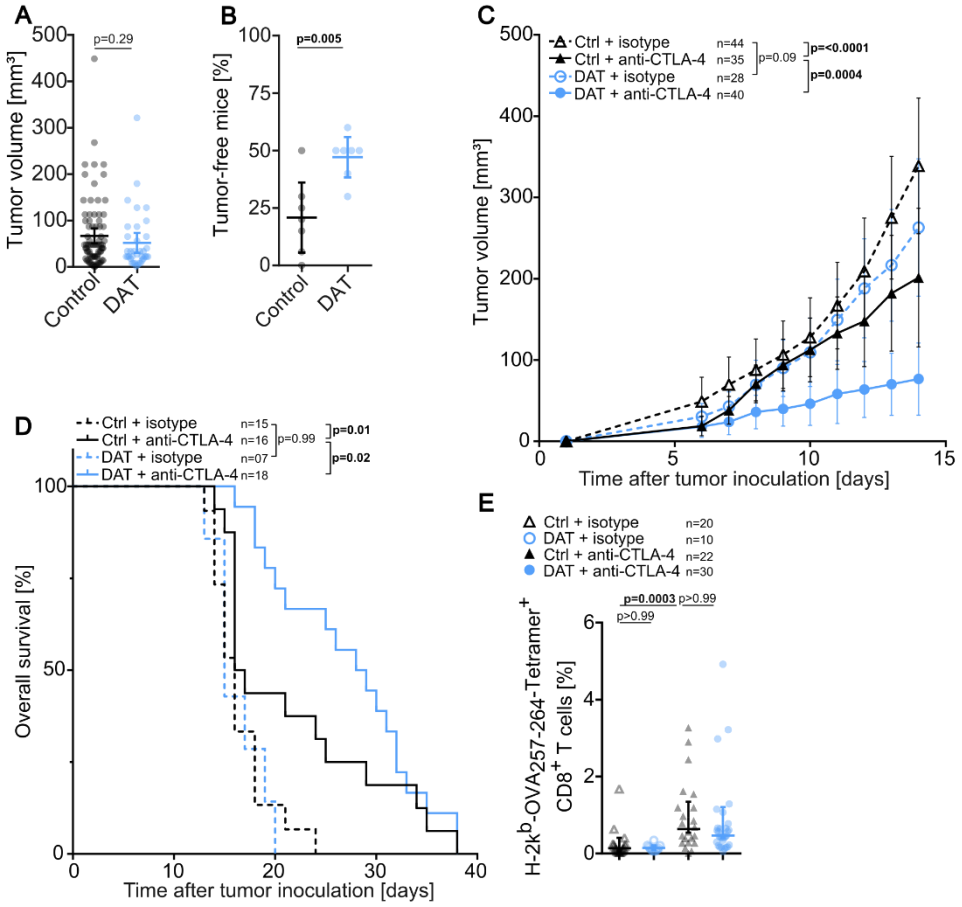

Figure 7: The additive effect of DAT and anti-CTLA-4 therapy varies based on dosage and method of administration
C57Bl/6j mice were injected s.c. with B16.OVA tumor cells on day 0 and treated with anti-CTLA-4 or isotype control antibodies on days 7, 10, and 13. From the day of tumor cell inoculation on mice were administered with DAT via drinking water until the end of the experiment. **(A)** Tumor volume and **(B)** percentage of tumor-free mice per experiment on day 7 comparing control mice with mice that received DAT [unpaired t-test]. **(C)** Tumor growth curves and **(D)** overall survival [two-way ANOVA with Tukey's multiple comparison test on day 14 for growth curves and Log-rank (Mantel-Cox) test for Kaplan-Meier survival]. **(E)** On day 15 tumor antigen-specific T cells were analyzed via flow cytometry [Kruskal-Wallis test with Dunn's multiple comparison test]. The data were obtained from 3-6 independent experiments. All graphs show mean with 95% CI or median with the CI at the requested confidence level of 95%.

To simulate the more commonly used combination of anti-CTLA-4 and anti-PD-1 in patients, mice were treated with a combination of both ICIs. Interestingly, while the combined ICI treatment was more effective than anti-CTLA-4 treatment alone, the addition of DAT supplementation had only a moderate influence on the overall therapy in this case (Fig. 8A and B). The percentages of circulating tumor antigen-specific T cells markedly increased with treatment with both ICIs compared to anti-CTLA-4 therapy. However, the additional administration of DAT did not further increase the numbers of these T cells (Fig. 8C). Taken together, the strong antitumor effect of combined anti-CTLA-4 and anti-PD-1 could be boosted modestly by additional DAT administration.

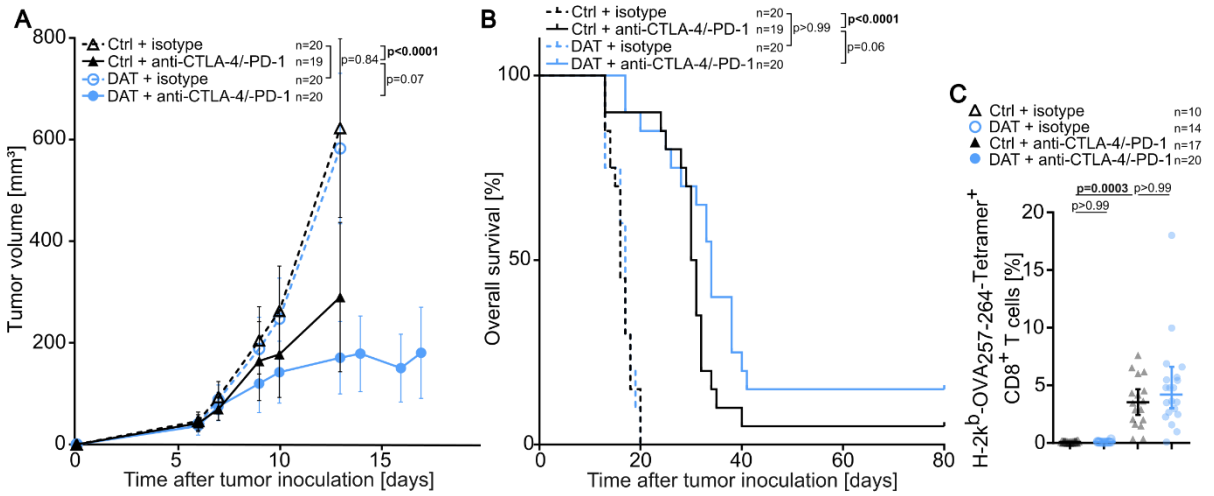

Figure 8: DAT moderately influences anti-CTLA-4 and anti-PD-1 combination therapy
C57Bl/6j mice were injected s.c. with B16.OVA tumor cells on day 0 and treated with anti-CTLA-4 and anti-PD-1 or isotype control antibodies on days 7, 10, and 13. From the day of tumor cell inoculation on mice were administered with DAT via drinking water until the end of the experiment. **(A)** Tumor growth curves and **(B)** overall survival [two-way ANOVA with Tukey's multiple comparison test on day 13 for growth curves and Log-rank (Mantel-Cox) test for Kaplan-Meier survival]. **(C)** On day 15 tumor antigen-specific T cells were analyzed via flow cytometry [Kruskal-Wallis test with Dunn's multiple comparison test]. The data were obtained from 2 independent experiments. All graphs show mean with 95% CI or median with the CI at the requested confidence level of 95%.

1.4 The timing of DAT administration influences its effect on anti-CTLA-4 treatment

Next, the evaluation focused on whether the timing of DAT administration could influence the effectiveness of ICI immunotherapy in this murine melanoma model. To investigate this, DAT administration through drinking water (100 mM) was initiated on day 5 following tumor inoculation, which is referred to as "late" treatment. In comparison to the early DAT supplementation starting from day 0, the late initiation of DAT administration from day 5 onwards resulted in a similar, though statistically non-significant, trend of delayed early tumor growth (Fig. 9A). However, when combined with anti-CTLA-4 therapy, late DAT treatment did not achieve the same favorable effects on tumor control and the corresponding survival of animals as observed with the early DAT treatment (Fig. 9B and C). Comparable to the early

DAT administration, the late DAT treatment did not result in increased frequencies of tumor antigen-specific T cells. To summarize, a later start of the DAT treatment dampened the efficacy of the combined treatment in comparison to an earlier start of DAT supplementation.

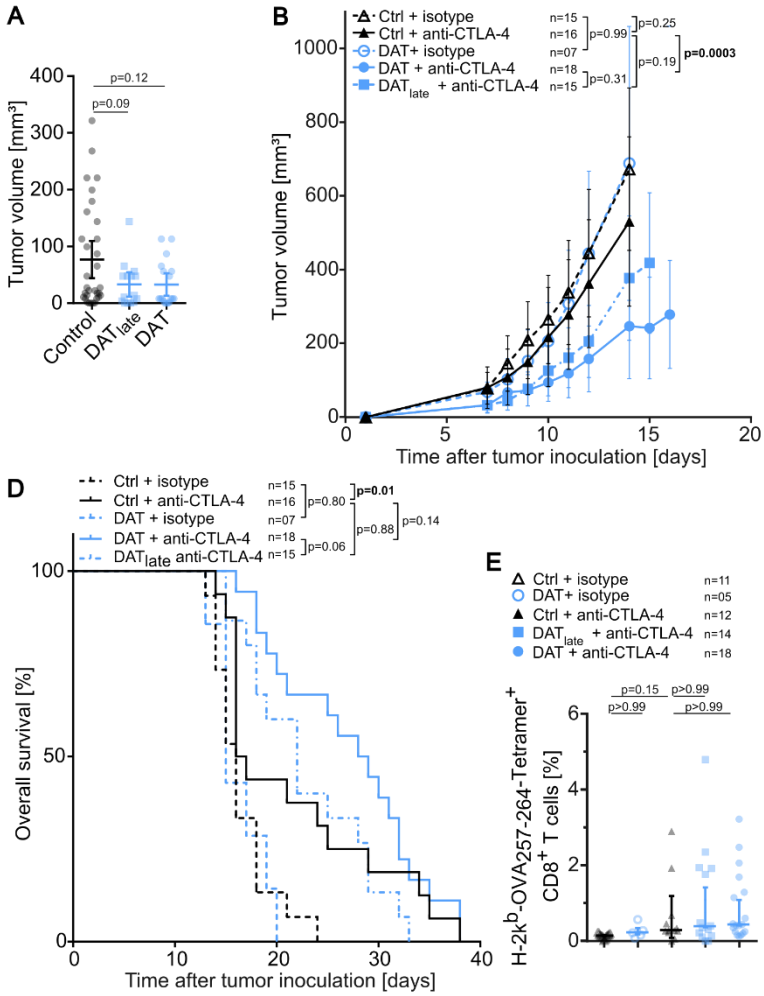

Figure 9: The additive effect of DAT and anti-CTLA-4 is time dependent
C57Bl/6j mice were injected s.c. with B16.OVA tumor cells on day 0 and treated with anti-CTLA-4 or isotype control antibodies on days 7, 10, and 13. From day 5 after tumor cell inoculation on mice were administered with DAT via drinking water until the end of the experiment. **(A)** Tumor volume on day 7 comparing control mice with mice that received DAT [one-way ANOVA with Tukey's multiple comparison test]. **(B)** Tumor growth curves and **(C)** overall survival [two-way ANOVA with Tukey's multiple comparison test on day 14 for growth curves and Log-rank (Mantel-Cox) test for Kaplan-Meier survival]. **(D)** On day 15 tumor antigen-specific T cells were analyzed via flow cytometry [Kruskal-Wallis test with Dunn's multiple comparison test]. The data were obtained from 3 independent experiments. All graphs show mean with 95% CI or median with the CI at the requested confidence level of 95%.

2. Potential ICI treatment-related changes in DAT and ICA levels poorly correlate with treatment response

Given the presence of numerous bacterial-derived metabolites in the gut and even the circulation, targeted metabolomics was conducted to identify the levels of the bacterial-derived metabolites DAT and ICA in murine stool samples from both responder and non-responder mice to anti-CTLA-4 therapy. One aim of the experiment was to explore if the pre-existing levels of the metabolites can serve as predictive markers for the success or failure of the anti-CTLA-4 treatment. The second aim was to investigate the impact of anti-CTLA-4 therapy on the levels of the metabolites, potentially linking them to treatment response or non-response. Stool samples of C57Bl/6j WT mice were collected one day prior to the subcutaneous injection of B16.OVA cells (referred to as 'steady state') and on the final day of the anti-CTLA-4 treatment ('anti-CTLA-4'). The mice were subsequently categorized into groups, including control mice receiving the isotype control, as well as responder and non-responder to the anti-CTLA-4 therapy.

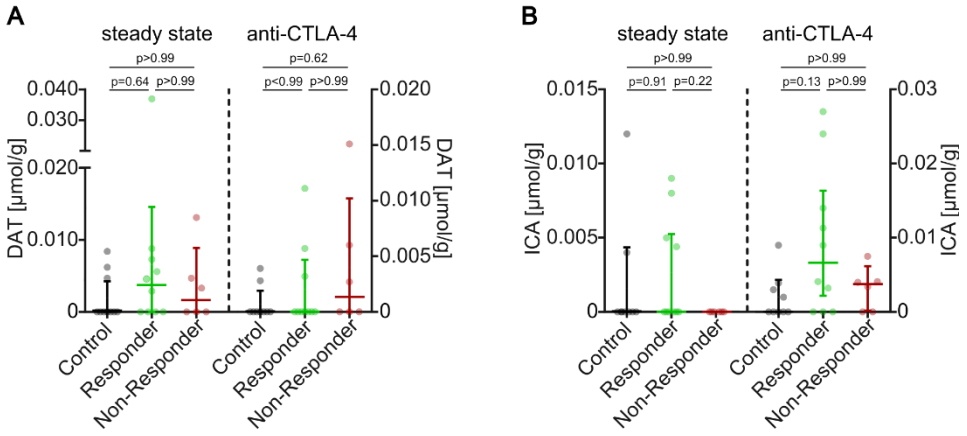

Figure 10: Treatment-related changes in metabolite levels following anti-CTLA-4 therapy
C57Bl/6j mice were injected s.c. with B16.OVA tumor cells on day 0 and treated with anti-CTLA-4 or isotype control antibodies on days 7, 10, and 13. Stool samples were collected on day 0 ("steady state") and day 13 ("anti-CTLA-4") and different bacterial-derived metabolites were measured utilizing targeted metabolomics. The mice were retrospectively classified as responder or non-responder to anti-CTLA-4 therapy. Control mice received the isotype control. Levels of **(A)** DAT and **(B)** ICA in stool samples of steady state and anti-CTLA-4 treated mice [Kruskal-Wallis test with Dunn's multiple comparison test]. The samples were obtained from mice from 3 independent experiments for each group with control n=9, responder n=10, and non-responder n=6. All graphs show median with the CI at the requested confidence level of 95%.

DAT was detected at very low levels in the initial steady state. In responder mice, there was a slight increase in levels, although this trend was not statistically significant (Fig. 10A). After the mice received anti-CTLA-4 this difference disappeared (Fig. 10A). ICA showed no significant differences in levels among control, responder, and non-responder mice in the steady state (Fig. 10B). However, unlike DAT levels following anti-CTLA-4 therapy, there was a slight, non-significant increase in ICA levels specifically observed in responder mice (Fig. 10B). Taken

together the results suggest potential treatment-related alterations in DAT and ICA levels but the results cannot be correlated with response due to the lack of statistical significance. Nevertheless, the higher DAT levels in the steady state might hint at a potential role as a predictive biomarker, but further investigation is needed to understand the biological significance of these observations.

3. DAT enhances the activation of DCs, T cells and NK cells

3.1 DAT supplementation modifies the TME and enhances T cell activation mediated by anti-CTLA-4

In order to investigate the effects of DAT on the tumor microenvironment, mice were supplemented with 100 mM DAT in the drinking water from the day of B16.OVA tumor cell inoculation and treated with anti-CTLA-4 as described previously on days 7, 10, and 13. On day 15 tumor tissue was analyzed via flow cytometry. Combined treatment with DAT and anti-CTLA-4 enhanced anti-CTLA-4 induced T cell activation characterized by an increased frequency and increased activity of IFN-γ^+ $CD4^+$ T cells (Fig. 11A and B). Likewise, DAT significantly enhanced the anti-CTLA-4-induced activation in $CD8^+$ T cells (Fig. 11C and D). As anticipated, anti-CTLA-4 immunotherapy had a significant impact on T cells in the TME. However, no additional effects from DAT supplementation in terms of the expansion and activation of OVA antigen-specific T cells (Fig. 11E and F), the frequency of $FoxP3^+$ regulatory T cells (Fig. 11G), or the T cell memory phenotype (Fig. 11H-M) could be observed. Moreover, the frequency and maturation of conventional $CD11c^+$ MHC-II^+ DCs in the TME, essential for presenting antigens during T cell priming, remained unchanged following oral DAT supplementation (Fig. 11N and O). Of interest, significantly higher frequencies of activated IFN-γ-producing NK cells were observed following DAT supplementation and combined anti-CTLA-4 treatment (Fig. 11P). In summary, these data collectively demonstrate that sole DAT supplementation did not significantly affect the TME. However, when administered alongside anti-CTLA-4 therapy, DAT potently enhanced the activation of both T and NK cells.

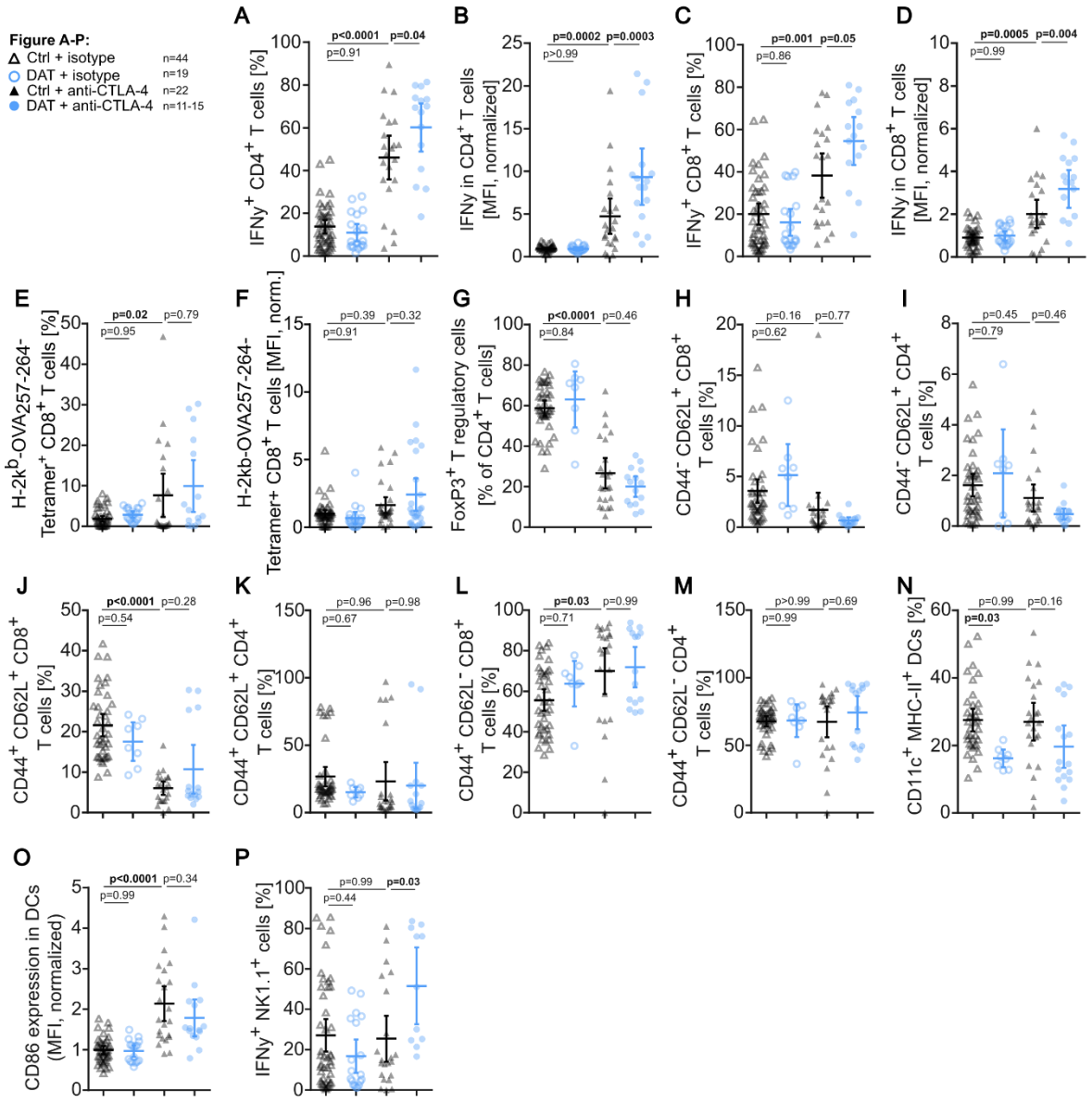

Figure 11: DAT supplementation alters the TME and enhances anti-CTLA-4-mediated T cell activation
On day 15 mice (described in figure 8) were sacrificed and tumors were extracted. The cells from the TME were analyzed via flow cytometry. **(A)** Frequencies of activated CD4+ T cells and **(B)** their expression of IFN-γ (MFI, normalized to the 'control + isotype' group). **(C)** Frequencies of activated CD8+ T cells and **(D)** their expression of IFN-γ (MFI, normalized to the 'control + isotype' group). **(E)** Frequencies of tumor antigen-specific T cells and **(F)** their expression of IFN-γ (MFI, normalized to the 'control + isotype' group). Frequencies of **(G)** regulatory T cells, **(H)** naïve CD8+ T cells, **(I)** naïve CD4+ T cells, **(J)** CD8+ TCMs, **(K)** CD4+ TCMs, **(L)** CD8+ TEMs, **(M)** CD4+ TEMs, **(N)** DCs and **(O)** their expression of IFN-γ (MFI, normalized to the 'control + isotype' group), and **(P)** IFN-γ expressing NK cells [one-way ANOVA with Tukey's multiple comparison test]. The data were obtained from 4 independent experiments. All graphs show mean with 95% CI.

The effects of DAT on T cell activation in the tdLNs were not as pronounced as in the TME (Fig. 12A and B). The expansion of OVA antigen-specific T cells (Fig. 12C), the frequency of FoxP3+ regulatory T cells (Fig. 12D), or the T cell memory phenotype (Fig. 12E-J) could not be influences by additional DAT supplementation. The lymph nodes presented with low frequencies of DCs which could neither be increased with anti-CTLA-4 treatment nor the combinatorial treatment (Fig. 12K). The activation of DCs was also unaffected by any of the

treatment combinations (Fig. 12L). While the frequencies of IFN-γ-expressing NK cells were significantly higher with the combinatorial treatment in the TME, the effect in the tdLNs was less pronounced and suggested a non-significant trend towards higher frequencies of activated NK cells with the combination of DAT and anti-CTLA-4 (Fig. 12M). Taken together, in contrast to the potent impact of DAT on the anti-CTLA-4-mediated effects in the TME, particularly with regard to T cell and NK cell activation, DAT in combination with anti-CTLA-4 just minimally affected the immune cell subsets in the tdLNs.

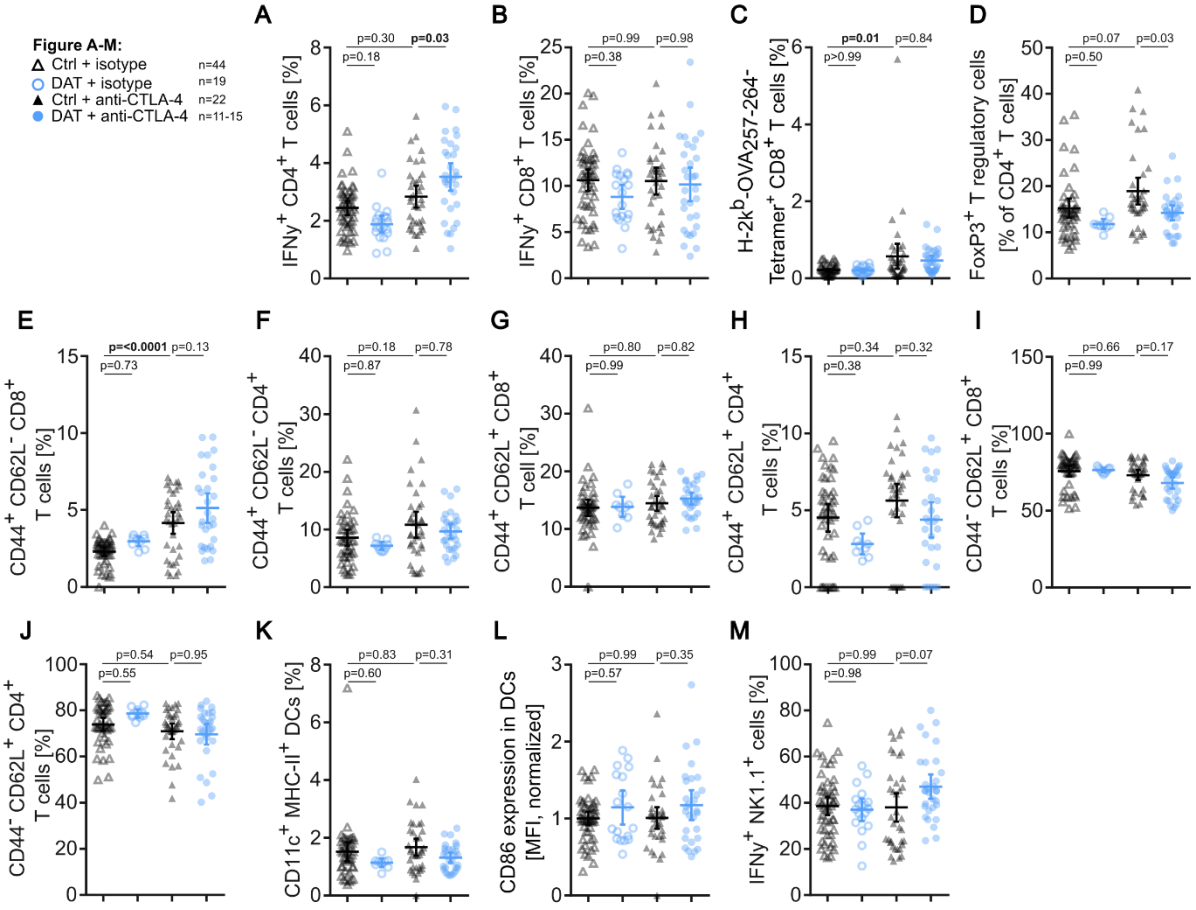

Figure 12: DAT supplementation minimally affects anti-CTLA-4-mediated effects on immune cells in tdLNs
On day 15 mice (described in figure 8) were sacrificed and tdLNs were extracted. The cells from the tdLNs were analyzed via flow cytometry. Frequencies **(A)** of activated $CD4^+$ T cells, **(B)** activated $CD8^+$ T cells, **(C)** tumor antigen-specific T cells, **(D)** regulatory T cells, **(E)** naïve $CD8^+$ T cells, **(F)** naïve $CD4^+$ T cells, **(G)** $CD8^+$ TCMs, **(H)** $CD4^+$ TCMs, **(I)** $CD8^+$ TEMs, **(J)** $CD4^+$ TEMs, **(K)** DCs and **(L)** their expression of IFN-γ (MFI, normalized to the 'control + isotype' group), and **(M)** IFN-γ expressing NK cells [one-way ANOVA with Tukey's multiple comparison test]. The data were obtained from 4 independent experiments. All graphs show mean with 95% CI.

3.2 Depletion of T cells and NK cells limits the additive effect of DAT and anti-CTLA-4

To assess if all cell types for which increased frequencies were observed after the combinatorial treatment are critical for the DAT-mediated antitumor immunity, depletion experiments were performed. The mice were treated as described above and depletion antibodies for CD4, CD8, and NK1.1 were injected i.p. prior to the tumor cell injection and afterwards every 7 days to maintain the depletion status. The depletion status was monitored by analyzing blood samples throughout the experiment using flow cytometry (Fig. 13A).

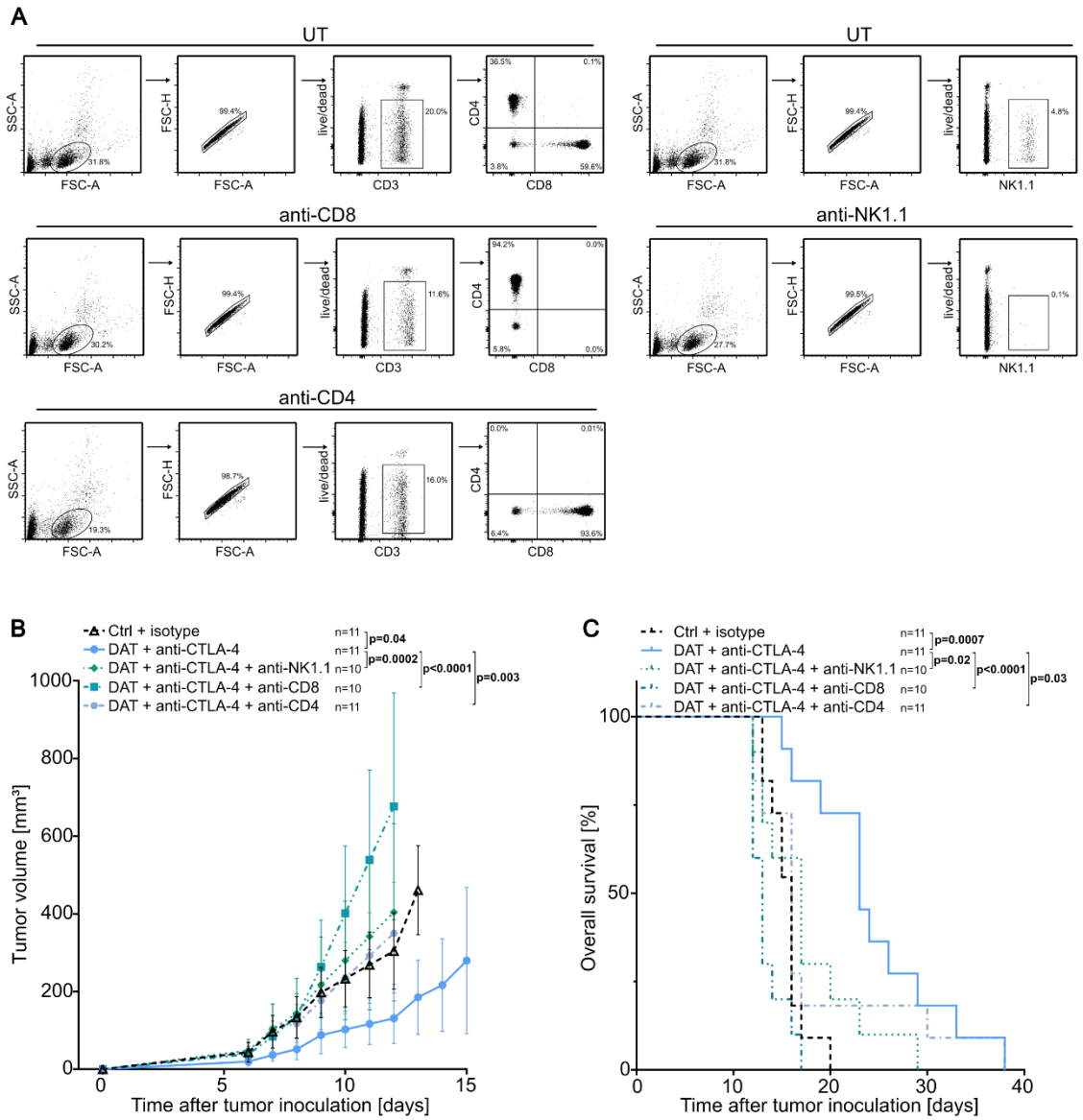

Figure 13: Depletion of T cells and NK cells limits the additive effect of DAT and anti-CTLA 4
C57Bl/6j mice were injected s.c. with B16.OVA tumor cells on day 0 and treated with anti-CTLA-4 or isotype control antibodies on days 7, 10, and 13. From the day of tumor cell inoculation on mice were administered with DAT via drinking water until the end of the experiment. Prior to the tumor cell inoculation and at defined time points throughout the experiment mice were injected i.p. with either anti-CD4, anti-CD8, or anti-NK1.1 antibodies. The depletion status was assessed via analysis of blood samples via flow cytometry. **(A)** Representative dot plots of UT (no depletion antibody), anti-CD8, anti-CD4, or anti-NK1.1 treated animals. **(B)** Tumor growth curves and **(C)** overall survival [two-way ANOVA with Tukey's multiple comparison test on day 12 for growth curves and Log-rank (Mantel-Cox) test for Kaplan-Meier survival]. The data were obtained from 2 independent experiments. All graphs show mean with 95% CI.

As cytotoxic T cells play a crucial role in antitumor immunity tumor control could not be achieved in mice with depleted $CD8^+$ T cells (Fig. 13B).[36,37] Similarly, mice with depleted $CD4^+$ and NK cells showed no improved tumor control with the combinatorial treatment compared to the isotype control (Fig. 13B). These results were confirmed by the long-term survival which demonstrated that DAT administration was not capable to compensate for the absence of any of the immune cell subsets (Fig. 13C). Altogether, the results outline that both T cells and NK cells are crucial in mediating the DAT effect and that this cannot be compensated by other still functional immune cell subsets.

3.3 DAT directly enhances T cell and DC activation *in vitro*

Bacterial metabolites can exert both direct and indirect effects on immune cells. While some metabolites mediate their effects on immune cells through systemic changes or alteration of the microbial composition, other metabolites directly activate or inhibit immune cells.[206,207,210,225,226] To validate whether the activation of T cells resulted from the direct impact of DAT, T cells were exposed to varying concentrations of DAT in a controlled *in vitro* environment.

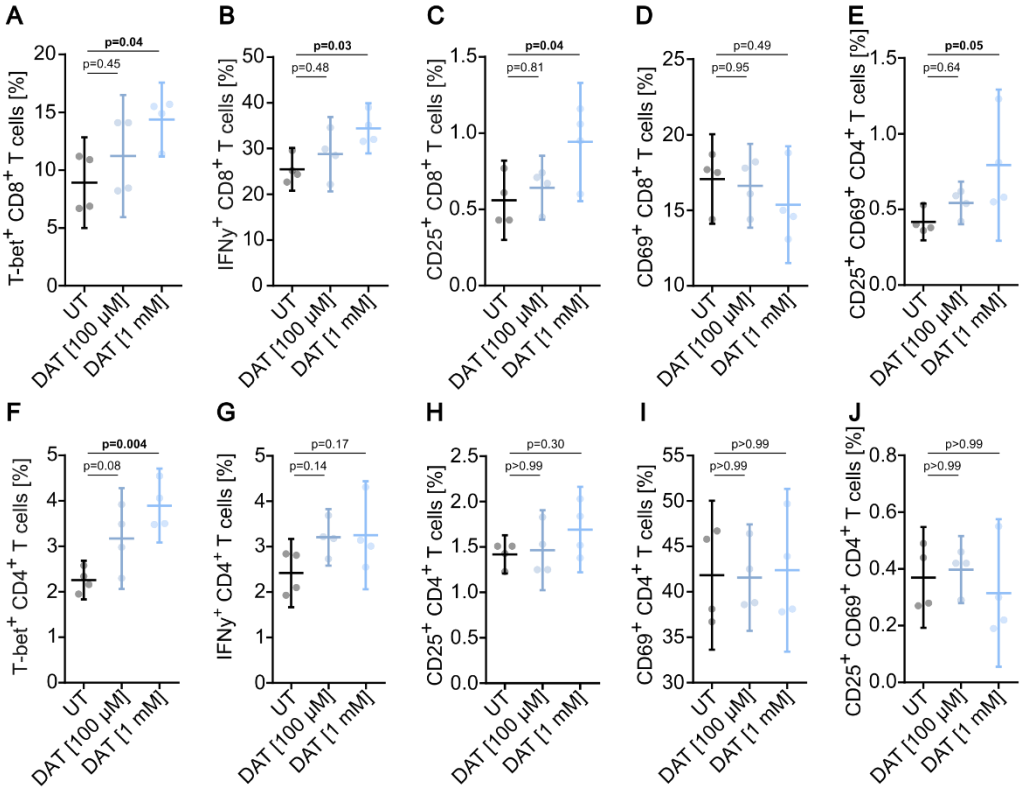

Figure 14: DAT directly enhances T cell activation *in vitro*
T cells from C57Bl/6j mouse spleens were treated with 100 µM DAT, 1 mM DAT, or left untreated under culture conditions providing IL-2 and TCR activating beads. Frequencies of $CD8^+$ T cells expressing **(A)** T-bet, **(B)** IFN-γ, **(C)** CD25, **(D)** CD69, and **(E)** CD25 and CD96. Frequencies of $CD4^+$ T cells expressing **(F)** T-bet, **(G)** IFN-γ, **(H)** CD25, **(I)** CD69, and **(J)** CD25 and CD96. [one-way ANOVA with Tukey's multiple comparison test]. The data were obtained from 4 independent experiments. All graphs show mean with 95% CI.

When T cells were exposed to a TCR stimulus along with co-stimulatory signals provided by CD3/CD28-coated beads and recombinant IL-2, DAT notably enhanced T cell activation (Fig. 14). DAT treatment under TCR stimulating conditions led to increased percentages of $CD8^+$ T cells expressing the transcription factor T-bet, the pro-inflammatory cytokine IFN-γ, and the activation marker CD25, but not the early activation marker CD69 (Fig. 14A-E). Concerning $CD4^+$ T cells, exposure to DAT under additional TCR stimulus resulted in an increased frequency of cells expressing T-bet (Fig. 14F). The proportions of $CD4^+$ T cells expressing IFN-γ and the activation markers CD25 and CD69 were not altered by additional DAT treatment (Fig. 14GH-K).

Interestingly, none of the investigated activation markers showed increased expression on $CD8^+$ T cells in the absence of a TCR stimulus (Fig. 15A-C). Similar to $CD8^+$ T cells, $CD4^+$ T cells showed no increased expression of any activation markers without an additional TCR stimulus (Fig. 15D-F).

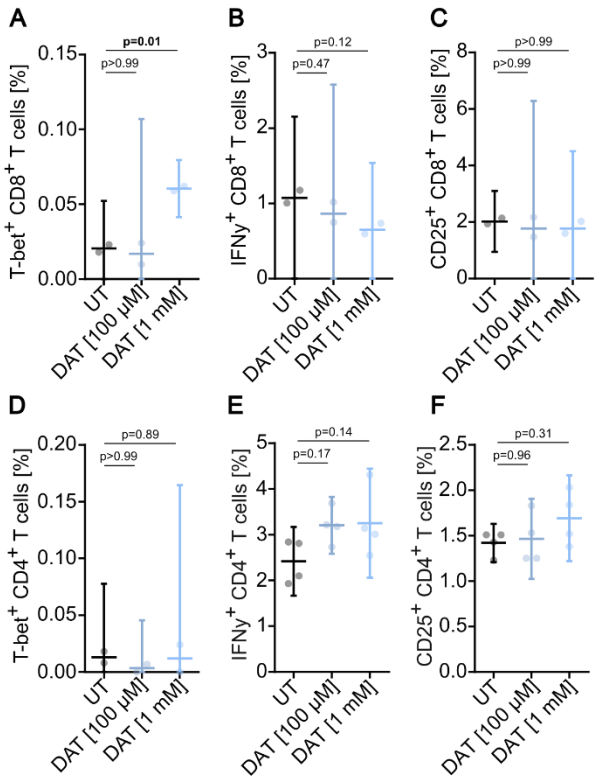

Figure 15: DAT-induced T cell activation needs a TCR stimulus
T cells from C57Bl/6j mouse spleens were treated with 100 µM DAT, 1 mM DAT, or left untreated under culture conditions providing IL-2. Frequencies of $CD8^+$ T cells expressing **(A)** T-bet, **(B)** IFN-γ, and **(C)** CD25. Frequencies of $CD4^+$ T cells expressing **(D)** T-bet, **(E)** IFN-γ, and **(F)** CD25. [one-way ANOVA with Tukey's multiple comparison test]. The data were obtained from 4 independent experiments. All graphs show mean with 95% CI.

Within DCs, DAT led to maturation characterized by heightened surface expression of the co-stimulatory molecules CD80 or CD86, but this effect was observed exclusively when DCs were

concurrently subjected to LPS (Fig. 16A-B). LPS is a constituent of the outer membrane of gram-negative bacteria and serves as a molecular pattern that activates Toll-like receptor.[173]

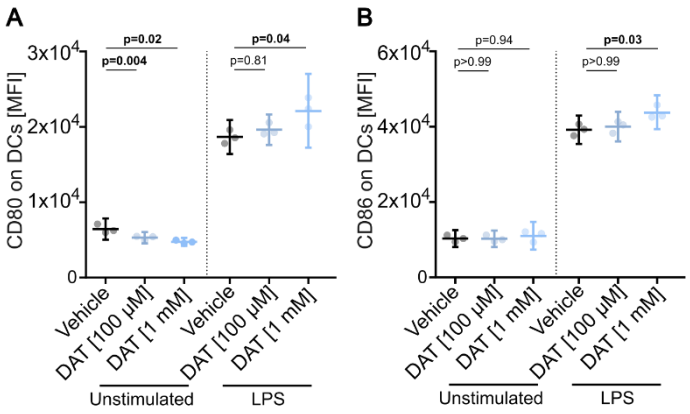

Figure 16: DAT directly enhances DC activation *in vitro*
DCs from C57Bl/6j mouse bone marrow were treated with 100 µM DAT, 1 mM DAT, or left untreated under culture conditions providing either LPS or no stimulus. The expression of the activation markers **(A)** CD80 and **(B)** CD86 were assessed via flow cytometry. The data were obtained from 3 independent experiments. All graphs show mean with 95% CI.

These findings provide evidence that DAT has the capacity to directly stimulate the activation of both T cells and DCs. However, it is important to note that this process may require additional signals, such as TCR engagement in the case of T cells or microbial co-stimulatory signals in DCs.

3.4 DAT amplifies the antigen-specific priming and proliferation of cytotoxic T cells

The analysis of the TME revealed an increased abundance of activated IFN-γ-producing T cells following DAT supplementation during anti-CTLA-4 immunotherapy. However, the data obtained did not allow differentiation regarding the impact of DAT on T-cell priming, effector function, or both. Subsequently, an evaluation was conducted to assess the potential of DAT to modulate T-cell priming in a controlled vaccination model without tumor development. This model employed purified OVA protein and the RIG-I ligand 3pRNA as an adjuvant in naïve mice. Starting on day 0, administration of DAT via drinking water was initiated, with a subsequent s.c. vaccination on day 7 involving OVA and 3pRNA.

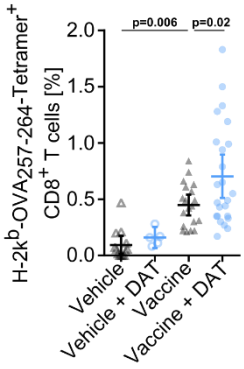

Figure 17: DAT amplifies the antigen-specific priming and proliferation of cytotoxic T cells
C57Bl/6j mice were injected with the vaccine containing 10 µg 3pRNA and 50 µg ovalbumin protein or the vehicle s.c. into the upper thigh 7 days after starting DAT administration via the drinking water. Seven days after the vaccination tumor antigen-specific T cells from the blood were analyzed via flow cytometry [Kruskal-Wallis test with Dunn's multiple comparison test]. The data were obtained from 5 independent experiments. All graphs show median with the CI at the requested confidence level of 95%.

In accordance with earlier observations, DAT supplementation alone failed to enhance the priming and proliferation of OVA antigen-specific T cells. Nevertheless, it significantly augmented the expansion of circulating OVA antigen-specific T cells when combined with the 3pRNA adjuvant (Fig. 17).

Following vaccination, mice were subjected to a tumor challenge involving bimodal inoculation of B16.OVA tumor cells, administered subcutaneously and intravenously. The i.v. injection of B16.OVA tumor cells results in the formation of lung pseudo-metastases, providing a more aggressive challenge than s.c. tumors.[227,228] Mice that received the combined vaccine, which included the 3pRNA adjuvant and oral DAT administration, demonstrated significant improvements in subcutaneous tumor control (Fig. 18A) and exhibited enhanced systemic tumor control, as evident from the reduction in the number of pulmonary pseudo-metastases (18B and C). These findings provide robust evidence that DAT treatment amplifies the antigen-specific priming and expansion of cytotoxic T cells, ultimately resulting in potent antitumor activity.

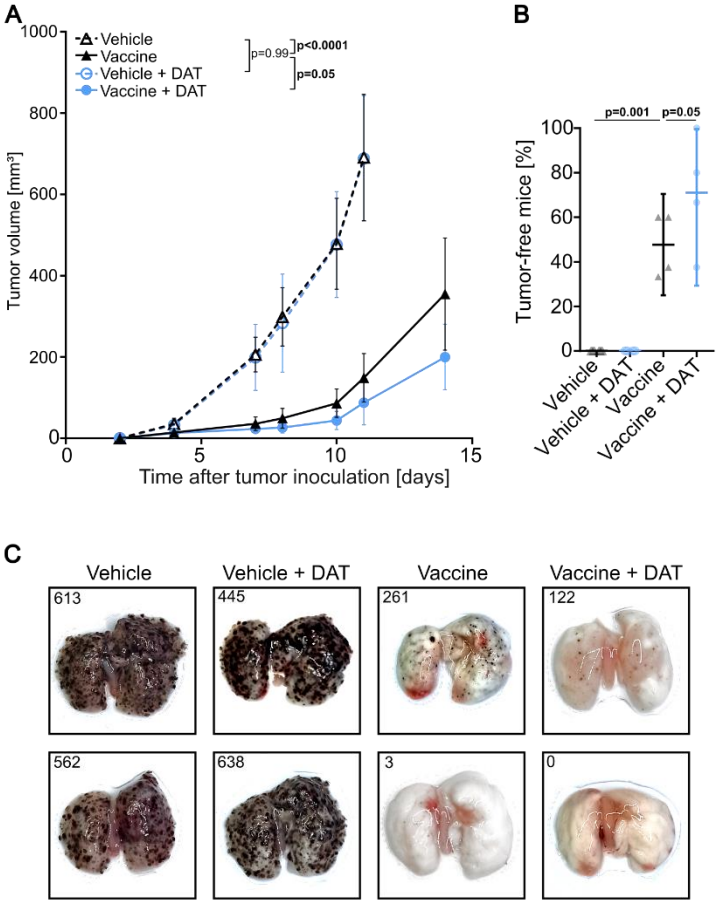

Figure 18: DAT enhances antitumor immunity after vaccination in tumor challenge models
C57Bl/6j mice were injected with the vaccine containing 10 µg 3pRNA and 50 µg ovalbumin protein or the vehicle s.c. into the upper thigh 7 days after starting DAT administration via the drinking water. Seven days after the vaccination mice were injected s.c. and i.v. with B16.OVA cells. **(A)** The tumor volume of s.c. tumors was measured frequently [two-way ANOVA with Tukey's multiple comparison test on day 11 and additional unpaired t-test with Welch's correction for 'vaccine' and 'vaccine + DAT' group on day 14]. 13 days after tumor cell inoculation lung pseud-metastases were counted and **(B)** the percentage of tumor-free mice per experiment (< 5 dots per lung) was calculated. **(C)** Representative images of lungs with pseud-metastases [one-way ANOVA with Bonferroni's multiple comparison test]. The data were obtained from 4 independent experiments. All graphs show mean with 95% CI.

4. Cytotoxicity assessment reveals no impact of DAT and ICA on B16.OVA tumor cells

As bacterial-derived metabolites like anacardic acid can induce apoptosis in tumor cells and reduce proliferation, the cytotoxicity of DAT on tumor cells and the potential to directly eliminate tumor cells was investigated.[207,226] Therefore, a MTT assay was performed. In the MTT assay, live cells with active mitochondria convert the colorless MTT reagent into a purple formazan product. The amount of formazan produced is directly proportional to the number of viable cells. Following 24 hours of DAT treatment, the viability of B16.OVA cells was analyzed and normalized to the untreated control. Cell transfected with 3pRNA served as the positive control for tumor cell killing. Interestingly, neither cells treated with DAT nor cells treated with ICA did exhibit any differences in viability, regardless of the dose applied (Fig. 19A and B).

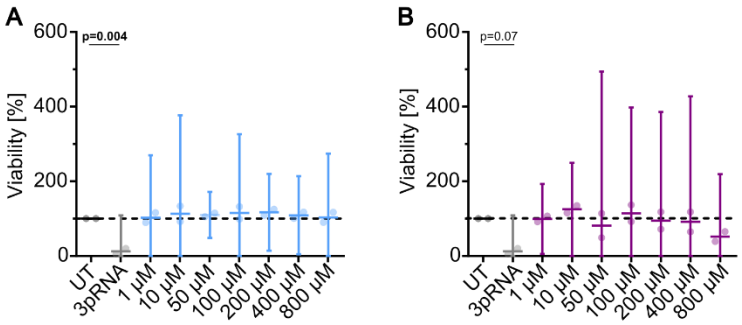

Figure 19: Cytotoxicity of DAT against B16.OVA tumor cells
B16.OVA cells were incubated with different concentrations of DAT for 24 h. Afterwards an MTT assays was performed to determine the viability of the B16.OVA cells treated with **(A)** DAT or **(B)** ICA [one-way ANOVA with Bonferroni's multiple comparison test with all not depicted comparisons being p>0.99]. The data were obtained from 2 independent experiments. All graphs show mean with 95% CI.

These results suggest that DAT and ICA are not cytotoxic to B16.OVA tumor cells, and the mechanism of action does not involve direct tumor cell killing.

5. The role of host-IFN-I signaling

5.1 Host-IFN-I signaling is required for the additive effect of DAT and anti-CTLA-4 on tumor control and survival

Considering its established function as an IFN modulator, the subsequent investigation explored the significance of host cell-intrinsic IFN-I signaling in the DAT-mediated enhancement of antitumor immunity.[178,229] As previously detailed, mice harboring a genetic deficiency in the common IFN-α receptor 1 (*Ifnar1*$^{-/-}$) exhibited an overall poor response to anti-CTLA-4 ICI treatment (Fig. 20).[224] Notably, the oral supplementation of DAT in *Ifnar1*$^{-/-}$ mice failed to exert any impact on early tumor control, as evidenced by the absence of DAT-mediated tumor growth delay (Fig. 20A-B). However, the additive effect of DAT and anti-CTLA-4 was entirely absent in *Ifnar1*$^{-/-}$ mice, leading to rapid tumor growth and diminished survival rates compared to their wild type counterparts (Fig.20C-D). Interestingly, mice treated with DAT and the isotype control presented with a survival benefit compared to the control mice which was not reflected in the tumor growth curves (Fig. 20C-D). However, there was no expansion of tumor antigen-specific T cells observed in mice treated with anti-CTLA-4, and DAT supplementation did not affect this result (Fig. 20E). The investigation of the role of host cell-intrinsic IFN-I signaling in DAT-mediated enhancement of antitumor immunity revealed that genetic deficiency in the IFN-α receptor 1 hindered anti-CTLA-4 efficacy. The oral DAT supplementation failed to delay early tumor growth and abrogated the additive effect of DAT and anti-CTLA-4 in *Ifnar1*$^{-/-}$ mice.

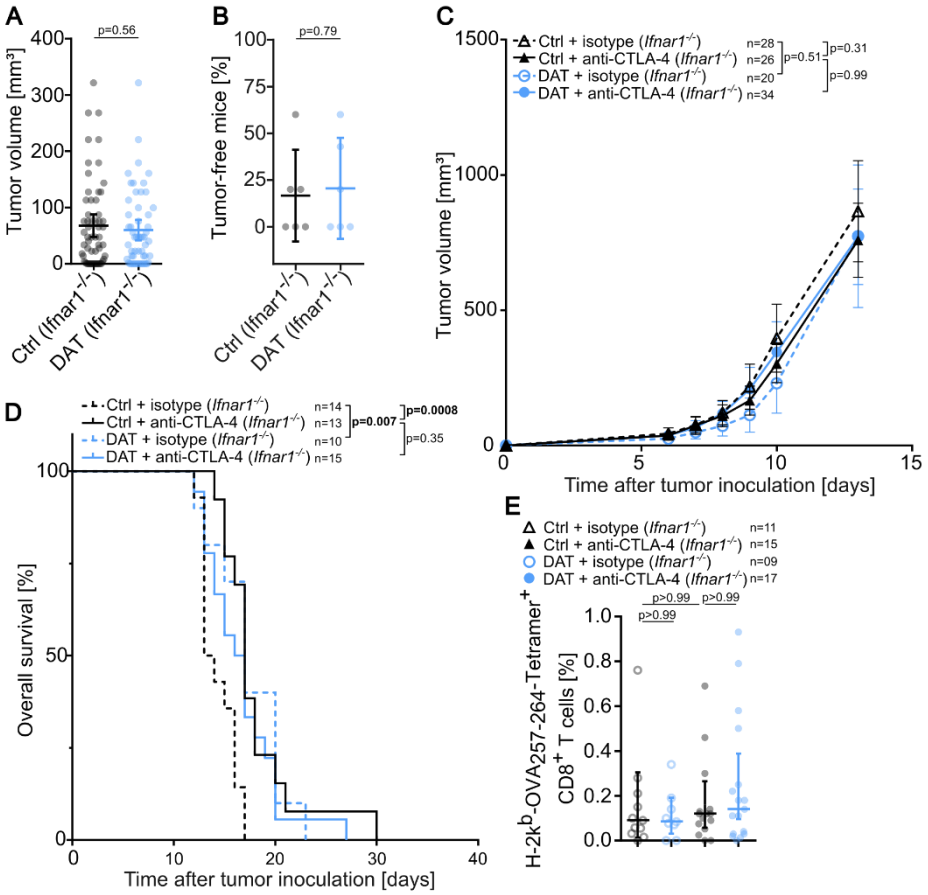

Figure 20: Host-IFN-I signaling is required for the additive effect of DAT and anti-CTLA-4 on tumor control and survival
Ifnar1$^{-/-}$ mice with C57Bl/6j background were injected s.c. with B16.OVA tumor cells on day 0 and treated with anti-CTLA-4 or isotype control antibodies on days 7, 10, and 13. From the day of tumor cell inoculation on mice were administered with DAT via drinking water until the end of the experiment. **(A)** Tumor volume and **(B)** percentage of tumor-free mice per experiment on day 7 comparing control mice with mice that received DAT [unpaired t-test]. **(C)** Tumor growth curves and **(D)** overall survival [two-way ANOVA with Tukey's multiple comparison test on day 13 for growth curves and Log-rank (Mantel-Cox) test for Kaplan-Meier survival]. **(E)** On day 15 tumor antigen-specific T cells were analyzed via flow cytometry [Kruskal-Wallis test with Dunn's multiple comparison test]. The data were obtained from 3-6 independent experiments. All graphs show mean with 95% CI or median with the CI at thr requested confidence level of 95%.

5.2 The additive impact of DAT and anti-CTLA-4 on immune cell activation in the TME requires host-IFN-I signaling

To confirm the previous results on cellular level, the TME of *Ifnar1*$^{-/-}$ mice was analyzed via flow cytometry. It is noteworthy that oral DAT supplementation did not mitigate the detrimental consequences of impaired host IFN-I signaling on the therapeutic efficacy of anti-CTLA-4. Consequently, when examining the TME in *Ifnar1*$^{-/-}$ mice, there was no observed increase in the abundance of activated T and NK cells in response to anti-CTLA-4, whether administered as monotherapy or in conjunction with oral DAT supplementation (Fig. 21A-L). Notable changes in other immune cell populations of the TME such as DCs could not be observed as well (Fig. 21M and N).

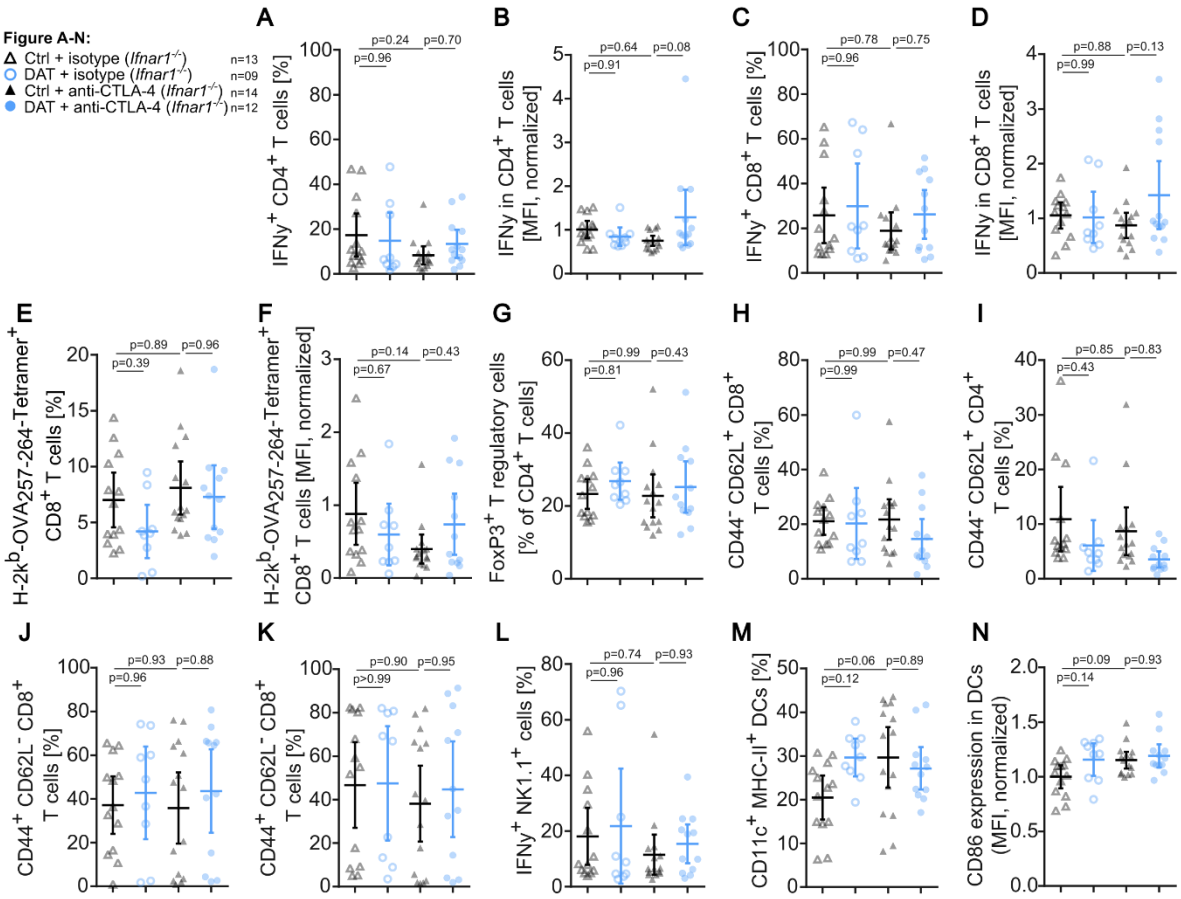

Figure 21: DAT supplementation does not alter the TME or enhance anti-CTLA-4-mediated T cell activation in *Ifnar1*$^{-/-}$ mice
On day 15 mice (described in figure 8) were sacrificed and tumors were extracted. The cells from the TME were analyzed via flow cytometry. **(A)** Frequencies of activated CD4$^+$ T cells and **(B)** their expression of IFN-γ (MFI, normalized to the 'control + isotype' group). **(C)** Frequencies of activated CD8$^+$ T cells and **(D)** their expression of IFN-γ (MFI, normalized to the 'control + isotype' group). **(E)** Frequencies of tumor antigen-specific T cells and **(F)** their expression of IFN-γ (MFI, normalized to the 'control + isotype' group). Frequencies of **(G)** regulatory T cells, **(H)** naïve CD8$^+$ T cells, **(I)** naïve CD4$^+$ T cells, **(J)** CD8$^+$ TEMs, **(K)** CD4$^+$ TEMs, **(L)** IFN-γ expressing NK cells, **(M)** DCs and **(N)** their expression of IFN-γ (MFI, normalized to the 'control + isotype' group) [one-way ANOVA with Tukey's multiple comparison test]. The data were obtained from 3 independent experiments. All graphs show mean with 95% CI.

These findings underscore the critical reliance of DAT-mediated enhancement of anti-CTLA-4 immunotherapy on intact host IFN-I signaling. However, it is important to note that these data do not elucidate whether DAT actively modulates IFN-I signaling or exerts its influence on downstream immunomodulatory functions within host (immune) cells mediated by IFNAR1.

6. The effect of DAT on anti-CTLA-4 therapy is not dependent on the gut microbiome but DAT is able to modify the microbial composition

6.1 DAT mitigates the antibiotic-induced efficacy reduction of anti-CTLA-4 therapy

The use of broad-spectrum antibiotics prior to ICI therapy remains a major clinical challenge as these antibiotics lead to adverse effects with associated gut dysbiosis on immunotherapy.[230–234] To assess whether oral DAT supplementation could mitigate the detrimental impacts of gut dysbiosis, mice were administered a mixture of broad-spectrum antibiotics (Abx), which included ampicillin, neomycin, vancomycin, metronidazole, and the antifungal agent amphotericin B prior to the inoculation of B16.OVA tumor cells and subsequent treatment. DAT was added to the Abx drinking water on the day of tumor cell inoculation. In fact, mice receiving the Abx solution displayed significant alterations in their gut microbiota characterized by poor bacterial growth in both conventional aerobic and anaerobic culture settings of stool samples (Fig. 22A). 16S-rRNA analysis was performed to confirm the depletion of the intestinal microbiome of Abx-treated mice (Fig. 22B).

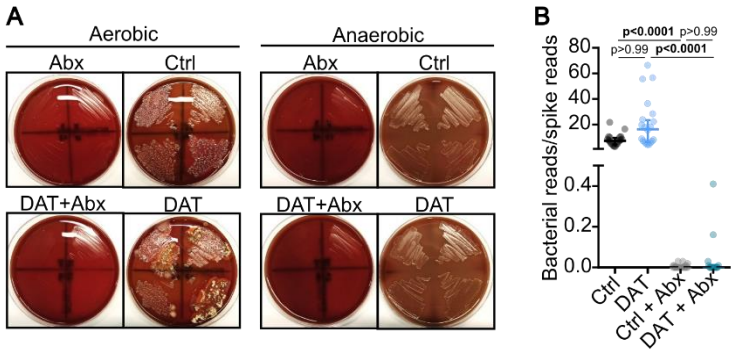

Figure 22: The gut microbiota was depleted successfully in mice treated with Abx
C57Bl/6j mice were injected s.c. with B16.OVA tumor cells on day 0 and treated with anti-CTLA-4 or isotype control antibodies on days 7, 10, and 13. From the day of tumor cell inoculation on mice were administered with DAT via drinking water until the end of the experiment. Additionally, mice were treated with broad-spectrum antibiotics (Abx) starting 5 days prior to the tumor cell injection until day 21. The depletion status of the gut microbiome was assessed by **(A)** plating stool samples on blood agar plates for 48 h under aerobic and anaerobic conditions (representative images) and by **(B)** 16S-rRNA sequencing of stool samples and the calculation of bacterial reads vs. spike reads [Kruskal-Wallis test with Dunn's multiple comparison test]. All graphs show median with the CI at the requested confidence level of 95%.

In line with prior studies, the administration of anti-CTLA-4 treatment did not lead to enhanced tumor control or prolonged survival in mice subjected to prior Abx treatment (Fig. 23A and B).[199] Intriguingly, oral administration of DAT resulted in partial restoration of the anti-CTLA-4 efficacy in Abx-treated mice. Although the intestinal bacterial population was significantly reduced, DAT in combination with anti-CTLA-4 led to enhanced tumor control and significantly prolonged survival in these mice (Fig. 23A and B). Interestingly, the decreased expansion of circulating tumor antigen-specific T cells in anti-CTLA-4 treated mice that were exposed to Abx treatment could be recovered by additional DAT supplementation (Fig. 23C). Control groups that did not

receive Abx treatment were run in parallel to validate the efficacy of the anti-CTLA-4 treatment and the additional impact of DAT. The corresponding data for these control groups are presented in additional graphs for readability (Fig. 23D-F). Comparing the mice that received the combination of DAT and anti-CTLA-4 under antibiotic (Abx) conditions with those that had the combined treatment without Abx-induced dysbiosis, it was observed that DAT could nearly restore the antitumor response to the level of non-dysbiotic mice. Collectively, these findings indicate that while oral DAT supplementation is unable to prevent intestinal dysbiosis subsequent to broad-spectrum antibiotic treatment, it has the capacity to reduce the negative effects of the dysbiosis on the effectiveness of anti-CTLA-4 immunotherapy.

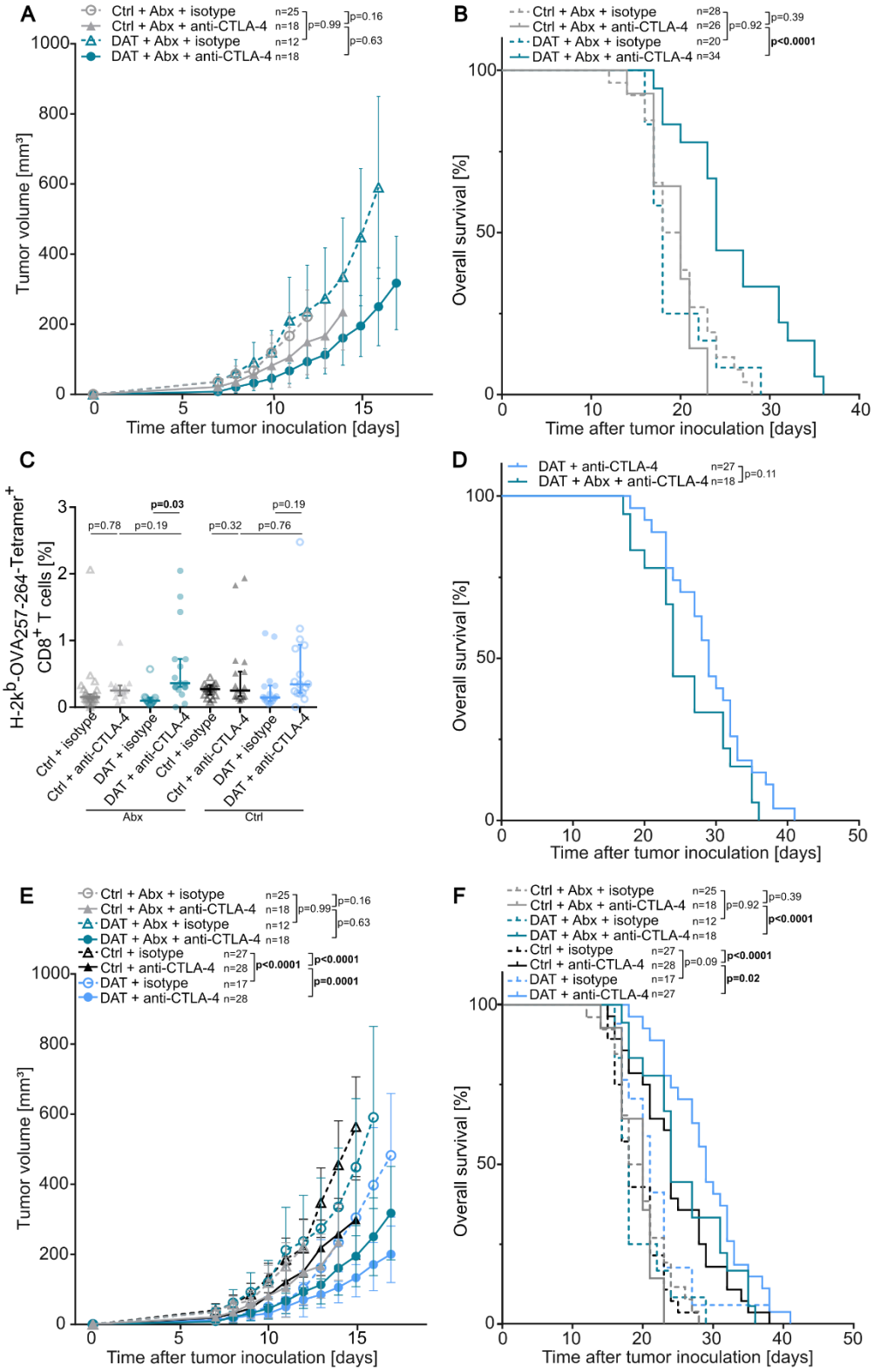

Figure 23: DAT ameliorates the Abx-induced efficacy reduction of anti-CTLA-4 therapy
C57Bl/6j mice were injected s.c. with B16.OVA tumor cells on day 0 and treated with anti-CTLA-4 or isotype control antibodies on days 7, 10, and 13. From the day of tumor cell inoculation on mice were administered with DAT via drinking water until the end of the experiment. Additionally, mice were treated with broad-spectrum antibiotics (Abx) starting 5 days prior to the tumor cell injection until day 21. **(A)** Tumor growth curves and **(B)** overall survival of Abx treated mice [two-way ANOVA with Tukey's multiple comparison test on day 12 for comparisons of 'Ctrl + isotype' and other groups and a two-way ANOVA with Tukey's multiple comparison test on day 14 excluding 'Ctrl + isotype' for all other comparisons (the statistical analysis was performed on the whole data set from fig. 21E) and Log-rank (Mantel-Cox) test for Kaplan-Meier survival]. **(C)** On day 15 tumor antigen-specific T cells were analyzed via flow

cytometry [Kruskal-Wallis test with Dunn's multiple comparison test]. **(D)** Comparison of the overall survival of mice treated with DAT and anti-CTLA-4 und Abx and non-Abx conditions [Log-rank (Mantel-Cox) test for Kaplan-Meier survival]. **(E)** Tumor growth curves and **(F)** overall survival of the whole data set [two-way ANOVA with Tukey's multiple comparison test on day 12 for comparisons of 'Ctrl + isotype' and other groups and a two-way ANOVA with Tukey's multiple comparison test on day 14 excluding 'Ctrl + isotype' for all other comparisons and Log-rank (Mantel-Cox) test for Kaplan-Meier survival]. The data were obtained from 3 independent experiments. All graphs show mean with 95% CI or median with the CI at the requested confidence level of 95%.

6.2 Oral DAT supplementation induces alterations in the gut microbial composition of mice

Previous research has indicated that specific bacterial taxa are enriched in patients who respond positively to treatment compared to non-responders.[184,185,187,188,196] Furthermore, it has been suggested that metabolites derived from bacteria may play a role in mediating varying antitumor immune responses.[206–210] To determine whether the favorable immunomodulatory effects of oral DAT administration were primarily due to compensating for insufficient endogenous DAT levels or actively influencing the gut microbiome composition, DAT was administered via the drinking water for a period of 7 days and fecal samples were analyzed via 16S-rRNA sequencing. The analysis revealed that the effective richness and Shannon effective diversity significantly decreased in DAT-treated mice. This suggests that the number of species and their relative abundances were lower in the stool samples of mice that received DAT supplementation (Fig. 24A and B). When examining beta-diversity, a notable dissimilarity between the gut microbiota of DAT-treated mice and untreated mice was found (Fig. 24C).

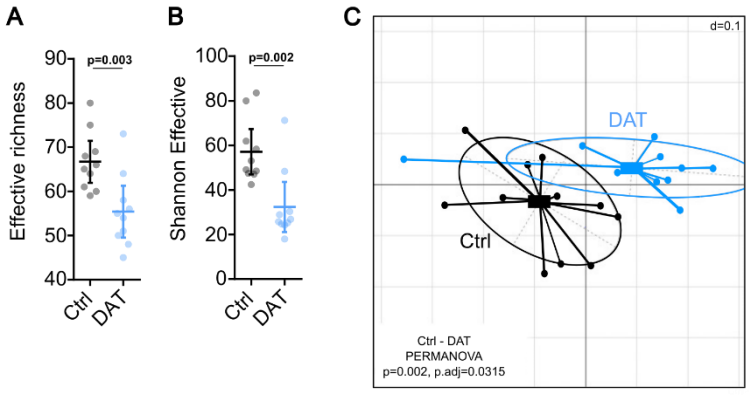

Figure 24: DAT changes the richness of the gut microbiome
C57Bl/6j mice were administered with DAT (n=10) or control (n=10) drinking water for 7 days. Stool samples were analyzed via 16S-rRNA sequencing and **(A)** the effective richness and **(B)** the Shannon effective were assessed [unpaired t-test]. **(C)** Beta-diversity was displayed as non-metric multidimensional scaling (NMDS) biplot with permutational multivariate analysis of variance (PERMANOVA). All graphs show mean with 95% CI.

Taxonomic binning was utilized to demonstrate differences among different bacterial taxa. Differences between mice administered with DAT in the drinking water and control mice could be detected on class, order, and family level, but not on genus level (Fig. 25A-D).

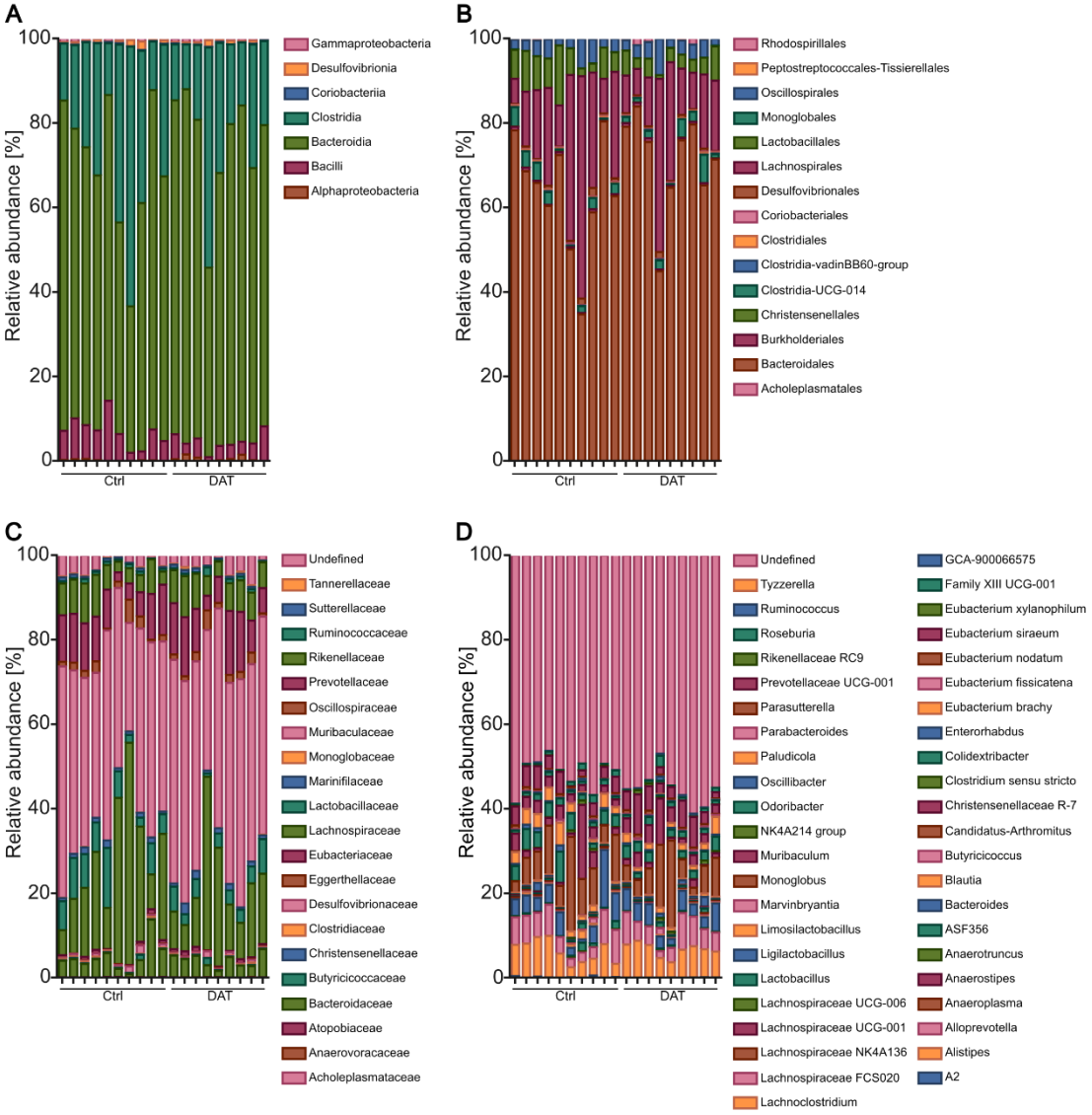

Figure 25: Taxonomic binning shows differences between DAT treated and control mice
C57Bl/6j mice were administered with DAT (n=10) or control (n=10) drinking water for 7 days. Stool samples were analyzed via 16S-rRNA sequencing and different taxa present in each sample were displayed on **(A)** class, **(B)** order, **(C)** family, and **(D)** genus level.

Analyzing the samples on class level, DAT application resulted in changes in the composition of the intestinal microbiota. Notably, the relative abundance of *Bacteroidia* significantly increased following DAT supplementation, while the relative abundance of *Clostridia*, the taxonomic class of the known DAT producer *Flavonifractor plautii* (NCBI:txid292800), decreased (Fig. 26A and B).[178,235] On order level, an increase in the relative abundance of *Bacteroidales* and *Burkholderiales* could be noticed, along with a decrease in the relative abundance of *Lachnospirales* following DAT supplementation (Fig. 26C-E). 16S-rRNA in stool

samples collected from mice before tumor inoculation and treatment with anti-CTLA-4 treatment was analyzed to retrospectively categorize them as responder or non-responder to ICI therapy. This retrospective analysis aimed to identify microbial signatures associated with therapy response, providing insight into the potential impact of DAT on modifying the gut microbiome in a way that aligns with the observed therapy response. Interestingly, *Burkholderiales* were found to be enriched in anti-CTLA-4 responder melanoma-bearing mice before treatment initiation, in the absence of DAT supplementation (Fig. 26F). On family level, an increased relative abundance of *Tannerellaceae*, alongside decreased abundances of *Lachnospiraceae* and *Oscillospiraceae* following DAT supplementation could be observed (Fig. 26G-I). Upon closer examination at the genus level, only a few distinct genera could be identified, none of which were influenced by oral DAT supplementation.

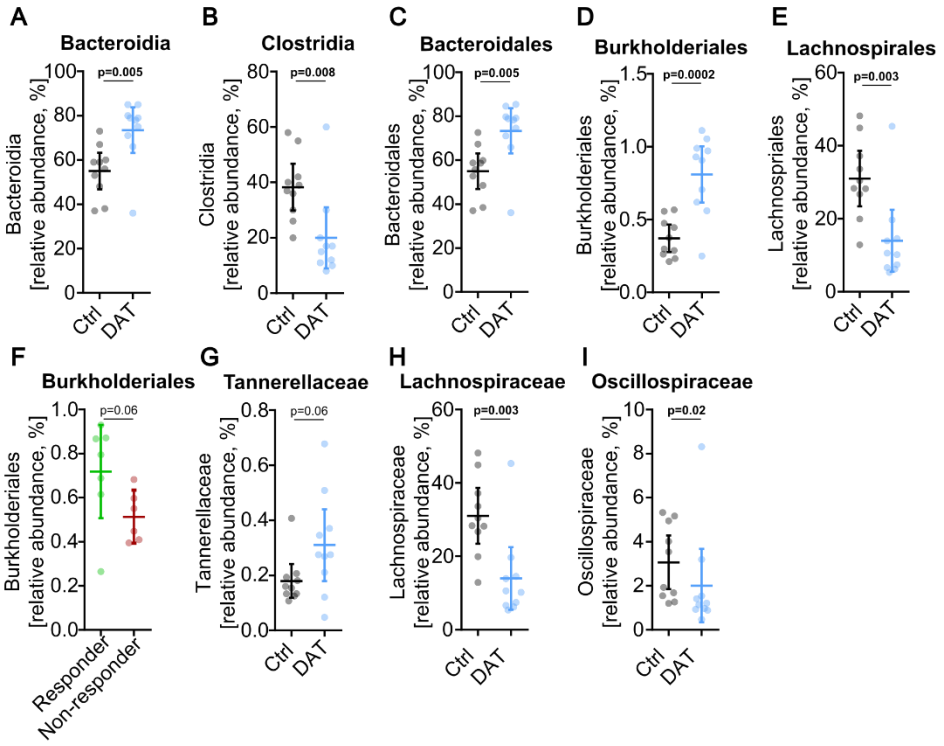

Figure 26: DAT induces differences in taxonomic composition of the gut microbiome
(A-E, G-I) C57Bl/6j mice were administered with DAT (n=10) or control (n=10) drinking water for 7 days. Stool samples were analyzed via 16S-rRNA sequencing and different taxa were compared between mice that received DAT and control mice. Relative abundances of **(A)** Bacteroidia and **(B)** Clostridia at class level, and **(C)** Bacteroidales, **(D)** Burkholderiales, and **(E)** Lachnospirales on order level [unpaired t-test]. **(F)** B16.OVA tumor bearing C57Bl/6j mice that were treated with anti-CTLA-4 were retrospectively categorized as responder and non-responder to the therapy. Stool samples from day 0 (before tumor cell inoculation) were analyzed [unpaired t-test with Welch's correction]. Relative abundances of **(G)** Tannerellaceae, **(H)** Lachnospiraceae, and **(I)** Oscillospiraceae on family level [unpaired t-test]. All graphs show mean with 95% CI.

In summary, these findings suggest that oral DAT supplementation can induce alterations in the gut microbial composition in mice. Some of the more abundant bacterial taxa can be associated with responder to anti-CTLA-4 treatment.

7. DAT and ICA do not exacerbate anti-CTLA-4-induced irAEs

One major clinical challenge associated with ICIs is the occurrence of immune-related adverse events. When considering combination therapies, concerns about these excessively stimulated and misguided immune responses become evident. Among the irAEs, colitis is a common concern in cancer patients undergoing ICI treatment, often leading to significant health issues.[106,137–140] In general, murine models exhibit low sensitivity to irAEs. Consequently, in the experimental mice clear clinical indications of ICI-induced colitis, such as bloody diarrhea or weight loss, could not be observed. Earlier reports have mentioned a subclinical form of colitis in mice treated with anti-CTLA-4 immunotherapy.[199] However, a promising approach to detect intestinal damage is via cleaved caspase-3 staining of colon sections.[199] Increased caspase-3 cleavage in large intestinal tissue sections from mice undergoing anti-CTLA-4 treatment, indicative of therapy-induced apoptosis of intestinal cells, was not observed (Fig. 27A and B). Given that the cleaved caspase-3 data yield statistical significant results, an established assay for measuring the influx of neutrophils into the gut lamina propria was employed as a highly sensitive surrogate marker for epithelial damage, loss of barrier function, and intestinal inflammation.[216] Notably, the previously reported outcome of anti-CTLA-4 treatment causing gut epithelial damage and subclinical colonic inflammation, characterized by significant neutrophil influx, could be successfully reproduced (Fig. 27C).[199] Oral supplementation with DAT appeared to completely ameliorate the gut damage induced by anti-CTLA-4 and the subsequent subclinical tissue inflammation (Fig. 27C). Yet, ICA administration resulted in a not as robust decrease of neutrophils in the lamina propria as DAT supplementation (Fig. 27C). To determine epithelial regeneration, an organoid recovery assay was employed. Increased numbers of organoids that recover from extracted crypts represent a healthy and intact epithelial barrier.[236] The assay failed to detect differences in mice treated with anti-CTLA-4 or control mice (Fig. 27D). Interestingly, crypts that were isolated from the small intestine of mice that were treated with anti-CTLA-4 and supplemented with DAT or ICA showed a higher recovery rate that led to increased numbers of organoids (Fig. 27D).

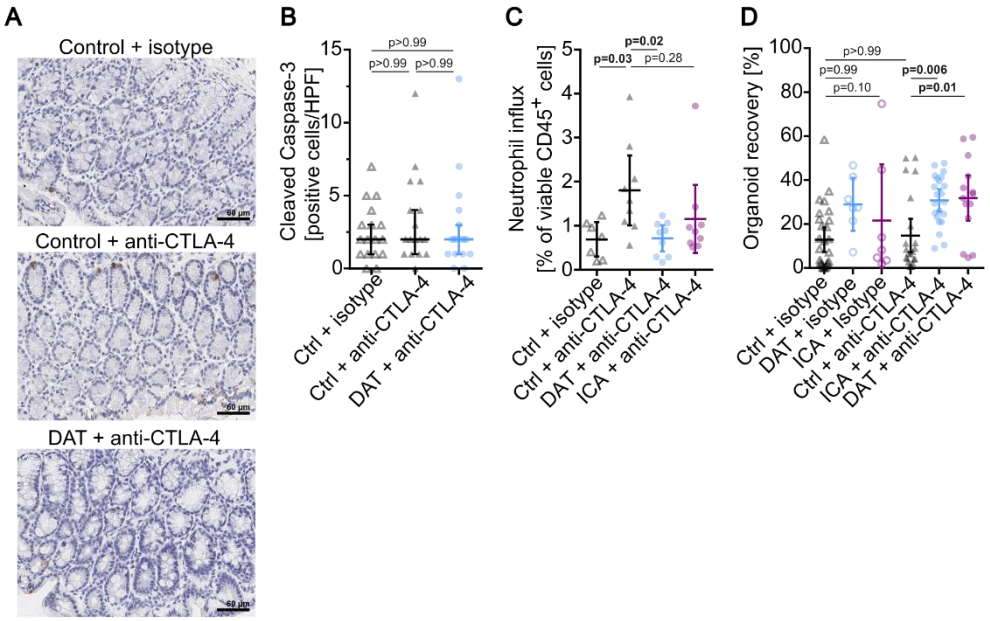

Figure 27: DAT and ICA do not aggravate anti-CTLA-4-induced immune related adverse events
C57Bl/6j mice were administered with DAT via the drinking water or gavaged with ICA from day 0 on and injected with anti-CTLA-4 or isotype control antibodies on days 7, 10, and 13. On day 15 mice were sacrificed and small intestine and colon were removed and processed. **(A)** Representative images of cleaved caspase-3 positive cells after immune histochemistry of the colon samples and **(B)** count of cleaved caspase-3 positive cells per high-power field (HPF) [Kruskal-Wallis test with Dunn's multiple comparison test]. **(C)** Neutrophil granulocyte influx into the small intestinal lamina propria was assessed via flow cytometry [one-way ANOVA with Tukey's multiple comparison test]. **(D)** Organoid recovery calculated as organoid count per 200 seeded crypts [one-way ANOVA with Tukey's multiple comparison test]. The data were obtained from 3-4 independent experiments. All graphs show mean with 95% CI or median with the CI at the requested confidence level of 95%.

In summary, these results suggest that combining oral DAT or ICA supplementation with anti-CTLA-4 does not exacerbate irAEs like colitis. Instead, DAT even has the potential to reduce colonic anti-CTLA-4-induced inflammation.

IV DISCUSSION

1. The experimental model and treatment schedule

The B16.OVA model is often used for studying primary tumor growth, whereas human melanoma is known for its propensity to metastasize to other organs, making it a more complex and lethal disease which is a critical aspect.[7,237,238] In patients, metastatic melanomas most commonly exhibit metastases in local and distant lymph nodes and lungs.[237,238] When injected intravenously into the tail vein B16.OVA migrate to the lungs and form aggressive pseudo-metastases as presented in the current study and in the literature.[227,228] Therefore, in addition to studying subcutaneous tumors, the current work here explored the more aggressive lung pseudo-metastases and revealed that DAT has a noteworthy impact in that context as well. The primary advantage of the B16.OVA model is the possibility to track antigen-specific immune responses, including the analysis of tumor antigen-specific T cells in the circulation or the TME, as well as its suitability for vaccination approaches as shown in the present study. The model antigen makes these tumors more immunogenic.[239] To circumvent the possibility that the observed effects were limited to B16.OVA some experiments were performed with the pancreatic adenocarcinoma cell line Panc02.

The timing and sequencing of treatments can significantly impact their efficacy. It is essential to determine when to administer ICI therapy, bacterial metabolites, or both to achieve the most potent antitumor effects. This may involve evaluating whether concurrent treatment, combination therapy, or sequential administration is more effective. In patients, ICIs are often administered at regular intervals, such as every two to three weeks.[12,13,15,95,100] This schedule allows for consistent and sustained immune checkpoint blockade to maintain the activation of immune responses against cancer cells. Here, an *in vivo* ICI application schedule that has been previously described and established, mirroring common treatment schedules found in the literature was employed.[224,240] This treatment schedule with anti-CTLA-4 significantly improved tumor control but still had room for further enhancement of tumor control and long-term survival through combination with metabolites.

Some studies have explored concurrent treatment, where probiotics or bacterial metabolites are administered alongside conventional cancer therapies. This approach aims to leverage the immune-boosting properties of bacterial metabolites while treating the tumor directly and can often be combined with a pretreatment approach. It can enhance immune responses and potentially improve treatment outcomes.[206,210,241–244] This is in line with the results presented here. The specific time point of treatment onset seems to be strongly dependent on the tumor entity and the bacterial metabolites (or probiotics) as it was shown in the B16.OVA murine model where pretreatment was combined with concurrent anti-CTLA-4 treatment. Starting the DAT administration on a later time point reduced the combinatorial treatment effect. As of today,

no studies investigated the administration of bacterial metabolites or specific bacterial species solely as a pretreatment to prepare the immune system or sensitize tumor cells to subsequent treatment. The only approach has been the colonization of GF or Abx treated mice with defined bacterial species.[206,245,246] The results with DAT in the B16.OVA model give a hint that the immune system was primed due to delayed tumor growth before onset of immunotherapy. Bacterial species and their metabolites can also be used as adjuvants after primary cancer treatment (e.g. surgery or chemotherapy). This approach seeks to prevent cancer recurrence, to promote long-term immune memory, or to reduce side effects. [243,247]

The effectiveness of oral administration can vary depending on factors like metabolite stability and gut absorption.[248] In contrast, intravenous administration ensures direct and rapid metabolite delivery into the bloodstream.[248] However, the administration of the metabolite inosine had the same effect whether given orally or intravenously.[206] Due to the superior outcomes achieved with continuous but slow high-dose administration throughout the day, as opposed to low-dose application via gavage, and considering its toxicity when administered as a single high dose, the most feasible method of application appeared to be the oral administration of DAT via the drinking water.

The effectiveness of these strategies may vary based on cancer type, stage, and patient characteristics. Here, ICA was shown to have an additive effect with combined anti-CTLA-4 treatment in the B16.OVA model but not with combined ant-PD-1 in the Panc02 model. Moreover, individualized treatment plans may be necessary to account for patient-specific factors, such as microbiome composition and immune status. In summary, the timing and application form of bacterial metabolites in cancer therapy depend on multiple factors and need further investigation.

2. The effect of bacterial metabolites on immune cells

The interplay between the gut microbiota and the immune system has gained increasing attention in recent years due to its profound impact on host health. Bacterial metabolites, particularly SCFAs and other bioactive compounds, play pivotal roles in regulating immune cell function.[181,206,208,210,244,249]

In the present study, DAT, when combined with anti-CTLA-4, significantly enhanced the activation of both $CD8^+$ and $CD4^+$ T cells *in vivo*. A study investigating the microbial metabolite inosine observed that tumor-bearing mice that received inosine, anti-CTLA-4, and a co-stimulus showed higher frequencies of IFN-γ expressing $CD4^+$ and $CD8^+$ T cells in the TME contributing to antitumor immunity against intestinal cancer, bladder cancer, and melanoma.[206]

In the present study, similar effects could be observed with DAT administration. Interestingly,

DAT could enhance the efficacy of anti-CTLA-4 and induce higher frequencies of activated T cells without the need for an additional stimulus *in vivo* whereas an additional TCR stimulus was necessary to ensure T cell activation *in vitro*. *In vivo*, various factors such as interactions with other cell types, signaling molecules, and the overall physiological context may contribute to a more nuanced and efficient T cell activation in the presence of DAT and anti-CTLA-4, compared to the simplified conditions of an *in vitro* setting. The tissue microenvironment plays a crucial role in immune cell activation. In some tissues, co-stimulatory molecules may be readily available, while in others, the microenvironment may lack the necessary co-stimulatory signals.[250,251] The effect of inosine relies on the presence of the adenosine A_{2A} receptor on T cells and, just like DAT *in vitro*, requires co-stimulation.[206] Furthermore, other bacterial-derived metabolites like SCFAs, such as butyrate, enhance $CD8^+$ T cell memory and promote memory differentiation of activated $CD8^+$ T cells. It has been demonstrated that butyrate enhances $CD8^+$ T cell function in a receptor-dependent manner, highlighting even more the role of bacterial metabolites in T cell responses.[249] Furthermore, aryl hydrocarbon receptor (AhR) agonist I3A was found to promote the activation of $CD8^+$ T cells and to enhance ICI therapy.[210] One study identified sodium butyrate to decrease the proportion of Tregs and to increase Th17 and NKT cells.[252] But bacterial-derived metabolites can also have opposite effects. Especially within the group of SCFAs opposing results have been published. For example, SCFAs butyrate and propionate have been shown to increase *de novo* Treg generation, shape the colonic Treg pool, and increase the numbers of Tregs in general, leading to immune tolerance.[181,212] Furthermore, one study noticed that butyrate hinders co-stimulatory signals that enhance the activation and proliferation of T cells and the accumulation of T cells that specifically target the tumor during anti-CTLA-4 therapy.[212]

Interestingly, DC activation could be triggered by DAT in combination with LPS in a controlled *in vitro* environment, but no increased DC activation was observed in the *in vivo* experiments. In general, bacterial-derived metabolites are capable to stimulate DCs in mice but conversely, they can also limit their activation.[212,253] Yet, tumors can create immunosuppressive microenvironments that inhibit the activation of DCs.[254] Even though DAT and anti-CTLA-4 may enhance T cell activation, immunosuppressive factors within the tumor could abrogate these effects on DCs *in vivo*. Even if the overall DC activation is not increased, the subset of DCs capable of cross-presentation may play a pivotal role in activating cytotoxic T cells.[255] To fully understand the role of DCs in the DAT melanoma model this aspect necessitates further exploration with the detailed analysis of multiple DC subsets.

Apart from T cells and DCs, other immune cells have been reported to be affected by microbial products and metabolites as well. The bacterial-derived metabolite anacardic acid was found to induce the production of neutrophil extracellular traps (NETs) which leads to NK cells, macrophages and CTLs infiltrating the tumor.[207,225,256,257] This aligns with the finding that DAT

also increases the frequencies of IFN-γ-expressing NK cells *in vivo*, in addition to T cells. The more increased frequencies of activated NK cells *in vivo* it might explain the counterintuitive observation of activated T cells but not the significant increase of DC activation. Cytokines released by other immune cells, such as macrophages or NK cells, can also contribute to T cell activation.[258,259] While DCs are considered to mainly present antigen, macrophages can present antigens to T cells as well.[255] These alternative APCs might compensate for any shortcomings in DC activation. Furthermore, it is suggested that DAT affects bone marrow-derived macrophages (BMDMs) as well by inducing an increase expression of ISGs *in vitro*.[178] Moreover, butyrate can induce the differentiation of macrophages and therefore enhance their antimicrobial capabilities.[260]

The gut microbiota is a complex ecosystem comprising various bacterial species, each capable of producing a unique array of metabolites. Understanding how different bacterial metabolites, such as DAT, ICA, inosine, or SCFAs, interact with one another and collectively influence immune cell behavior is an ongoing area of research. Bacterial metabolites are a diverse group of molecules, and their effects on immune cells can vary widely. The immune system likely integrates signals from multiple metabolites to fine-tune immune responses in a context-specific manner. The intricate interplay between these bacterial metabolites and immune cells underscores the complexity of the gut-immune axis.

3. The composition of the gut microbiome

3.1 Broad-spectrum antibiotics-induced changes and implications

The use of broad-spectrum antibiotics in cancer patients, though crucial for preventing life-threatening bacterial infections, raises concerns regarding their impact on the efficacy of ICIs.[261,262] On the one hand infections can lead to treatment interruptions, delaying the administration of ICIs and potentially compromising their effectiveness. On the other hand broad-spectrum antibiotics lead to gut dysbiosis, characterized by a loss of diversity, depletion of essential microbial species, and a diminished capacity for defense against invasive pathogens.[263] Following exposure to antibiotics, gut dysbiosis sets in rapidly, and it can require more than six weeks for the human microbiome to recover after the administration of broad-spectrum antibiotics.[264,265] Multiple studies associate the use of broad-spectrum antibiotics prior to ICI therapy with poor response, decreased PFS and OS, and a higher tumor burden in different tumor entities.[230–234,266,267] In the present study, the administration of antibiotics equally led to impaired response to anti-CTLA-4 and thus decreased OS in mice.

Notably, microbial-derived metabolites like DAT can be utilized even during continuous antibiotic treatment, a possibility not afforded by the administration of specific bacterial species or consortia, thus opening up new opportunities for application. In this study, DAT administration could reverse the adverse effects of antibiotic treatment on anti-CTLA-4 efficacy. With the underlying depletion of the gut microbiome, this demonstrates that DAT can act independently of a functional gut microbiome and supports the hypothesis that its antitumor efficacy, according to the TME and *in vitro* data, is achieved through direct effects on immune cells. One study found that while some probiotic bacteria are commonly prescribed to prevent antibiotic-associated dysbiosis, they delay and have an incomplete effect on reconstituting the gut mucosal microbiome in both mice and humans after antibiotic treatment.[268] The effect of probiotic bacteria on the recovery of the intestinal microbiome after antibiotic administration has been poorly studied so far, and bacterial metabolites have not been thoroughly examined either. It cannot be ruled out that DAT may have similar effects due to its potential influence on the intestinal microbiome. On the other hand, positive effects on recolonization cannot be ruled out either and further investigation on this topic is necessary.

The use of broad-spectrum antibiotics prior to ICI therapy in cancer patients is a complex issue. Decisions regarding antibiotic use should be made on a case-by-case basis, weighing the risks of infection against the potential consequences of microbiome disruption. By harnessing bacterial-derived metabolites, it becomes possible to overcome certain challenges associated with the use of broad-spectrum antibiotics.

3.2 Metabolite-induced changes and implications

The results highlighting the impact of DAT on immune cells, combined with the findings from the antibiotic experiments, clearly indicate that DAT can influence immune cells and thus the antitumor response is independent of the gut microbiome or in compensation for missing microbial signals. However, it is important to assess to what extent DAT may influence the microbiome and thus potentially other signaling pathways.

Although a high α-diversity is typically viewed as a sign of a healthy gut microbiota, several meta-analyses have failed to establish a link between gut microbial diversity and responsiveness of patients to immunotherapy involving ICIs.[269,270] DAT did even decrease the α-diversity but still was efficient in tumor control. DAT supplementation led to a decline in the relative abundance of *Clostridia*, a group of microorganisms that are obligate anaerobes. Among the members of this class, certain species like *Flavonifractor plautii* (formerly known as *Clostridium orbiscindens*) have been identified as contributors to DAT production[178]. Interestingly, a high abundance of DAT producing *F. plautii* is associated with CRC in an Indian

cohort.[271] Assuming a dysbiosis with increased numbers of *F. plautii* leads to enhanced degradation of flavonoids, it implies that beneficial flavonoids and their bioavailability are missing, which could promote CRC. Nonetheless, the function of naturally occurring DAT originating from the predominant gut microbiota, as opposed to therapeutically administered DAT, remains uncertain. The data here indicate a potential link between endogenous DAT levels in stool samples and the subsequent response to anti-CTLA-4 immunotherapy, but this association must be approached with caution, as the levels of DAT in murine stool samples were close to the detection limit of the mass spectrometry technique employed.

Based on the data obtained from melanoma-bearing mice, it was observed that DAT supplementation had the capacity to augment the abundance of *Burkholderiales* in the gut microbiome. The correlation with the increased abundance of *Burkholderiales* in responder mice suggests that the increase in *Burkholderiales* in DAT treated mice indicates a potential beneficial effect of DAT on the gut microbiome. Furthermore, *Bacteroidales* which were enriched upon DAT supplementation are also positively correlated with disease control in mice.[199] *Lachnospirales*, and more specifically *Lachnospiraceae*, are generally described as beneficial taxa in the immunotherapy setting.[272,273] However, DAT supplementation resulted in a decrease in their abundance. Notably, the interpretation of the significance of these results is controversial. In microbiome 16S-rRNA studies, nucleic acid extraction is a critical step, and debates have emerged about the best protocol to accurately represent microbial diversity.[274] The accuracy of taxonomic classification also depends on the quality and comprehensiveness of the reference databases. In comparison to shotgun sequencing 16S-rRNA sequencing recovered less data regarding low-abundance genera and phyla.[275,276] Furthermore, microbiome research involves choices regarding the hypervariable regions of the 16S-rRNA gene, primers, sequencing platforms, databases, and computational tools. These choices can impact the results and comparability of studies, and a standardized approach in this field is still lacking.[274] These differences among different studies may explain the discrepancy between some results in the literature. Interestingly, most studies on other bacterial metabolites, such as inosine or SCFAs, have not investigated the potential effects of these metabolites on the gut microbiome.[206,209]

Moreover, the interpretation of microbial data is significantly influenced by niche-specific interaction networks and the progression of disease.[277,278] It is established that microbes can form diverse microbial networks, interact with each other, and create correlation or co-occurrence networks, potentially leading to microbe translocation.[279,280] Microbes can impact tumor responses at distant locations through systemic effects, such as microbial-derived metabolites in the bloodstream or the translocation of microorganisms through the gut epithelium.[281–283] Apart from potential direct impacts on immune cells, the early tumor control observed in this study could be partly attributed to the influence of DAT on the gut microbiome.

While DAT supplementation impacts microbial diversity and specific taxa in the gut, the nuanced interplay of these changes in the context of disease progression and microbial networks necessitates further investigation.

4. DAT as an IFN-I modulator in antitumor immunity

Recent research has shed light on the intricate interplay between the host's immune response and the efficacy of ICIs, particularly emphasizing the role of host IFN-I signaling. *Ifnar1*$^{-/-}$ mice present with enhanced angiogenesis and tumorigenesis.[284] Interestingly, the tumors extracted from *Ifnar1*$^{-/-}$ mice contained more blood than tumors from WT mice (data not available) which is in line with this observation. As described before, the treatment with ICIs is dependent on intact host-IFN-I signaling.[55,224] In line with these results, tumor growth was observed to be more aggressive in *Ifnar1*$^{-/-}$ mice and the mice responded poorly to anti-CTLA-4 treatment in the present study. Oral DAT supplementation could not circumvent or neutralize the severe defect of anti-CTLA-4-induced antitumor immunity which reinforces the idea that DAT strengthens antitumor immunity through IFN-I signaling. It could potentially be one of the microbial factors needed to sustain the production of basal IFN-I in this particular scenario. Additionally, the protective effect of a DAT-producing bacterial strain against influenza, by increasing interferon levels and suppressing viral replication, provides additional evidence for this hypothesis.[179] In line with these results, other bacterial-derived metabolites such as acetate have been shown to be dependent on IFN-I signaling via IFNAR to ameliorate signs of disease.[285] Earlier studies have recognized that the intestinal microbiota plays a role in sustaining constitutive host IFN-I expression through nucleic acid-sensing PRRs like cGAS/STING or RIG-I, thus enabling both anti-viral and antitumor immune responses.[176,286] Another study reveals that certain lactic acid bacteria stimulate the production of IFN-I through intracellular sensors STING and MAVS.[287] One study determined whether DAT exerts its effects through augmentation of IFN-I induction or IFN-I amplification with experiments using BMDMs from mice lacking key mediators of both pathways. The results showed that DAT still enhances the expression of IFN-γ–induced protein 10 (IP-10) when BMDMs lacking a component of the induction pathway (MAVS) are used, suggesting that DAT is more likely involved in the amplification of IFN-I rather than the induction process. Further experiments with BMDMs from mice lacking STAT1, a downstream signaling molecule of IFNAR, confirmed that the effect of DAT on IP-10 expression depends on IFN amplification through IFNAR and STAT1.[178] A study suggests that despite its presence in serum, DAT may not primarily function through direct IFN-I induction at infection or tumor sites, as serum levels of DAT remain largely unchanged in a virus infection model. Instead, it indicates that the efficacy of DAT may be

linked to immune cell migration, a vital process for orchestrating effective immune responses at sites of infection or tumors.[179] These findings highlight the need for further investigation into the precise mechanisms through which DAT operates and its potential role in orchestrating local immune responses in dependence of host IFN-I signaling.

Not only does host-IFN-I signaling play a pivotal role in antitumor immunity but tumor cell intrinsic IFNAR signaling could play a role as well. One the one hand tumor cell intrinsic IFNAR signaling can decrease the response to ICIs or radiotherapy.[288] On the other hand, IFNAR signaling in tumor cells can enhance the expression of MHC-I molecules, which are crucial for presenting tumor antigens to T cells.[289] Furthermore, IFNAR activation can increase the expression of PD-L1 on tumor cells, making them more susceptible to ICIs while IFNAR downregulation can enhance cancer progression.[290,291] In cancer patients the absence of IFNAR in tumors is associated with decreased OS and increased tumor growth.[292,293] Whether tumor cell intrinsic IFNAR is required for the efficacy of DAT in antitumor immunity is unknown. As DAT affects host immune cells and exerts its function via direct effects on these cells, it can be assumed that host-IFN-I signaling plays the major role compared to tumor-intrinsic IFN-I signaling. The effects of IFNAR signaling in tumor cells can be context dependent. While activation of IFNAR signaling is generally associated with antitumor immunity, in some cases, chronic or excessive IFNAR signaling may promote immune suppression or tolerance. The balance between immune activation and tolerance depends on various factors, including the tumor microenvironment, the type of immune cells present, and the specific molecular pathways involved.[294]

5. Clinical application and advantages of bacterial-derived metabolites

Bacterial-derived metabolites have the potential to be incorporated into clinical applications, not only as standalone addition to ICI therapy, but also in conjunction with existing approaches, such as probiotics or engineered microbes. Metabolites could potentially contribute to probiotic treatment. As an example, probiotic bacteria *Akkermansia muciniphila* and *Bifidobacterium pseudolongum* are associated with a better response to ICI treatment, regulating immune responses, and furthermore, producing the beneficial metabolite inosine.[198,200,202,206,233] Hence, microbes that are not directly related may share similar immune-modulating properties by generating the same or similar metabolites and activating a common host signaling pathway. Furthermore, *Akkermansia muciniphila* produces the SCFA PA that is suggested to inhibit cancer cell proliferation and improve antitumor response together with ICIs.[295] Importantly, the tryptophan metabolite I3A derived from *Lactobacillus reuteri* was found to enhance ICI efficacy and being more enriched in responder patients.[210] This is in line with the results of the current

study that ICA, another tryptophan metabolite, was able to improve anti-CTLA-4 therapy. DAT-producing bacteria also merit consideration as potential probiotic candidates due to the recognized benefits of DAT in cancer immunotherapy. However, a critical aspect in evaluating these probiotics is the safety concern. As mentioned earlier, a high abundance of *F. plautii* has been linked to CRC in a cohort study.[271] This association raises questions about the potential for F. plautii to produce other metabolites that may interact negatively with the disease, making it crucial to thoroughly assess the safety profile of any probiotic bacteria under consideration for cancer therapy. In the case of DAT further research is needed to assess the effects of *F. plautii* as a probiotic. Interestingly, one DAT producer, *Lactiplantibacillus pentoses*, demonstrates enhanced antiviral activity via the IFN-I pathway when compared to another strain of the same bacterium that lacks DAT production.[179] This additionally indicates that bacterial-derived metabolites might play a pivotal role in probiotics applications. Moreover, it would be conceivable to combine safe probiotics that enhance the antitumor effect of ICIs with other bacterial metabolites that also have combinatorial effects with ICI therapy and these probiotics.

Bacteria can also be engineered to deliver immune-modulating proteins or substances to the TME.[296–298] The bacterial delivery of bacterial-derived metabolites such as DAT, ICA, or SCFAs has not been tested yet. This approach could be promising as bacterial-derived metabolites might be more effective when transported directly into the tumor. That might be feasible for metabolites that inhibit tumor cell proliferation, like PA, or directly activate immune cells, like inosine, SCFAs, or DAT in this study.[206,208,295] Furthermore, tumor-targeting bacteria might be able to convert amino acids or other products into beneficial metabolites in the TME. *Escherichia coli Nissl 1917* colonizes tumors and is capable of converting ammonia to L-arginine which enhances T cell survival and antitumor activity.[299] Moreover, *Lactobacilli* can convert tryptophan into indole derivates like I3A which then could improve antitumor immunity[210,300]

Using isolated bacterial metabolites in cancer treatment with ICIs offers certain advantages compared to other microbiome-related therapy approaches like FMT, probiotics, or engineered microbes. Bacterial metabolites can be isolated and administered in a more targeted and controlled manner. This allows for precise dosing and avoids introducing a wide variety of microorganisms, reducing the risk of unwanted side effects. The reduced immunogenicity of bacterial metabolites is another significant advantage. They are less likely to trigger unwanted off-tumor/off-target immune responses in the recipient when compared to live bacteria or engineered microbes as they are specific molecules and do not carry a variety of antigens and molecular patterns.[173,301,302] This lower immunogenicity could improve treatment tolerance and efficacy. Unlike probiotics or FMT, they do not carry the risk of causing infections, overgrowth, or other adverse effects within the recipient. This might make bacterial-derived metabolites a

suitable alternative for high-risk patients.[303–305] Even though FMT is generally considered safe when appropriate donor screening and preparation procedures are followed, there are risks, including the potential transmission of infections or unknown pathogens from the donor. Two patients who underwent FMT in separate clinical trials experienced extended-spectrum beta-lactamase (ESBL)–producing *Escherichia coli* bacteremia, linked to the same stool donor through genomic sequencing, emphasizing the need for enhanced donor screening to prevent adverse infectious events.[304] Furthermore, FMT requires suitable donors whereas bacterial metabolites can be produced and purified in a standardized way, ensuring consistency in their composition and quality. This is important for clinical applications where reproducibility and reliability are essential.[306,307]

Moreover, Bacterial-derived metabolites offer a solution where concerns about colonization efficacy, typically in the context of probiotics, become less relevant. Direct quantification of mucosal probiotics colonization, observed in some studies through endoscopies in humans and pigs, suggests variable and limited colonization patterns, while a metagenomic assessment revealed mucosal association of probiotics in 60% of supplemented individuals. The persistence of probiotics in colonizing the gut mucosa after cessation of consumption remains uncertain, with studies indicating strain- and person-specific variability in shedding patterns, including detectable shedding of specific probiotic strains in stool samples for weeks or even months following supplement discontinuation, influenced by the individual microbiome composition.[308] In the case of engineered bacteria the effective dose of live bacteria in the target tissue may also not correlate directly with the administered dose. Factors like tissue accessibility, extent of tumor necrosis or hypoxia, and pre-existing tumor-infiltrating inflammatory cells determine the effectiveness. While concerns may persist about the gut absorption capacity with the oral administration of bacterial-derived metabolites, alternative methods such as i.v. application provide additional possibilities, setting them apart from probiotics.[206,248]

Another advantage could be the potential discovery of biologically active derivates that could mimic the functions of bacterial-derived metabolites, but with an even more specific targeting mechanism. But the application of this approach requires the precise elucidation of underlying mechanisms and the molecular targets of the bacterial-derived metabolites.

Furthermore, certain bacterial-derived metabolites, as demonstrated in this study, can potentially protect the host from irAEs without impeding or even enhancing the efficacy of antitumor immunotherapy.[229,244] This capability facilitates the uninterrupted administration of ICIs without the need for treatment termination resulting from these irAEs. By utilizing bacterial metabolites, it might still be feasible to apply antibiotics, if necessary, provided that the bacterial metabolite functions independently of the gut microbiome's composition, similar to DAT in the current study or inosine which exerted its function in GF mice.[206] Especially in cases where

antibiotic treatment needs to be applied concurrently with ICI therapy, limiting the use of live bacteria, bacterial-derived metabolites could offer a significant advantage.

In summary, the utilization of metabolites in tandem with ICI therapy, alongside approaches like FMT and probiotics, holds considerable promise for antitumor effects. The safety, antibiotic resilience, and ease of isolation and control make metabolites a compelling alternative to live bacteria, presenting a potentially impactful avenue for innovative cancer treatments.

6. Concluding remarks

In conclusion, this study unveils the crucial role of bacterial-derived metabolites, particularly the IFN-I modulator DAT, in enhancing the efficacy and safety of anti-CTLA-4 immunotherapy for melanoma. The significance of IFN-I in the antitumor response underscores the pivotal role that IFN-I modulating metabolites might play in shaping and optimizing the immune response against cancer. Importantly, the ability to restore the efficacy of anti-CTLA-4 with DAT under antibiotic conditions and its independent yet modulatory role in the gut microbiome composition offer novel perspectives in the dynamic interplay between metabolites and microbial environments. These findings hold significant promise for advancing therapeutic strategies that harness bacterial-derived metabolites to optimize the outcomes of ICI therapy.

V REFERENCES

1. Joachim L, Göttert S, Sax A, et al. The microbial metabolite desaminotyrosine enhances T-cell priming and cancer immunotherapy with immune checkpoint inhibitors. *EBioMedicine*. 2023;97:104834. doi:10.1016/j.ebiom.2023.104834
2. Sulaimon SS, Kitchell BE. The Basic Biology of Malignant Melanoma: Molecular Mechanisms of Disease Progression and Comparative Aspects. *J Vet Intern Med*. 2003;17(6):760-772. doi:10.1111/j.1939-1676.2003.tb02513.x
3. Millet A, Martin AR, Ronco C, Rocchi S, Benhida R. Metastatic Melanoma: Insights Into the Evolution of the Treatments and Future Challenges. *Med Res Rev*. 2017;37(1):98-148. doi:10.1002/med.21404
4. Dzwierzynski WW. Melanoma Risk Factors and Prevention. *Clin Plast Surg*. 2021;48(4):543-550. doi:10.1016/j.cps.2021.05.001
5. Siegel RL, Miller KD, Wagle NS, Jemal A. Cancer statistics, 2023. *CA Cancer J Clin*. 2023;73(1):17-48. doi:10.3322/caac.21763
6. Garbe C, Amaral T, Peris K, et al. European consensus-based interdisciplinary guideline for melanoma. Part 1: Diagnostics: Update 2022. *Eur J Cancer*. 2022;170:236-255. doi:10.1016/j.ejca.2022.03.008
7. Davis LE, Shalin SC, Tackett AJ. Current state of melanoma diagnosis and treatment. *Cancer Biol Ther*. 2019;20(11):1366-1379. doi:10.1080/15384047.2019.1640032
8. Gorayski P, Burmeister B, Foote M. Radiotherapy for cutaneous melanoma: Current and future applications. *Future Oncology*. 2015;11(3):525-534. doi:10.2217/fon.14.300
9. Gupta A, Gomes F, Lorigan P. The role for chemotherapy in the modern management of melanoma. *Melanoma Manag*. 2017;4(2):125-136. doi:10.2217/mmt-2017-0003
10. Di Trolio R, Simeone E, Di Lorenzo G, Buonerba C, Ascierto PA. The use of interferon in melanoma patients: A systematic review. *Cytokine Growth Factor Rev*. 2015;26(2):203-212. doi:10.1016/j.cytogfr.2014.11.008
11. Marabondo S, Kaufman HL. High-dose interleukin-2 (IL-2) for the treatment of melanoma: safety considerations and future directions. *Expert Opin Drug Saf*. 2017;16(12):1347-1357. doi:10.1080/14740338.2017.1382472
12. Larkin J, Chiarion-Sileni V, Gonzalez R, et al. Combined Nivolumab and Ipilimumab or Monotherapy in Untreated Melanoma. *New England Journal of Medicine*. 2015;373(1):23-34. doi:10.1056/nejmoa1504030
13. Wolchok JD, Chiarion-Sileni V, Gonzalez R, et al. Overall Survival with Combined Nivolumab and Ipilimumab in Advanced Melanoma. *New England Journal of Medicine*. 2017;377(14):1345-1356. doi:10.1056/nejmoa1709684

14. Carlino MS, Menzies AM, Atkinson V, et al. Long-term Follow-up of Standard-Dose Pembrolizumab Plus Reduced-Dose Ipilimumab in Patients with Advanced Melanoma: KEYNOTE-029 Part 1B. *Clinical Cancer Research*. 2020;26(19):5086-5091. doi:10.1158/1078-0432.CCR-20-0177

15. Tawbi HA, Schadendorf D, Lipson EJ, et al. Relatlimab and Nivolumab versus Nivolumab in Untreated Advanced Melanoma. *New England Journal of Medicine*. 2022;386(1):24-34. doi:10.1056/nejmoa2109970

16. Schoenfeld AJ, Hellmann MD. Acquired Resistance to Immune Checkpoint Inhibitors. *Cancer Cell*. 2020;37(4):443-455. doi:10.1016/j.ccell.2020.03.017

17. Schadendorf D, Hodi FS, Robert C, et al. Pooled analysis of long-term survival data from phase II and phase III trials of ipilimumab in unresectable or metastatic melanoma. *Journal of Clinical Oncology*. 2015;33(17):1889-1894. doi:10.1200/JCO.2014.56.2736

18. Ribas A, Hamid O, Daud A, et al. Association of pembrolizumab with tumor response and survival among patients with advanced melanoma. In: *JAMA - Journal of the American Medical Association*. Vol 315. American Medical Association; 2016:1600-1609. doi:10.1001/jama.2016.4059

19. Das S, Johnson DB. Immune-related adverse events and anti-tumor efficacy of immune checkpoint inhibitors. *J Immunother Cancer*. 2019;7(1). doi:10.1186/s40425-019-0805-8

20. Larocca CA, LeBoeuf NR, Silk AW, Kaufman HL. An Update on the Role of Talimogene Laherparepvec (T-VEC) in the Treatment of Melanoma: Best Practices and Future Directions. *Am J Clin Dermatol*. 2020;21(6):821-832. doi:10.1007/s40257-020-00554-8

21. Li D, Wu M. Pattern recognition receptors in health and diseases. *Signal Transduct Target Ther*. 2021;6(1). doi:10.1038/s41392-021-00687-0

22. Fitzgerald KA, Kagan JC. Toll-like Receptors and the Control of Immunity. *Cell*. 2020;180(6):1044-1066. doi:10.1016/j.cell.2020.02.041

23. Franchi L, Warner N, Viani K, Nuñez G. Function of Nod-like receptors in microbial recognition and host defense. *Immunol Rev*. 2009;227(1):106-128. doi:10.1111/j.1600-065X.2008.00734.x

24. Rehwinkel J, Gack MU. RIG-I-like receptors: their regulation and roles in RNA sensing. *Nat Rev Immunol*. 2020;20(9):537-551. doi:10.1038/s41577-020-0288-3

25. Liu H, Wang F, Cao Y, Dang Y, Ge B. The multifaceted functions of cGAS. *J Mol Cell Biol*. 2022;14(5). doi:10.1093/jmcb/mjac031

26. Turvey SE, Broide DH. Innate immunity. *Journal of Allergy and Clinical Immunology*. 2010;125(2). doi:10.1016/j.jaci.2009.07.016

27. Delves PJ, Roitt IM. The Immune System. Mackay IR, Rosen FS, eds. *New England Journal of Medicine*. 2000;343(1):37-49. doi:10.1056/NEJM200007063430107

28. Iwasaki A, Medzhitov R. Control of adaptive immunity by the innate immune system. *Nat Immunol*. 2015;16(4):343-353. doi:10.1038/ni.3123

29. Alcover A, Alarcón B, Di Bartolo V. Cell Biology of T Cell Receptor Expression and Regulation. *Annu Rev Immunol*. 2018;36(1):103-125. doi:10.1146/annurev-immunol-042617-053429

30. Smith-Garvin JE, Koretzky GA, Jordan MS. T cell activation. *Annu Rev Immunol*. 2009;27:591-619. doi:10.1146/annurev.immunol.021908.132706

31. Takahama Y. Journey through the thymus: Stromal guides for T-cell development and selection. *Nat Rev Immunol*. 2006;6(2):127-135. doi:10.1038/nri1781

32. Dong C, Flavell RA. Th1 and Th2 cells. *Curr Opin Hematol*. 2001;8(1):47-51. doi:10.1097/00062752-200101000-00009

33. Zhu J, Paul WE. Heterogeneity and plasticity of T helper cells. *Cell Res*. 2010;20(1):4-12. doi:10.1038/cr.2009.138

34. Terabe M, Berzofsky JA. Immunoregulatory T cells in tumor immunity. *Curr Opin Immunol*. 2004;16(2):157-162. doi:10.1016/j.coi.2004.01.010

35. Beissert S, Schwarz A, Schwarz T. Regulatory T cells. *Journal of Investigative Dermatology*. 2006;126(1):15-24. doi:10.1038/sj.jid.5700004

36. Andersen MH, Schrama D, thor Straten P, Becker JC. Cytotoxic T Cells. *Journal of Investigative Dermatology*. 2006;126(1):32-41. doi:10.1038/sj.jid.5700001

37. Maher J, Davies ET. Targeting cytotoxic T lymphocytes for cancer immunotherapy. *Br J Cancer*. 2004;91(5):817-821. doi:10.1038/sj.bjc.6602022

38. Shipkova M, Wieland E. Surface markers of lymphocyte activation and markers of cell proliferation. *Clinica Chimica Acta*. 2012;413(17-18):1338-1349. doi:10.1016/j.cca.2011.11.006

39. Boehm U, Klamp T, Groot M, Howard JC. Cellular responses to interferon-γ. *Annu Rev Immunol*. 1997;15(1):749-795. doi:10.1146/annurev.immunol.15.1.749

40. Farber DL, Yudanin NA, Restifo NP. Human memory T cells: Generation, compartmentalization and homeostasis. *Nat Rev Immunol*. 2014;14(1):24-35. doi:10.1038/nri3567

41. Corrado M, Pearce EL. Targeting memory T cell metabolism to improve immunity. *Journal of Clinical Investigation*. 2022;132(1). doi:10.1172/JCI148546

42. Liu K, Nussenzweig MC. Origin and development of dendritic cells. *Immunol Rev*. 2010;234(1):45-54. doi:10.1111/j.0105-2896.2009.00879.x

43. Ye Y, Gaugler B, Mohty M, Malard F. Plasmacytoid dendritic cell biology and its role in immune-mediated diseases. *Clin Transl Immunology*. 2020;9(5). doi:10.1002/cti2.1139

44. Durai V, Murphy KM. Functions of Murine Dendritic Cells. *Immunity*. 2016;45(4):719-736. doi:10.1016/j.immuni.2016.10.010

45. Yin X, Chen S, Eisenbarth SC. Dendritic Cell Regulation of T Helper Cells. *Annu Rev Immunol*. 2021;39(1):759-790. doi:10.1146/annurev-immunol-101819-025146

46. León B, Ardavín C. Monocyte-derived dendritic cells in innate and adaptive immunity. *Immunol Cell Biol*. 2008;86(4):320-324. doi:10.1038/icb.2008.14

47. Wu SY, Fu T, Jiang YZ, Shao ZM. Natural killer cells in cancer biology and therapy. *Mol Cancer*. 2020;19(1). doi:10.1186/s12943-020-01238-x

48. Mah AY, Cooper MA. Metabolic regulation of natural killer cell IFN-γ production. *Crit Rev Immunol*. 2016;36(2):131-147. doi:10.1615/CritRevImmunol.2016017387

49. Lucas M, Schachterle W, Oberle K, Aichele P, Diefenbach A. Dendritic Cells Prime Natural Killer Cells by trans-Presenting Interleukin 15. *Immunity*. 2007;26(4):503-517. doi:10.1016/j.immuni.2007.03.006

50. Zitvogel L, Galluzzi L, Kepp O, Smyth MJ, Kroemer G. Type I interferons in anticancer immunity. *Nat Rev Immunol*. 2015;15(7):405-414. doi:10.1038/nri3845

51. Jiang J, Zhao M, Chang C, Wu H, Lu Q. Type I Interferons in the Pathogenesis and Treatment of Autoimmune Diseases. *Clin Rev Allergy Immunol*. 2020;59(2):248-272. doi:10.1007/s12016-020-08798-2

52. Hervas-Stubbs S, Perez-Gracia JL, Rouzaut A, Sanmamed MF, Le Bon A, Melero I. Direct effects of type I interferons on cells of the immune system. *Clinical Cancer Research*. 2011;17(9):2619-2627. doi:10.1158/1078-0432.CCR-10-1114

53. Rizza P, Moretti F, Capone I, Belardelli F. Role of type I interferon in inducing a protective immune response: Perspectives for clinical applications. *Cytokine Growth Factor Rev*. 2015;26(2):195-201. doi:10.1016/j.cytogfr.2014.10.002

54. Cheon HJ, Wang Y, Wightman SM, Jackson MW, Stark GR. How cancer cells make and respond to interferon-I. *Trends Cancer*. 2023;9(1):83-92. doi:10.1016/j.trecan.2022.09.003

55. Fuertes MB, Kacha AK, Kline J, et al. Host type I IFN signals are required for antitumor CD8+ T cell responses through CD8α+ dendritic cells. *Journal of Experimental Medicine*. 2011;208(10):2005-2016. doi:10.1084/jem.20101159

56. Diamond MS, Kinder M, Matsushita H, et al. Type I interferon is selectively required by dendritic cells for immune rejection of tumors. *Journal of Experimental Medicine*. 2011;208(10):1989-2003. doi:10.1084/jem.20101158

57. Gresser I, Belardelli F. Endogenous type I interferons as a defense against tumors. *Cytokine Growth Factor Rev*. 2002;13(2):111-118. doi:10.1016/S1359-6101(01)00035-1

58. Dunn GP, Bruce AT, Sheehan KCF, et al. A critical function for type I interferons in cancer immunoediting. *Nat Immunol*. 2005;6(7):722-729. doi:10.1038/ni1213

59. Tivol EA, Borriello F, Schweitzer AN, Lynch WP, Bluestone JA, Sharpe AH. Loss of CTLA-4 leads to massive lymphoproliferation and fatal multiorgan tissue destruction, revealing a critical negative regulatory role of CTLA-4. *Immunity*. 1995;3(5):541-547. doi:10.1016/1074-7613(95)90125-6

60. Nishimura H, Nose M, Hiai H, Minato N, Honjo T. Development of lupus-like autoimmune diseases by disruption of the PD-1 gene encoding an ITIM motif-carrying immunoreceptor. *Immunity*. 1999;11(2):141-151. doi:10.1016/s1074-7613(00)80089-8

61. Kuehn HS, Ouyang W, Lo B, et al. Immune dysregulation in human subjects with heterozygous germline mutations in CTLA4. *Science (1979)*. 2014;345(6204):1623-1627. doi:10.1126/science.1255904

62. Lee YH, Bae SC, Kim JH, Song GG. Meta-analysis of genetic polymorphisms in programmed cell death 1. *Z Rheumatol*. 2015;74(3):230-239. doi:10.1007/s00393-014-1415-y

63. Paluch C, Santos AM, Anzilotti C, Cornall RJ, Davis SJ. Immune checkpoints as therapeutic targets in autoimmunity. *Front Immunol*. 2018;9(OCT). doi:10.3389/fimmu.2018.02306

64. Hosseini A, Gharibi T, Marofi F, Babaloo Z, Baradaran B. CTLA-4: From mechanism to autoimmune therapy. *Int Immunopharmacol*. 2020;80:106221. doi:10.1016/j.intimp.2020.106221

65. Weiss A, Imboden JB. Cell Surface Molecules and Early Events Involved in Human T Lymphocyte Activation. In: *Advances in Immunology*. Vol 41. ; 1987:1-38. doi:10.1016/S0065-2776(08)60029-2

66. Kucuk ZY, Charbonnier LM, McMasters RL, Chatila T, Bleesing JJ. CTLA-4 haploinsufficiency in a patient with an autoimmune lymphoproliferative disorder. *Journal of Allergy and Clinical Immunology*. 2017;140(3):862-864.e4. doi:10.1016/j.jaci.2017.02.032

67. Waterhouse P, Penninger JM, Timms E, et al. Lymphoproliferative Disorders with Early Lethality in Mice Deficient in Ctla-4. *Science (1979)*. 1995;270(5238):985-988. doi:10.1126/science.270.5238.985

68. Tivol EA, Boyd SD, McKeon S, et al. CTLA4Ig prevents lymphoproliferation and fatal multiorgan tissue destruction in CTLA-4-deficient mice. *Journal of immunology*. 1997;158(11):5091-5094.

69. Erfani N, Mehrabadi SM, Ghayumi MA, et al. Increase of regulatory T cells in metastatic stage and CTLA-4 over expression in lymphocytes of patients with non-small cell lung cancer (NSCLC). *Lung Cancer*. 2012;77(2):306-311. doi:10.1016/j.lungcan.2012.04.011

70. Huang PY, Guo SS, Zhang Y, et al. Tumor CTLA-4 overexpression predicts poor survival in patients with nasopharyngeal carcinoma. *Oncotarget*. 2016;7(11):13060-13068. doi:10.18632/oncotarget.7421

71. Mao H, Zhang L, Yang Y, et al. New Insights of CTLA-4 into Its Biological Function in Breast Cancer. *Curr Cancer Drug Targets*. 2010;10(7):728-736. doi:10.2174/156800910793605811

72. Zhang B, Dang J, Ba D, Wang C, Han J, Zheng F. Potential function of CTLA-4 in the tumourigenic capacity of melanoma stem cells. *Oncol Lett*. 2018;16(5):6163-6170. doi:10.3892/ol.2018.9354

73. Pistillo MP, Carosio R, Grillo F, et al. Phenotypic characterization of tumor CTLA-4 expression in melanoma tissues and its possible role in clinical response to Ipilimumab. *Clinical Immunology*. 2020;215. doi:10.1016/j.clim.2020.108428

74. Patsoukis N, Wang Q, Strauss L, Boussiotis VA. *Revisiting the PD-1 Pathway*. Vol 6.; 2020. doi:10.1126/sciadv.abd2712

75. Lázár-Molnár E, Chen B, Sweeney KA, et al. Programmed death-1 (PD-1)-deficient mice are extraordinarily sensitive to tuberculosis. *Proc Natl Acad Sci U S A*. 2010;107(30):13402-13407. doi:10.1073/pnas.1007394107

76. Ogishi M, Yang R, Aytekin C, et al. Inherited PD-1 deficiency underlies tuberculosis and autoimmunity in a child. *Nat Med*. 2021;27(9):1646-1654. doi:10.1038/s41591-021-01388-5

77. Kleffel S, Posch C, Barthel SR, et al. Melanoma Cell-Intrinsic PD-1 Receptor Functions Promote Tumor Growth. *Cell*. 2015;162(6):1242-1256. doi:10.1016/j.cell.2015.08.052

78. Jiang Z, Yan Y, Dong J, Duan L. PD-1 expression on uveal melanoma induces tumor proliferation and predicts poor patient survival. *International Journal of Biological Markers*. 2020;35(3):50-58. doi:10.1177/1724600820943610

79. Li H, Li X, Liu S, et al. Programmed cell death-1 (PD-1) checkpoint blockade in combination with a mammalian target of rapamycin inhibitor restrains hepatocellular carcinoma growth induced by hepatoma cell–intrinsic PD-1. *Hepatology*. 2017;66(6):1920-1933. doi:10.1002/hep.29360

80. Du S, McCall N, Park K, et al. Blockade of Tumor-Expressed PD-1 promotes lung cancer growth. *Oncoimmunology*. 2018;7(4). doi:10.1080/2162402X.2017.1408747

81. Konishi J, Yamazaki K, Azuma M, Kinoshita I, Dosaka-Akita H, Nishimura M. B7-H1 Expression on Non-Small Cell Lung Cancer Cells and Its Relationship with Tumor-Infiltrating Lymphocytes and Their PD-1 Expression. *Clinical Cancer Research*. 2004;10(15):5094-5100. doi:10.1158/1078-0432.CCR-04-0428

82. Nomi T, Sho M, Akahori T, et al. Clinical significance and therapeutic potential of the programmed death-1 ligand/programmed death-1 pathway in human pancreatic cancer. *Clinical Cancer Research*. 2007;13(7):2151-2157. doi:10.1158/1078-0432.CCR-06-2746

83. Dong H, Strome SE, Salomao DR, et al. Tumor-associated B7-H1 promotes T-cell apoptosis: A potential mechanism of immune evasion. *Nat Med*. 2002;8(8):793-800. doi:10.1038/nm730

84. Hamanishi J, Mandai M, Iwasaki M, et al. Programmed cell death 1 ligand 1 and tumor-infiltrating CD8+ T lymphocytes are prognostic factors of human ovarian cancer. *Proceedings of the National Academy of Sciences*. 2007;104(9):3360-3365. doi:10.1073/pnas.0611533104

85. Saito R, Abe H, Kunita A, Yamashita H, Seto Y, Fukayama M. Overexpression and gene amplification of PD-L1 in cancer cells and PD-L1 + immune cells in Epstein-Barr virus-associated gastric cancer: The prognostic implications. *Modern Pathology*. 2017;30(3):427-439. doi:10.1038/modpathol.2016.202

86. Nakanishi J, Wada Y, Matsumoto K, Azuma M, Kikuchi K, Ueda S. Overexpression of B7-H1 (PD-L1) significantly associates with tumor grade and postoperative prognosis in human urothelial cancers. *Cancer Immunology, Immunotherapy*. 2007;56(8):1173-1182. doi:10.1007/s00262-006-0266-z

87. Chabner BA, Roberts TGJ. Timeline: Chemotherapy and the war on cancer. *Nat Rev Cancer*. 2005;5(1):65-72. doi:10.1038/nrc1529

88. Baskar R, Lee KA, Yeo R, Yeoh KW. Cancer and radiation therapy: Current advances and future directions. *Int J Med Sci*. 2012;9(3):193-199. doi:10.7150/ijms.3635

89. Wolchok JD, Chiarion-Sileni V, Gonzalez R, et al. Long-Term Outcomes With Nivolumab Plus Ipilimumab or Nivolumab Alone Versus Ipilimumab in Patients With Advanced Melanoma. *J Clin Oncol*. 2021;40:127-137. doi:10.1200/JCO.21

90. Huo JL, Wang YT, Fu WJ, Lu N, Liu ZS. The promising immune checkpoint LAG-3 in cancer immunotherapy: from basic research to clinical application. *Front Immunol*. 2022;13. doi:10.3389/fimmu.2022.956090

91. Leach DR, Krummel MF, Allison JP. Enhancement of Antitumor Immunity by CTLA-4 Blockade. *Science (1979)*. 1996;271(5256):1734-1736. doi:10.1126/science.271.5256.1734

92. Yang YF, Zou JP, Mu J, et al. Enhanced induction of antitumor T-cell responses by cytotoxic T lymphocyte-associated molecule-4 blockade: the effect is manifested only at the restricted tumor-bearing stages. *Cancer Res*. 1997;57(18):4036-4041.

93. Hurwitz AA, Foster BA, Kwon ED, et al. Combination immunotherapy of primary prostate cancer in a transgenic mouse model using CTLA-4 blockade. *Cancer Res*. 2000;60(9):2444-2448.

94. van Elsas A, Hurwitz AA, Allison JP. Combination Immunotherapy of B16 Melanoma Using Anti–Cytotoxic T Lymphocyte–Associated Antigen 4 (Ctla-4) and Granulocyte/Macrophage Colony-Stimulating Factor (Gm-Csf)-Producing Vaccines Induces Rejection of Subcutaneous and Metastatic Tumors Accompanied by Autoimmune Depigmentation. *J Exp Med*. 1999;190(3):355-366. doi:10.1084/jem.190.3.355

95. Bristol-Myers Squibb Company. *FDA Approves YERVOY™ (Ipilimumab) for the Treatment of Patients with Newly Diagnosed or Previously-Treated Unresectable or Metastatic Melanoma, the Deadliest Form of Skin Cancer*.; 2011.

96. Hodi FS, O'Day SJ, McDermott DF, et al. Improved Survival with Ipilimumab in Patients with Metastatic Melanoma. *New England Journal of Medicine*. 2010;363(8):711-723. doi:10.1056/NEJMoa1003466

97. Wolchok JD, Neyns B, Linette G, et al. Ipilimumab monotherapy in patients with pretreated advanced melanoma: a randomised, double-blind, multicentre, phase 2, dose-ranging study. *Lancet Oncology*. 2010;11:155-164. doi:10.1016/S1470

98. Wei SC, Levine JH, Cogdill AP, et al. Distinct Cellular Mechanisms Underlie Anti-CTLA-4 and Anti-PD-1 Checkpoint Blockade. *Cell*. 2017;170(6):1120-1133.e17. doi:10.1016/j.cell.2017.07.024

99. McGranahan N, Furness AJS, Rosenthal R, et al. Clonal neoantigens elicit T cell immunoreactivity and sensitivity to immune checkpoint blockade. *Science (1979)*. 2016;351(6280):1463-1469. doi:10.1126/science.aaf1490

100. Bristol Myers Squibb Company. *U.S. Food and Drug Administration Approves Opdivo® (Nivolumab) as Adjuvant Treatment for Eligible Patients with Completely Resected Stage IIB or Stage IIC Melanoma*. www.fda.gov/medwatch.

101. Robert C, Long G V., Brady B, et al. Nivolumab in Previously Untreated Melanoma without BRAF Mutation . *New England Journal of Medicine*. 2015;372(4):320-330. doi:10.1056/nejmoa1412082

102. Brahmer JR, Tykodi SS, Chow LQM, et al. Safety and Activity of Anti–PD-L1 Antibody in Patients with Advanced Cancer. *New England Journal of Medicine*. 2012;366(26):2455-2465. doi:10.1056/nejmoa1200694

103. Yarchoan M, Albacker LA, Hopkins AC, et al. PD-L1 expression and tumor mutational burden are independent biomarkers in most cancers. *JCI Insight*. 2019;4(6). doi:10.1172/jci.insight.126908

104. Yarchoan M, Hopkins A, Jaffee EM. Tumor Mutational Burden and Response Rate to PD-1 Inhibition. *New England Journal of Medicine*. 2017;377(25):2500-2501. doi:10.1056/nejmc1713444

105. Doroshow DB, Bhalla S, Beasley MB, et al. PD-L1 as a biomarker of response to immune-checkpoint inhibitors. *Nat Rev Clin Oncol*. 2021;18(6):345-362. doi:10.1038/s41571-021-00473-5

106. Hodi FS, O'Day SJ, McDermott DF, et al. Improved Survival with Ipilimumab in Patients with Metastatic Melanoma. *New England Journal of Medicine*. 2010;363(8):711-723. doi:10.1056/nejmoa1003466

107. Mittal SK, Roche PA. Suppression of antigen presentation by IL-10. *Curr Opin Immunol*. 2015;34:22-27. doi:10.1016/j.coi.2014.12.009

108. Park SJ, Nakagawa T, Kitamura H, et al. IL-6 Regulates In Vivo Dendritic Cell Differentiation through STAT3 Activation. *The Journal of Immunology*. 2004;173(6):3844-3854. doi:10.4049/jimmunol.173.6.3844

109. Hegde S, Pahne J, Smola-Hess S. Novel immunosuppressive properties of interleukin-6 in dendritic cells: inhibition of NF-κB binding activity and CCR7 expression. *The FASEB Journal*. 2004;18(12):1439-1441. doi:10.1096/fj.03-0969fje

110. Gabrilovich DI, Chen HL, Girgis KR, et al. Production of vascular endothelial growth factor by human tumors inhibits the functional maturation of dendritic cells. *Nat Med*. 1996;2(10):1096-1103. doi:10.1038/nm1096-1096

111. Fiorentino DF, Zlotnik A, Vieira P, et al. IL-10 acts on the antigen-presenting cell to inhibit cytokine production by Th1 cells. *Journal of immunology*. 1991;146(10):3444-3451. http://www.ncbi.nlm.nih.gov/pubmed/1827484

112. Steinbrink K, Wölfl M, Jonuleit H, Knop J, Enk AH. Induction of tolerance by IL-10-treated dendritic cells. *Journal of immunology*. 1997;159(10):4772-4780.

113. Enk AH, Jonuleit H, Saloga J, Knop J. Dendritic cells as mediators of tumor-induced tolerance in metastatic melanoma. *Int J Cancer*. 1997;73(3):309-316. doi:10.1002/(SICI)1097-0215(19971104)73:3<309::AID-IJC1>3.0.CO;2-3

114. Yang Z, Qi Y, Lai N, et al. Notch1 signaling in melanoma cells promoted tumor-induced immunosuppression via upregulation of TGF-β1. *Journal of Experimental and Clinical Cancer Research*. 2018;37(1). doi:10.1186/s13046-017-0664-4

115. Brand A, Singer K, Koehl GE, et al. LDHA-Associated Lactic Acid Production Blunts Tumor Immunosurveillance by T and NK Cells. *Cell Metab*. 2016;24(5):657-671. doi:10.1016/j.cmet.2016.08.011

116. Ma X, Bi E, Lu Y, et al. Cholesterol Induces CD8+ T Cell Exhaustion in the Tumor Microenvironment. *Cell Metab*. 2019;30(1):143-156.e5. doi:10.1016/j.cmet.2019.04.002

117. Gemta LF, Siska PJ, Nelson ME, et al. Impaired enolase 1 glycolytic activity restrains effector functions of tumor-infiltrating CD8+ T cells. *Sci Immunol*. 2019;4(31). doi:10.1126/sciimmunol.aap9520

118. Uyttenhove C, Pilotte L, Théate I, et al. Evidence for a tumoral immune resistance mechanism based on tryptophan degradation by indoleamine 2,3-dioxygenase. *Nat Med*. 2003;9(10):1269-1274. doi:10.1038/nm934

119. Kudo Y, Boyd CAR, Sargent IL, Redman CWG. Tryptophan degradation by human placental indoleamine 2,3-dioxygenase regulates lymphocyte proliferation. *J Physiol*. 2001;535(1):207-215. doi:10.1111/j.1469-7793.2001.00207.x

120. Frumento G, Rotondo R, Tonetti M, Ferrara GB. T cell proliferation is blocked by indoleamine 2,3-dioxygenase. *Transplant Proc*. 2001;33(1-2):428-430. doi:10.1016/S0041-1345(00)02078-9

121. Holmgaard RB, Zamarin D, Li Y, et al. Tumor-Expressed IDO Recruits and Activates MDSCs in a Treg-Dependent Manner. *Cell Rep*. 2015;13(2):412-424. doi:10.1016/j.celrep.2015.08.077

122. Brody JR, Costantino CL, Berger AC, et al. Expression of indoleamine 2,3-dioxygenase in metastatic malignant melanoma recruits regulatory T cells to avoid immune detection and affects survival. *Cell Cycle*. 2009;8(12):1930-1934. doi:10.4161/cc.8.12.8745

123. Salmi S, Lin A, Hirschovits-Gerz B, et al. The role of FoxP3+ regulatory T cells and IDO+ immune and tumor cells in malignant melanoma – an immunohistochemical study. *BMC Cancer*. 2021;21(1). doi:10.1186/s12885-021-08385-4

124. Lee HW, Choi HJ, Ha SJ, Lee KT, Kwon YG. Recruitment of monocytes/macrophages in different tumor microenvironments. *Biochim Biophys Acta Rev Cancer*. 2013;1835(2):170-179. doi:10.1016/j.bbcan.2012.12.007

125. Philips RL, Wang Y, Cheon HJ, et al. The JAK-STAT pathway at 30: Much learned, much more to do. *Cell*. 2022;185(21):3857-3876. doi:10.1016/j.cell.2022.09.023

126. Stenzinger A, Allen JD, Maas J, et al. Tumor mutational burden standardization initiatives: Recommendations for consistent tumor mutational burden assessment in

clinical samples to guide immunotherapy treatment decisions. *Genes Chromosomes Cancer*. 2019;58(8):578-588. doi:10.1002/gcc.22733

127. Samstein RM, Lee CH, Shoushtari AN, et al. Tumor mutational load predicts survival after immunotherapy across multiple cancer types. *Nat Genet*. 2019;51(2):202-206. doi:10.1038/s41588-018-0312-8

128. Madore J, Strbenac D, Vilain R, et al. PD-L1 Negative Status is Associated with Lower Mutation Burden, Differential Expression of Immune-Related Genes, and Worse Survival in Stage III Melanoma. *Clinical Cancer Research*. 2016;22(15):3915-3923. doi:10.1158/1078-0432.CCR-15-1714

129. Dubin K, Callahan MK, Ren B, et al. Intestinal microbiome analyses identify melanoma patients at risk for checkpoint-blockade-induced colitis. *Nat Commun*. 2016;7(1):10391. doi:10.1038/ncomms10391

130. Chaput N, Lepage P, Coutzac C, et al. Baseline gut microbiota predicts clinical response and colitis in metastatic melanoma patients treated with ipilimumab. *Annals of Oncology*. 2017;28(6):1368-1379. doi:10.1093/annonc/mdx108

131. Andrews LP, Yano H, Vignali DAA. Inhibitory receptors and ligands beyond PD-1, PD-L1 and CTLA-4: breakthroughs or backups. *Nat Immunol*. 2019;20(11):1425-1434. doi:10.1038/s41590-019-0512-0

132. Del Campo AB, Kyte JA, Carretero J, et al. Immune escape of cancer cells with beta2-microglobulin loss over the course of metastatic melanoma. *Int J Cancer*. 2014;134(1):102-113. doi:10.1002/ijc.28338

133. Restifo NP, Marincola FM, Kawakami Y, Taubenberger J, Yannelli JR, Rosenberg SA. Loss of Functional Beta2-Microglobulin in Metastatic Melanomas From Five Patients Receiving Immunotherapy. *JNCI Journal of the National Cancer Institute*. 1996;88(2):100-108. doi:10.1093/jnci/88.2.100

134. Zaretsky JM, Garcia-Diaz A, Shin DS, et al. Mutations Associated with Acquired Resistance to PD-1 Blockade in Melanoma. *New England Journal of Medicine*. 2016;375(9):819-829. doi:10.1056/nejmoa1604958

135. Minn AJ. Interferons and the Immunogenic Effects of Cancer Therapy. *Trends Immunol*. 2015;36(11):725-737. doi:10.1016/j.it.2015.09.007

136. Pathak R, Pharaon RR, Mohanty A, Villaflor VM, Salgia R, Massarelli E. Acquired resistance to pd-1/pd-l1 blockade in lung cancer: Mechanisms and patterns of failure. *Cancers (Basel)*. 2020;12(12):1-13. doi:10.3390/cancers12123851

137. Kumar V, Chaudhary N, Garg M, Floudas CS, Soni P, Chandra AB. Current diagnosis and management of immune related adverse events (irAEs) induced by immune

checkpoint inhibitor therapy. *Front Pharmacol*. 2017;8(FEB). doi:10.3389/fphar.2017.00049

138. Weber JS, Postow M, Lao CD, Schadendorf D. Management of Adverse Events Following Treatment With Anti-Programmed Death-1 Agents. *Oncologist*. 2016;21(10):1230-1240. doi:10.1634/theoncologist.2016-0055

139. Larkin J, Chmielowski B, Lao CD, et al. Neurologic Serious Adverse Events Associated with Nivolumab Plus Ipilimumab or Nivolumab Alone in Advanced Melanoma, Including a Case Series of Encephalitis. *Oncologist*. 2017;22(6):709-718. doi:10.1634/theoncologist.2016-0487

140. Suo A, Chan Y, Beaulieu C, et al. Anti-PD1-Induced Immune-Related Adverse Events and Survival Outcomes in Advanced Melanoma. *Oncologist*. 2020;25(5):438-446. doi:10.1634/theoncologist.2019-0674

141. Naidoo J, Wang X, Woo KM, et al. Pneumonitis in patients treated with anti-programmed death-1/programmed death ligand 1 therapy. *Journal of Clinical Oncology*. 2017;35(7):709-717. doi:10.1200/JCO.2016.68.2005

142. Morganstein DL, Lai Z, Spain L, et al. Thyroid abnormalities following the use of cytotoxic T-lymphocyte antigen-4 and programmed death receptor protein-1 inhibitors in the treatment of melanoma. *Clin Endocrinol (Oxf)*. 2017;86(4):614-620. doi:10.1111/cen.13297

143. Kähler KC, Eigentler TK, Gesierich A, et al. Ipilimumab in metastatic melanoma patients with pre-existing autoimmune disorders. *Cancer Immunology, Immunotherapy*. 2018;67(5):825-834. doi:10.1007/s00262-018-2134-z

144. Chaput N, Lepage P, Coutzac C, et al. Baseline gut microbiota predicts clinical response and colitis in metastatic melanoma patients treated with ipilimumab. *Annals of Oncology*. 2017;28(6):1368-1379. doi:10.1093/annonc/mdx108

145. Guarner F, Malagelada JR. Gut flora in health and disease. *The Lancet*. 2003;361(9356):512-519. doi:10.1016/S0140-6736(03)12489-0

146. Turnbaugh PJ, Ley RE, Hamady M, Fraser-Liggett CM, Knight R, Gordon JI. The Human Microbiome Project. *Nature*. 2007;449(7164):804-810. doi:10.1038/nature06244

147. Lozupone CA, Stombaugh JI, Gordon JI, Jansson JK, Knight R. Diversity, stability and resilience of the human gut microbiota. *Nature*. 2012;489(7415):220-230. doi:10.1038/nature11550

148. The Human Microbiome Project Consortium. Structure, function and diversity of the healthy human microbiome. *Nature*. 2012;486(7402):207-214. doi:10.1038/nature11234

149. Rinninella E, Raoul P, Cintoni M, et al. What is the healthy gut microbiota composition? A changing ecosystem across age, environment, diet, and diseases. *Microorganisms*. 2019;7(1). doi:10.3390/microorganisms7010014

150. Singh RK, Chang HW, Yan D, et al. Influence of diet on the gut microbiome and implications for human health. *J Transl Med*. 2017;15(1). doi:10.1186/s12967-017-1175-y

151. Topping DL, Clifton PM. Short-Chain Fatty Acids and Human Colonic Function: Roles of Resistant Starch and Nonstarch Polysaccharides. *Physiol Rev*. 2001;81(3):1031-1064. doi:10.1152/physrev.2001.81.3.1031

152. Bielik V, Kolisek M. Bioaccessibility and bioavailability of minerals in relation to a healthy gut microbiome. *Int J Mol Sci*. 2021;22(13). doi:10.3390/ijms22136803

153. Kamada N, Chen GY, Inohara N, Núñez G. Control of pathogens and pathobionts by the gut microbiota. *Nat Immunol*. 2013;14(7):685-690. doi:10.1038/ni.2608

154. Khosravi A, Mazmanian SK. Disruption of the gut microbiome as a risk factor for microbial infections. *Curr Opin Microbiol*. 2013;16(2):221-227. doi:10.1016/j.mib.2013.03.009

155. Cammarota G, Ianiro G, Ahern A, et al. Gut microbiome, big data and machine learning to promote precision medicine for cancer. *Nat Rev Gastroenterol Hepatol*. 2020;17(10):635-648. doi:10.1038/s41575-020-0327-3

156. Aprile F, Bruno G, Palma R, et al. Microbiota Alterations in Precancerous Colon Lesions: A Systematic Review. *Cancers (Basel)*. 2021;13(12):3061. doi:10.3390/cancers13123061

157. Multhoff G, Molls M, Radons J. Chronic inflammation in cancer development. *Front Immunol*. 2011;2(JAN):98. doi:10.3389/fimmu.2011.00098

158. Singh V, Yeoh BS, Chassaing B, et al. Dysregulated Microbial Fermentation of Soluble Fiber Induces Cholestatic Liver Cancer. *Cell*. 2018;175(3):679-694.e22. doi:10.1016/j.cell.2018.09.004

159. Liévin-Le Moal V, Servin AL. The front line of enteric host defense against unwelcome intrusion of harmful microorganisms: Mucins, antimicrobial peptides, and Microbiota. *Clin Microbiol Rev*. 2006;19(2):315-337. doi:10.1128/CMR.19.2.315-337.2006

160. Jakobsson HE, Rodríguez-Piñeiro AM, Schütte A, et al. The composition of the gut microbiota shapes the colon mucus barrier. *EMBO Rep*. 2015;16(2):164-177. doi:10.15252/embr.201439263

161. Bergström A, Kristensen MB, Bahl MI, et al. Nature of bacterial colonization influences transcription of mucin genes in mice during the first week of life. *BMC Res Notes*. 2012;5. doi:10.1186/1756-0500-5-402

162. Desai MS, Seekatz AM, Koropatkin NM, et al. A Dietary Fiber-Deprived Gut Microbiota Degrades the Colonic Mucus Barrier and Enhances Pathogen Susceptibility. *Cell*. 2016;167(5):1339-1353.e21. doi:10.1016/j.cell.2016.10.043

163. Mörbe UM, Jørgensen PB, Fenton TM, et al. Human gut-associated lymphoid tissues (GALT); diversity, structure, and function. *Mucosal Immunol*. 2021;14(4):793-802. doi:10.1038/s41385-021-00389-4

164. Abreu MT. Toll-like receptor signalling in the intestinal epithelium: How bacterial recognition shapes intestinal function. *Nat Rev Immunol*. 2010;10(2):131-143. doi:10.1038/nri2707

165. Miettinen M, Matikainen S, Vuopio-Varkila J, et al. Lactobacilli and streptococci induce interleukin-12 (IL-12), IL-18, and gamma interferon production in human peripheral blood mononuclear cells. *Infect Immun*. 1998;66(12):6058-6062. doi:10.1128/IAI.66.12.6058-6062.1998

166. Park H, Li Z, Yang XO, et al. A distinct lineage of CD4 T cells regulates tissue inflammation by producing interleukin 17. *Nat Immunol*. 2005;6(11):1133-1141. doi:10.1038/ni1261

167. Khader SA, Gaffen SL, Kolls JK. Th17 cells at the crossroads of innate and adaptive immunity against infectious diseases at the mucosa. *Mucosal Immunol*. 2009;2(5):403-411. doi:10.1038/mi.2009.100

168. Mazmanian SK, Cui HL, Tzianabos AO, Kasper DL. An immunomodulatory molecule of symbiotic bacteria directs maturation of the host immune system. *Cell*. 2005;122(1):107-118. doi:10.1016/j.cell.2005.05.007

169. Östman S, Rask C, Wold AE, Hultkrantz S, Telemo E. Impaired regulatory T cell function in germ-free mice. *Eur J Immunol*. 2006;36(9):2336-2346. doi:10.1002/eji.200535244

170. Umesaki Y, Setoyama H, Matsumoto S, Okada Y. Expansion of alpha beta T-cell receptor-bearing intestinal intraepithelial lymphocytes after microbial colonization in germ-free mice and its independence from thymus. *Immunology*. 1993;79(1):32-37. http://www.ncbi.nlm.nih.gov/pubmed/8509140

171. Ivanov II, Frutos R de L, Manel N, et al. Specific Microbiota Direct the Differentiation of IL-17-Producing T-Helper Cells in the Mucosa of the Small Intestine. *Cell Host Microbe*. 2008;4(4):337-349. doi:10.1016/j.chom.2008.09.009

172. Gaboriau-Routhiau V, Rakotobe S, Lécuyer E, et al. The Key Role of Segmented Filamentous Bacteria in the Coordinated Maturation of Gut Helper T Cell Responses. *Immunity*. 2009;31(4):677-689. doi:10.1016/j.immuni.2009.08.020

173. Caroff M, Karibian D, Cavaillon JM, Haeffner-Cavaillon N. Structural and functional analyses of bacterial lipopolysaccharides. *Microbes Infect*. 2002;4(9):915-926. doi:10.1016/S1286-4579(02)01612-X

174. Adib-Conquy M, Scott-Algara D, Cavaillon JM, Souza-Fonseca-Guimaraes F. TLR-mediated activation of NK cells and their role in bacterial/viral immune responses in mammals. *Immunol Cell Biol*. 2014;92(3):256-262. doi:10.1038/icb.2013.99

175. Kosaka A, Yan H, Ohashi S, et al. Lactococcus lactis subsp. cremoris FC triggers IFN-γ production from NK and T cells via IL-12 and IL-18. *Int Immunopharmacol*. 2012;14(4):729-733. doi:10.1016/j.intimp.2012.10.007

176. Lam KC, Araya RE, Huang A, et al. Microbiota triggers STING-type I IFN-dependent monocyte reprogramming of the tumor microenvironment. *Cell*. 2021;184(21):5338-5356.e21. doi:10.1016/j.cell.2021.09.019

177. Nicolai CJ, Wolf N, Chang IC, et al. NK cells mediate clearance of CD8+ T cell-resistant tumors in response to STING agonist. *Sci Immunol*. 2020;5(45). doi:10.1126/sciimmunol.aaz2738

178. Steed AL, Christophi GP, Kaiko GE, et al. The microbial metabolite desaminotyrosine protects from influenza through type I interferon. *Science (1979)*. Published online 2017. doi:10.1126/science.aam5336

179. Wang Q, Fang Z, Xiao Y, et al. Lactiplantibacillus pentoses CCFM1227 Produces Desaminotyrosine to Protect against Influenza Virus H1N1 Infection through the Type I Interferon in Mice. *Nutrients*. 2023;15(16). doi:10.3390/nu15163659

180. Chang P V., Hao L, Offermanns S, Medzhitov R. The microbial metabolite butyrate regulates intestinal macrophage function via histone deacetylase inhibition. *Proc Natl Acad Sci U S A*. 2014;111(6):2247-2252. doi:10.1073/pnas.1322269111

181. Smith PM, Howitt MR, Panikov N, et al. The microbial metabolites, short-chain fatty acids, regulate colonic T reg cell homeostasis. *Science (1979)*. 2013;341(6145):569-573. doi:10.1126/science.1241165

182. Round JL, Mazmanian SK. Inducible Foxp3+ regulatory T-cell development by a commensal bacterium of the intestinal microbiota. *Proc Natl Acad Sci U S A*. 2010;107(27):12204-12209. doi:10.1073/pnas.0909122107

183. Round JL, O'Connell RM, Mazmanian SK. Coordination of tolerogenic immune responses by the commensal microbiota. *J Autoimmun*. 2010;34(3):J220-J225. doi:10.1016/j.jaut.2009.11.007

184. Davar D, Dzutsev AK, McCulloch JA, et al. Fecal microbiota transplant overcomes resistance to anti–PD-1 therapy in melanoma patients. *Science (1979)*. 2021;371(6529):595-602. doi:10.1126/science.abf3363

185. Peters BA, Wilson M, Moran U, et al. Relating the gut metagenome and metatranscriptome to immunotherapy responses in melanoma patients. *Genome Med*. 2019;11(1):61. doi:10.1186/s13073-019-0672-4

186. Gopalakrishnan V, Spencer CN, Nezi L, et al. Gut microbiome modulates response to anti-PD-1 immunotherapy in melanoma patients. *Science (1979)*. 2018;359(6371):97-103. doi:10.1126/science.aan4236

187. Jin Y, Dong H, Xia L, et al. The Diversity of Gut Microbiome is Associated With Favorable Responses to Anti–Programmed Death 1 Immunotherapy in Chinese Patients With NSCLC. *Journal of Thoracic Oncology*. 2019;14(8):1378-1389. doi:10.1016/j.jtho.2019.04.007

188. Zheng Y, Wang T, Tu X, et al. Gut microbiome affects the response to anti-PD-1 immunotherapy in patients with hepatocellular carcinoma. *J Immunother Cancer*. 2019;7(1). doi:10.1186/s40425-019-0650-9

189. Matson V, Fessler J, Bao R, et al. The commensal microbiome is associated with anti-PD-1 efficacy in metastatic melanoma patients. *Science (1979)*. 2018;359(6371):104-108. doi:10.1126/science.aao3290

190. Baruch EN, Youngster I, Ben-Betzalel G, et al. Fecal microbiota transplant promotes response in immunotherapy-refractory melanoma patients. *Science (1979)*. 2021;371(6529):602-609. doi:10.1126/science.abb5920

191. Frankel AE, Coughlin LA, Kim J, et al. Metagenomic Shotgun Sequencing and Unbiased Metabolomic Profiling Identify Specific Human Gut Microbiota and Metabolites Associated with Immune Checkpoint Therapy Efficacy in Melanoma Patients. *Neoplasia (United States)*. 2017;19(10):848-855. doi:10.1016/j.neo.2017.08.004

192. Andrews MC, Duong CPM, Gopalakrishnan V, et al. Gut microbiota signatures are associated with toxicity to combined CTLA-4 and PD-1 blockade. *Nat Med*. 2021;27(8):1432-1441. doi:10.1038/s41591-021-01406-6

193. Wind TT, Gacesa R, Vich Vila A, et al. Gut microbial species and metabolic pathways associated with response to treatment with immune checkpoint inhibitors in metastatic melanoma. *Melanoma Res*. 2020;30(3):235-246. doi:10.1097/CMR.0000000000000656

194. Kelly BJ, Tebas P. Clinical Practice and Infrastructure Review of Fecal Microbiota Transplantation for Clostridium difficile Infection. *Chest*. 2018;153(1):266-277. doi:10.1016/j.chest.2017.09.002

195. Routy B, Le Chatelier E, Derosa L, et al. Gut microbiome influences efficacy of PD-1-based immunotherapy against epithelial tumors. *Science (1979)*. 2018;359(6371):91-97. doi:10.1126/science.aan3706

196. Gopalakrishnan V, Spencer CN, Nezi L, et al. Gut microbiome modulates response to anti–PD-1 immunotherapy in melanoma patients. *Science (1979)*. 2018;359(6371):97-103. doi:10.1126/science.aan4236

197. Parvez S, Malik KA, Ah Kang S, Kim HY. Probiotics and their fermented food products are beneficial for health. *J Appl Microbiol*. 2006;100(6):1171-1185. doi:10.1111/j.1365-2672.2006.02963.x

198. Sivan A, Corrales L, Hubert N, et al. Commensal Bifidobacterium promotes antitumor immunity and facilitates anti-PD-L1 efficacy. *Science (1979)*. 2015;350(6264):1084-1089. doi:10.1126/science.aac4255

199. Vétizou M, Pitt JM, Daillère R, et al. Anticancer immunotherapy by CTLA-4 blockade relies on the gut microbiota. *Science (1979)*. 2015;350(6264):1079-1084. doi:10.1126/science.aad1329

200. Derosa L, Zitvogel L. A probiotic supplement boosts response to cancer immunotherapy. *Nat Med*. 2022;28(4):633-634. doi:10.1038/s41591-022-01723-4

201. Tomita Y, Ikeda T, Sakata S, et al. Association of probiotic clostridium butyricum therapy with survival and response to immune checkpoint blockade in patients with lung cancer. *Cancer Immunol Res*. 2020;8(10):1236-1242. doi:10.1158/2326-6066.CIR-20-0051

202. Cheng D, Xie MZ. A review of a potential and promising probiotic candidate—Akkermansia muciniphila. *J Appl Microbiol*. 2021;130(6):1813-1822. doi:10.1111/jam.14911

203. Goderska K, Nowak J, Czarnecki Z. Comparision of growth of Lactobacillus acidophilus and Bifidobacterium Bifidum species in media suplemented with selected saccharides including prebiotics. *ACTA Acta Sci Pol, Technol Aliment*. 2008;7(2):5-20.

204. Manning TS, Gibson GR. Prebiotics. *Best Pract Res Clin Gastroenterol*. 2004;18(2):287-298. doi:10.1016/j.bpg.2003.10.008

205. Spencer CN, McQuade JL, Gopalakrishnan V, et al. Dietary fiber and probiotics influence the gut microbiome and melanoma immunotherapy response. *Science (1979)*. 2021;374(6575):1632-1640. doi:10.1126/science.aaz7015

206. Mager LF, Burkhard R, Pett N, et al. Microbiome-derived inosine modulates response to checkpoint inhibitor immunotherapy. *Science (1979)*. 2020;369(6510):1481-1489. doi:10.1126/science.abc3421

207. Gnanaprakasam JNR, López-Bañuelos L, Vega L. Anacardic 6-pentadecyl salicylic acid induces apoptosis in breast cancer tumor cells, immunostimulation in the host and decreases blood toxic effects of taxol in an animal model. *Toxicol Appl Pharmacol*. 2021;410. doi:10.1016/j.taap.2020.115359

208. Luu M, Riester Z, Baldrich A, et al. Microbial short-chain fatty acids modulate CD8+ T cell responses and improve adoptive immunotherapy for cancer. *Nat Commun*. 2021;12(1). doi:10.1038/s41467-021-24331-1

209. Nomura M, Nagatomo R, Doi K, et al. Association of Short-Chain Fatty Acids in the Gut Microbiome With Clinical Response to Treatment With Nivolumab or Pembrolizumab in Patients With Solid Cancer Tumors. *JAMA Netw Open*. 2020;3(4):e202895. doi:10.1001/jamanetworkopen.2020.2895

210. Bender MJ, McPherson AC, Phelps CM, et al. Dietary tryptophan metabolite released by intratumoral Lactobacillus reuteri facilitates immune checkpoint inhibitor treatment. *Cell*. 2023;186(9):1846-1862.e26. doi:10.1016/j.cell.2023.03.011

211. Son MY, Cho HS. Anticancer Effects of Gut Microbiota-Derived Short-Chain Fatty Acids in Cancers. *J Microbiol Biotechnol*. 2023;33(7):849-856. doi:10.4014/jmb.2301.01031

212. Coutzac C, Jouniaux JM, Paci A, et al. Systemic short chain fatty acids limit antitumor effect of CTLA-4 blockade in hosts with cancer. *Nat Commun*. 2020;11(1). doi:10.1038/s41467-020-16079-x

213. Stutz MR, Dylla NP, Pearson SD, et al. Immunomodulatory fecal metabolites are associated with mortality in COVID-19 patients with respiratory failure. *Nat Commun*. 2022;13(1):6615. doi:10.1038/s41467-022-34260-2

214. Müller U, Steinhoff U, Reis LFL, et al. Functional Role of Type I and Type II Interferons in Antiviral Defense. *Science (1979)*. 1994;264(5167):1918-1921. doi:10.1126/science.8009221

215. Poeck H, Besch R, Maihoefer C, et al. 5′-triphosphate-siRNA: turning gene silencing and Rig-I activation against melanoma. *Nat Med*. 2008;14(11):1256-1263. doi:10.1038/nm.1887

216. Fischer JC, Wintges A, Haas T, Poeck H. Assessment of mucosal integrity by quantifying neutrophil granulocyte influx in murine models of acute intestinal injury. *Cell Immunol*. 2017;316:70-76. doi:10.1016/j.cellimm.2017.04.003

217. Han J, Lin K, Sequeira C, Borchers CH. An isotope-labeled chemical derivatization method for the quantitation of short-chain fatty acids in human feces by liquid chromatography-tandem mass spectrometry. *Anal Chim Acta*. 2015;854:86-94. doi:10.1016/j.aca.2014.11.015

218. Reitmeier S, Kiessling S, Clavel T, et al. Arrhythmic Gut Microbiome Signatures Predict Risk of Type 2 Diabetes. *Cell Host Microbe*. 2020;28(2):258-272.e6. doi:10.1016/j.chom.2020.06.004

219. Klindworth A, Pruesse E, Schweer T, et al. Evaluation of general 16S ribosomal RNA gene PCR primers for classical and next-generation sequencing-based diversity studies. *Nucleic Acids Res*. 2013;41(1). doi:10.1093/nar/gks808

220. Kioukis A, Pourjam M, Neuhaus K, Lagkouvardos I. Taxonomy Informed Clustering, an Optimized Method for Purer and More Informative Clusters in Diversity Analysis and Microbiome Profiling. *Frontiers in Bioinformatics*. 2022;2. doi:10.3389/fbinf.2022.864597

221. Lagkouvardos I, Joseph D, Kapfhammer M, et al. IMNGS: A comprehensive open resource of processed 16S rRNA microbial profiles for ecology and diversity studies. *Sci Rep*. 2016;6. doi:10.1038/srep33721

222. Lagkouvardos I, Fischer S, Kumar N, Clavel T. Rhea: a transparent and modular R pipeline for microbial profiling based on 16S rRNA gene amplicons. *PeerJ*. 2017;5(1):e2836. doi:10.7717/peerj.2836

223. Reitmeier S, Hitch TCA, Treichel N, et al. Handling of spurious sequences affects the outcome of high-throughput 16S rRNA gene amplicon profiling. *ISME Communications*. 2021;1(1). doi:10.1038/s43705-021-00033-z

224. Heidegger S, Wintges A, Stritzke F, et al. RIG-I activation is critical for responsiveness to checkpoint blockade. *Sci Immunol*. 2019;4(39). doi:10.1126/sciimmunol.aau8943

225. Gnanaprakasam JNR, Estrada-Muñiz E, Vega L. The anacardic 6-pentadecyl salicylic acid induces macrophage activation via the phosphorylation of ERK1/2, JNK, P38 kinases and NF-κB. *Int Immunopharmacol*. 2015;29(2):808-817. doi:10.1016/j.intimp.2015.08.038

226. Schultz DJ, Wickramasinghe NS, Ivanova MM, et al. Anacardic acid inhibits estrogen receptor α-DNA binding and reduces target gene transcription and breast cancer cell proliferation. *Mol Cancer Ther*. 2010;9(3):594-605. doi:10.1158/1535-7163.MCT-09-0978

227. Amirkhosravi A, Meyer T, Chang JY, et al. Tissue factor pathway inhibitor reduces experimental lung metastasis of B16 melanoma. *Thromb Haemost*. 2002;87(6):930-936. http://www.ncbi.nlm.nih.gov/pubmed/12083498

228. Heidegger S, Kreppel D, Bscheider M, et al. RIG-I activating immunostimulatory RNA boosts the efficacy of anticancer vaccines and synergizes with immune checkpoint blockade. *EBioMedicine*. 2019;41:146-155. doi:10.1016/j.ebiom.2019.02.056

229. Wei Y, Gao J, Kou Y, et al. The intestinal microbial metabolite desaminotyrosine is an anti-inflammatory molecule that modulates local and systemic immune homeostasis. *The FASEB Journal*. 2020;34(12):16117-16128. doi:10.1096/fj.201902900RR

230. Ahmed J, Kumar A, Parikh K, et al. Use of broad-spectrum antibiotics impacts outcome in patients treated with immune checkpoint inhibitors. *Oncoimmunology*. 2018;7(11). doi:10.1080/2162402X.2018.1507670

231. Elkrief A, El Raichani L, Richard C, et al. Antibiotics are associated with decreased progression-free survival of advanced melanoma patients treated with immune checkpoint inhibitors. *Oncoimmunology*. 2019;8(4). doi:10.1080/2162402X.2019.1568812

232. Tinsley N, Zhou C, Tan G, et al. Cumulative Antibiotic Use Significantly Decreases Efficacy of Checkpoint Inhibitors in Patients with Advanced Cancer. *Oncologist*. 2020;25(1):55-63. doi:10.1634/theoncologist.2019-0160

233. Derosa L, Hellmann MD, Spaziano M, et al. Negative association of antibiotics on clinical activity of immune checkpoint inhibitors in patients with advanced renal cell and non-small-cell lung cancer. *Annals of Oncology*. 2018;29(6):1437-1444. doi:10.1093/annonc/mdy103

234. Pinato DJ, Howlett S, Ottaviani D, et al. Association of prior antibiotic treatment with survival and response to immune checkpoint inhibitor therapy in patients with cancer. *JAMA Oncol*. 2019;5(12):1774-1778. doi:10.1001/jamaoncol.2019.2785

235. Schoch CL, Ciufo S, Domrachev M, et al. NCBI Taxonomy: a comprehensive update on curation, resources and tools. *Database (Oxford)*. 2020;2020. doi:10.1093/database/baaa062

236. d'Aldebert E, Quaranta M, Sébert M, et al. Characterization of Human Colon Organoids From Inflammatory Bowel Disease Patients. *Front Cell Dev Biol*. 2020;8. doi:10.3389/fcell.2020.00363

237. Dickson P V., Gershenwald JE. Staging and prognosis of cutaneous melanoma. *Surg Oncol Clin N Am*. 2011;20(1):1-17. doi:10.1016/j.soc.2010.09.007

238. Bartlett EK, Karakousis GC. Current staging and prognostic factors in melanoma. *Surg Oncol Clin N Am*. 2015;24(2):215-227. doi:10.1016/j.soc.2014.12.001

239. Jin Y, Wang PS, Li Z, et al. Abstract A010: Development of OVA-expressing immunogenic syngeneic mouse tumor models: CT26-OVA and B16-OVA. *Mol Cancer Ther*. 2019;18(12_Supplement):A010-A010. doi:10.1158/1535-7163.TARG-19-A010

240. Ruocco MG, Pilones KA, Kawashima N, et al. Suppressing T cell motility induced by anti-CTLA-4 monotherapy improves antitumor effects. *Journal of Clinical Investigation*. 2012;122(10):3718-3730. doi:10.1172/JCI61931

241. Mikó E, Vida A, Kovács T, et al. Lithocholic acid, a bacterial metabolite reduces breast cancer cell proliferation and aggressiveness. *Biochim Biophys Acta Bioenerg*. 2018;1859(9):958-974. doi:10.1016/j.bbabio.2018.04.002

242. Shi L, Sheng J, Wang M, et al. Combination Therapy of TGF-β Blockade and Commensal-derived Probiotics Provides Enhanced Antitumor Immune Response and Tumor Suppression. *Theranostics*. 2019;9(14):4115-4129. doi:10.7150/thno.35131

243. Yu AQ, Li L. The Potential Role of Probiotics in Cancer Prevention and Treatment. *Nutr Cancer*. 2016;68(4):535-544. doi:10.1080/01635581.2016.1158300

244. Renga G, Nunzi E, Pariano M, et al. Optimizing therapeutic outcomes of immune checkpoint blockade by a microbial tryptophan metabolite. *J Immunother Cancer*. 2022;10(3). doi:10.1136/jitc-2021-003725

245. Zhan Y, Chen PJ, Sadler WD, et al. Gut microbiota protects against gastrointestinal tumorigenesis caused by epithelial injury. *Cancer Res*. 2013;73(24):7199-7210. doi:10.1158/0008-5472.CAN-13-0827

246. Wang CSE, Li W Bin, Wang HY, et al. VSL#3 can prevent ulcerative colitis-associated carcinogenesis in mice. *World J Gastroenterol*. 2018;24(37):4254-4262. doi:10.3748/wjg.v24.i37.4254

247. Levit R, Savoy de Giori G, de Moreno de LeBlanc A, LeBlanc JG. Evaluation of vitamin-producing and immunomodulatory lactic acid bacteria as a potential co-adjuvant for cancer therapy in a mouse model. *J Appl Microbiol*. 2021;130(6):2063-2074. doi:10.1111/jam.14918

248. Cyriac JM, James E. Switch over from intravenous to oral therapy: A concise overview. *J Pharmacol Pharmacother*. 2014;5(2):83-87. doi:10.4103/0976-500X.130042

249. Bachem A, Makhlouf C, Binger KJ, et al. Microbiota-Derived Short-Chain Fatty Acids Promote the Memory Potential of Antigen-Activated CD8+ T Cells. *Immunity*. 2019;51(2):285-297.e5. doi:10.1016/j.immuni.2019.06.002

250. Ulmer AJ, Flad HD, Rietschel Th, Mattern T. Induction of proliferation and cytokine production in human T lymphocytes by lipopolysaccharide (LPS). *Toxicology*. 2000;152(1-3):37-45. doi:10.1016/S0300-483X(00)00290-0

251. Driessens G, Kline J, Gajewski TF. Costimulatory and coinhibitory receptors in anti-tumor immunity. *Immunol Rev*. 2009;229(1):126-144. doi:10.1111/j.1600-065X.2009.00771.x

252. Ma X, Zhou Z, Zhang X, et al. Sodium butyrate modulates gut microbiota and immune response in colorectal cancer liver metastatic mice. *Cell Biol Toxicol*. 2020;36(5):509-515. doi:10.1007/s10565-020-09518-4

253. Ihekweazu FD, Engevik MA, Ruan W, et al. Bacteroides ovatus Promotes IL-22 Production and Reduces Trinitrobenzene Sulfonic Acid–Driven Colonic Inflammation. *American Journal of Pathology*. 2021;191(4):704-719. doi:10.1016/j.ajpath.2021.01.009

254. Tuccitto A, Shahaj E, Vergani E, et al. Immunosuppressive circuits in tumor microenvironment and their influence on cancer treatment efficacy. *Virchows Archiv*. 2019;474(4):407-420. doi:10.1007/s00428-018-2477-z

255. Lin ML, Zhan Y, Villadangos JA, Lew AM. The cell biology of cross-presentation and the role of dendritic cell subsets. *Immunol Cell Biol*. 2008;86(4):353-362. doi:10.1038/icb.2008.3

256. Hollands A, Corriden R, Gysler G, et al. Natural product anacardic acid from cashew nut shells stimulates neutrophil extracellular trap production and bactericidal activity. *Journal of Biological Chemistry*. 2016;291(27):13964-13973. doi:10.1074/jbc.M115.695866

257. Garley M, Jabłońska E, Dąbrowska D. NETs in cancer. *Tumor Biology*. 2016;37(11):14355-14361. doi:10.1007/s13277-016-5328-z

258. Zingoni A, Sornasse T, Cocks BG, Tanaka Y, Santoni A, Lanier LL. NK cell regulation of T cell-mediated responses. *Mol Immunol*. 2005;42(4 SPEC. ISS.):451-454. doi:10.1016/j.molimm.2004.07.025

259. Cox MA, Harrington LE, Zajac AJ. Cytokines and the inception of CD8 T cell responses. *Trends Immunol*. 2011;32(4):180-186. doi:10.1016/j.it.2011.01.004

260. Schulthess J, Pandey S, Capitani M, et al. The Short Chain Fatty Acid Butyrate Imprints an Antimicrobial Program in Macrophages. *Immunity*. 2019;50(2):432-445.e7. doi:10.1016/j.immuni.2018.12.018

261. Gafter-Gvili A, Fraser A, Paul M, et al. Antibiotic prophylaxis for bacterial infections in afebrile neutropenic patients following chemotherapy. *Cochrane Database of Systematic Reviews*. 2012;2018(7). doi:10.1002/14651858.CD004386.pub3

262. Freifeld AG, Bow EJ, Sepkowitz KA, et al. Clinical practice guideline for the use of antimicrobial agents in neutropenic patients with cancer: 2010 Update by the Infectious Diseases Society of America. *Clinical Infectious Diseases*. 2011;52(4). doi:10.1093/cid/cir073

263. Lange K, Buerger M, Stallmach A, Bruns T. Effects of Antibiotics on Gut Microbiota. *Digestive Diseases*. 2016;34(3):260-268. doi:10.1159/000443360

264. Raymond F, Déraspe M, Boissinot M, Bergeron MG, Corbeil J. Partial recovery of microbiomes after antibiotic treatment. *Gut Microbes*. 2016;7(5):428-434. doi:10.1080/19490976.2016.1216747

265. Palleja A, Mikkelsen KH, Forslund SK, et al. Recovery of gut microbiota of healthy adults following antibiotic exposure. *Nat Microbiol*. 2018;3(11):1255-1265. doi:10.1038/s41564-018-0257-9

266. Castello A, Rossi S, Toschi L, Lopci E. Impact of antibiotic therapy and metabolic parameters in non-small cell lung cancer patients receiving checkpoint inhibitors. *J Clin Med*. 2021;10(6):1-12. doi:10.3390/jcm10061251

267. Thompson J, Szabo A, Arce-Lara C, Menon S. Antibiotic Use Is Associated with Inferior Survival for Lung Cancer Patients Receiving PD-1 Inhibitors. *Journal of Thoracic Oncology*. 2017;12(11):S1998. doi:10.1016/j.jtho.2017.09.926

268. Suez J, Zmora N, Zilberman-Schapira G, et al. Post-Antibiotic Gut Mucosal Microbiome Reconstitution Is Impaired by Probiotics and Improved by Autologous FMT. *Cell*. 2018;174(6):1406-1423.e16. doi:10.1016/j.cell.2018.08.047

269. Limeta A, Ji B, Levin M, Gatto F, Nielsen J. Meta-analysis of the gut microbiota in predicting response to cancer immunotherapy in metastatic melanoma. *JCI Insight*. 2020;5(23). doi:10.1172/jci.insight.140940

270. Fernandes MR, Aggarwal P, Costa RGF, Cole AM, Trinchieri G. Targeting the gut microbiota for cancer therapy. *Nat Rev Cancer*. 2022;22(12):703-722. doi:10.1038/s41568-022-00513-x

271. Gupta A, Dhakan DB, Maji A, et al. Association of Flavonifractor plautii, a Flavonoid-Degrading Bacterium, with the Gut Microbiome of Colorectal Cancer Patients in India. *mSystems*. 2019;4(6). doi:10.1128/msystems.00438-19

272. McCulloch JA, Davar D, Rodrigues RR, et al. Intestinal microbiota signatures of clinical response and immune-related adverse events in melanoma patients treated with anti-PD-1. *Nat Med*. 2022;28(3):545-556. doi:10.1038/s41591-022-01698-2

273. Hexun Z, Miyake T, Maekawa T, et al. High abundance of Lachnospiraceae in the human gut microbiome is related to high immunoscores in advanced colorectal cancer. *Cancer Immunology, Immunotherapy*. 2023;72(2):315-326. doi:10.1007/s00262-022-03256-8

274. Osman MA, Neoh HM, Mutalib NSA, Chin SF, Jamal R. 16S rRNA gene sequencing for deciphering the colorectal cancer gut microbiome: Current protocols and workflows. *Front Microbiol*. 2018;9(APR). doi:10.3389/fmicb.2018.00767

275. Durazzi F, Sala C, Castellani G, Manfreda G, Remondini D, De Cesare A. Comparison between 16S rRNA and shotgun sequencing data for the taxonomic characterization of the gut microbiota. *Sci Rep*. 2021;11(1). doi:10.1038/s41598-021-82726-y

276. Campanaro S, Treu L, Kougias PG, Zhu X, Angelidaki I. Taxonomy of anaerobic digestion microbiome reveals biases associated with the applied high throughput sequencing strategies. *Sci Rep*. 2018;8(1). doi:10.1038/s41598-018-20414-0

277. Coker OO, Dai Z, Nie Y, et al. Mucosal microbiome dysbiosis in gastric carcinogenesis. *Gut*. 2018;67(6):1024-1032. doi:10.1136/gutjnl-2017-314281

278. Ferreira RM, Pereira-Marques J, Pinto-Ribeiro I, et al. Gastric microbial community profiling reveals a dysbiotic cancer-associated microbiota. *Gut*. 2018;67(2):226-236. doi:10.1136/gutjnl-2017-314205

279. Matsukawa H, Iida N, Kitamura K, et al. *Dysbiotic Gut Microbiota in Pancreatic Cancer Patients Form Correlation Networks with the Oral Microbiota and Prognostic Factors*. Vol 11.; 2021. www.ajcr.us/

280. Yu J, Feng Q, Wong SH, et al. Metagenomic analysis of faecal microbiome as a tool towards targeted non-invasive biomarkers for colorectal cancer. *Gut*. 2017;66(1):70-78. doi:10.1136/gutjnl-2015-309800

281. Atarashi K, Suda W, Luo C, et al. Ectopic colonization of oral bacteria in the intestine drives TH1 cell induction and inflammation. *Science (1979)*. 2017;358(6361):359-365. doi:10.1126/science.aan4526

282. Tezal M, Sullivan MA, Hyland A, et al. Chronic periodontitis and the incidence of head and neck squamous cell carcinoma. *Cancer Epidemiology Biomarkers and Prevention*. 2009;18(9):2406-2412. doi:10.1158/1055-9965.EPI-09-0334

283. Mai X, LaMonte MJ, Hovey KM, et al. History of periodontal disease diagnosis and lung cancer incidence in the Women's Health Initiative Observational Study. *Cancer Causes and Control*. 2014;25(8):1045-1053. doi:10.1007/s10552-014-0405-3

284. McCarty MF, Bielenberg D, Donawho C, Bucana CD, Fidler IJ. Evidence for the causal role of endogenous interferon-alpha/beta in the regulation of angiogenesis, tumorigenicity, and metastasis of cutaneous neoplasms. *Clin Exp Metastasis*. 2002;19(7):609-615. doi:10.1023/a:1020923326441

285. Antunes KH, Fachi JL, de Paula R, et al. Microbiota-derived acetate protects against respiratory syncytial virus infection through a GPR43-type 1 interferon response. *Nat Commun*. 2019;10(1). doi:10.1038/s41467-019-11152-6

286. Schaupp L, Muth S, Rogell L, et al. Microbiota-Induced Type I Interferons Instruct a Poised Basal State of Dendritic Cells. *Cell*. 2020;181(5):1080-1096.e19. doi:10.1016/j.cell.2020.04.022

287. Gutierrez-Merino J, Isla B, Combes T, Martinez-Estrada F, Maluquer De Motes C. Beneficial bacteria activate type-I interferon production via the intracellular cytosolic sensors STING and MAVS. *Gut Microbes*. 2020;11(4):771-788. doi:10.1080/19490976.2019.1707015

288. Chen J, Cao Y, Markelc B, Kaeppler J, Vermeer JAF, Muschel RJ. Type i IFN protects cancer cells from CD8+ T cell-mediated cytotoxicity after radiation. *Journal of Clinical Investigation*. 2019;129(10):4224-4238. doi:10.1172/JCI127458

289. Wan S, Pestka S, Jubin RG, Lyu YL, Tsai YC, Liu LF. Chemotherapeutics and radiation stimulate MHC class i expression through elevated interferon-beta signaling in breast cancer cells. *PLoS One*. 2012;7(3). doi:10.1371/journal.pone.0032542

290. Yang YQ, Dong WJ, Yin XF, et al. Interferon-related secretome from direct interaction between immune cells and tumor cells is required for upregulation of PD-L1 in tumor cells. *Protein Cell*. 2016;7(7):538-543. doi:10.1007/s13238-016-0281-6

291. Katlinskaya Y V., Katlinski K V., Yu Q, et al. Suppression of Type I Interferon Signaling Overcomes Oncogene-Induced Senescence and Mediates Melanoma Development and Progression. *Cell Rep*. 2016;15(1):171-180. doi:10.1016/j.celrep.2016.03.006

292. Katlinski K V., Gui J, Katlinskaya Y V., et al. Inactivation of Interferon Receptor Promotes the Establishment of Immune Privileged Tumor Microenvironment. *Cancer Cell*. 2017;31(2):194-207. doi:10.1016/j.ccell.2017.01.004

293. Chang LC, Fan CW, Tseng WK, et al. IFNAR1 is a predictor for overall survival in colorectal cancer and its mRNA expression correlated with IRF7 but not TLR9. *Medicine (United States)*. 2014;93(29):e349. doi:10.1097/MD.0000000000000349

294. Boukhaled GM, Harding S, Brooks DG. Opposing Roles of Type I Interferons in Cancer Immunity. *Annu Rev Pathol Mech Dis 2021*. 2020;16:167-198. doi:10.1146/annurev-pathol-031920

295. Santoni M, Piva F, Conti A, et al. Gut Microbiome Influences Efficacy of PD-1-based Immunotherapy Against Epithelial Tumors. *Eur Urol*. 2018;74(4):521-522. doi:10.1016/j.eururo.2018.05.033

296. Tumas S, Meldgaard TS, Vaaben TH, et al. Engineered E. coli Nissle 1917 for delivery of bioactive IL-2 for cancer immunotherapy. *Sci Rep*. 2023;13(1). doi:10.1038/s41598-023-39365-2

297. Skeate JG, Otsmaa ME, Prins R, Fernandez DJ, Da Silva DM, Kast WM. TNFSF14: LIGHTing the Way for Effective Cancer Immunotherapy. *Front Immunol*. 2020;11. doi:10.3389/fimmu.2020.00922

298. Zheng JH, Nguyen VH, Jiang SN, et al. Two-step enhanced cancer immunotherapy with engineered Salmonella typhimurium secreting heterologous flagellin. *Sci Transl Med*. 2017;9(376). doi:10.1126/scitranslmed.aak9537

299. Canale FP, Basso C, Antonini G, et al. Metabolic modulation of tumours with engineered bacteria for immunotherapy. *Nature*. 2021;598(7882):662-666. doi:10.1038/s41586-021-04003-2

300. Zelante T, Iannitti RG, Cunha C, et al. Tryptophan catabolites from microbiota engage aryl hydrocarbon receptor and balance mucosal reactivity via interleukin-22. *Immunity*. 2013;39(2):372-385. doi:10.1016/j.immuni.2013.08.003

301. Bae M, Cassilly CD, Liu X, et al. Akkermansia muciniphila phospholipid induces homeostatic immune responses. *Nature*. 2022;608(7921):168-173. doi:10.1038/s41586-022-04985-7

302. Liu Y, Zhang X, Chen S, et al. Gut-derived lipopolysaccharide promotes alcoholic hepatosteatosis and subsequent hepatocellular carcinoma by stimulating neutrophil extracellular traps through toll-like receptor 4. *Clin Mol Hepatol*. 2022;28(3):522-539. doi:10.3350/cmh.2022.0039

303. Dore MP, Bibbò S, Fresi G, Bassotti G, Pes GM. Side effects associated with probiotic use in adult patients with inflammatory bowel disease: A systematic review and meta-analysis of randomized controlled trials. *Nutrients*. 2019;11(12). doi:10.3390/nu11122913

304. DeFilipp Z, Bloom PP, Torres Soto M, et al. Drug-Resistant E. coli Bacteremia Transmitted by Fecal Microbiota Transplant . *New England Journal of Medicine*. 2019;381(21):2043-2050. doi:10.1056/nejmoa1910437

305. Dailey FE, Turse EP, Daglilar E, Tahan V. The dirty aspects of fecal microbiota transplantation: a review of its adverse effects and complications. *Curr Opin Pharmacol*. 2019;49:29-33. doi:10.1016/j.coph.2019.04.008

306. The european parliament and the council of the european union. Regulation (EU) No 536/2014 on clinical trials on medicinal products for human use, and repealing Directive 2001/20/EC. Official Journal of the European Union. Published 2014. Accessed November 13, 2023. https://eur-lex.europa.eu/eli/reg/2014/536/2022-12-05

307. European Commission. Guidelines on Good Manufacturing Practice specific to Advanced Therapy Medicinal Products. *EudraLex - The Rules Governing Medicinal Products in the European Union*. 2017;4.

308. Suez J, Zmora N, Segal E, Elinav E. The pros, cons, and many unknowns of probiotics. *Nat Med*. 2019;25(5):716-729. doi:10.1038/s41591-019-0439-x

VI ACKNOWLEDGEMENTS

First, I would like to thank my supervisors Hendrik Poeck and Simon Heidegger who made this project possible and gave me the opportunity to delve into a challenging and rewarding research journey.

My gratitude also goes to Michael Sattler who, as second advisor and member of my thesis committee, reviewed and evaluated this work.

Furthermore, I would like to thank all collaborators, whose collective efforts enriched the quality of this research.

Special thanks are extended to all my colleagues from AG Poeck and AG Heidegger. I want to express my deepest appreciation to Sascha for not only being a valuable colleague but also a wonderful friend. His advice and the delicious cakes, croissants, and tomatoes he shared made the journey truly enjoyable. I am also grateful to Tatiana and Lena for their consistent assistance in various capacities, the flowers, and all the fun we had together. A heartfelt thank you to Nardine, Nadia, and Anna for their unwavering support and all the joyful moments and lunch breaks. Gratitude is also extended to all the supportive, (s)trong, and humorous individuals from TranslaTUM who made the work environment truly special.

I would like to acknowledge Monika, Abebe, Niki, Susanne, and Lukas, whose dedication and excellent work made my time in MR1 special and transformed it into a second home. They not only ensured my residence in MR1 was as pleasant as possible but also consistently provided outstanding care for our little fluffy companions.

I extend my sincere appreciation to my family - first and foremost my parents and my brother - for their constant support and understanding. Despite the family-wide occasional inquiries about the completion date, their encouragement has remained a constant source of motivation. Lastly, I am deeply grateful for Leon's invaluable support and for being my procrastination partner in crime.